THE OHIO STATE UNIVERSITY

Atomic Data and Spectral Analysis Of Carbon, Nitrogen, Oxygen and Silicon Ions Observed with the International Ultraviolet Explorer

A. K. Pradhan
Department of Astronomy

Goddard Space Flight Center
Greenbelt, Maryland 20771

Grant No. NAG 5-1644
Progress Report

November 1992

T · H · E
OHIO
STATE
UNIVERSITY

Atomic Data and Spectral Analysis Of Carbon, Nitrogen, Oxygen and Silicon Ions Observed with the International Ultraviolet Explorer

A. K. Pradhan
Department of Astronomy

Goddard Space Flight Center
Greenbelt, Maryland 20771

Grant No. NAG 5-1644
Progress Report
RF Project No. 769157/724904

November 1992

PROGRESS REPORT: ADP GRANT NAG 5-1644

Atomic Data And Spectral Analysis of Carbon, Nitrogen Oxygen and Silicon Ions Observed with IUE

A.K.Pradhan,
Department of Astronomy, The Ohio State University, Columbus Ohio 43210.

According to the plan presented in the original proposal we have now completed most of the atomic calculations involving collision strengths and rate coeffcients for electron impact excitation of C II, N III and O IV ions. These have been reported in the first two publications appended with this report. We have now moved into the applications phase of the project with the new data being used to analyze the IUE observations of a variety of objects, as described in the third publication recently submitted (also appended). The analysis and interpretaion of archival data will continue well into the next year with several collaborators that the PI and Co-PI (P.G. Judge) are involved with. In addition, the atomic calculations on Si II have been started.

An extension of the present project is also under way. We are calculating collision cross sections and rates for other, highly ionized members of the Boron sequence: Ne VI, Mg VIII, Si X, S XII, A XIV, Ca XVI and Fe XXII, including relativistic effects which are likely to influence the intercombination lines due the transitions $^4P_J - ^2P^o_{J'}$. A new line ratios code has also been written to obtain the intensities of the prominent UV lines for direct comparison with observations.

It is expected that the work will continue beyond the tenure of the grant, however no addtional request for funding is intended and we shall adhere to the budget as outlined and approved.

Appendices

THE ASTROPHYSICAL JOURNAL SUPPLEMENT SERIES, 80:425–452, 1992 May

RATE COEFFICIENTS FOR THE EXCITATION OF INFRARED AND ULTRAVIOLET LINES IN C II, N III, AND O IV

ROBERT D. BLUM AND ANIL K. PRADHAN
Department of Astronomy, Ohio State University, Columbus, OH 43210
Received 1991 June 10; accepted 1991 October 8

ABSTRACT

Electron impact excitation of boron-like C, N, and O is the primary mechanism for the formation of a number of IR and UV emission lines that are useful density and temperature diagnostics for a variety of astrophysical sources. New and improved collision strengths and Maxwellian-averaged rate coefficients for temperatures between 1000 and 40,000 K are presented for all the prominent transitions in the spectra of C II, N III, and O IV. The collision strengths show extensive autoionization structures that are delineated in detail and which enhance the rate coefficients for several transitions by a considerable amount. Particular attention is directed toward the fine-structure IR transition $^2P^o_{1/2}$–$^2P^o_{3/2}$ and the dipole-allowed and intercombination UV transitions $^2P^o_{1/2,3/2}$–$^2D^2_{3/2,5/2}$, $^2S^2_{1/2}$, $^2P_{1/2,3/2}$, and $^2P^o_{1/2,3/2}$–$^4P_{1/2,3/2,5/2}$, respectively, in the three ions. Maxwellian-averaged collision strengths are calculated for all possible fine-structure transitions among the states included in the eigenfunction expansion of the target ion. All calculations are carried out in the close-coupling approximation using the *R*-matrix method as adapted for the Opacity Project.

Subject heading: atomic processes

1. INTRODUCTION

The emission lines of C II, N III, and O IV have long been recognized as important temperature and density diagnostics in the UV and the IR from sources as diverse as novae, planetary nebulae, symbiotic stars, Seyfert galaxies, quasars, the interstellar medium, and the Sun. For example, the UV spectra of C II from planetary nebulae, mainly the multiplets λλ 1335 and 2325 of transitions $^2P^o_J$–$^2D_{J'}$ and $^2P^o_J$–$^4P_{J'}$, have been reported by Pwa, Mo, & Pottasch (1984), and Stencel et al. (1981) at densities $10^3 < N_e < 10^5$ cm^{-3}. Observations of C II are also reported at much higher densities prevalent in solar chromosphere and the transition region, with $N_e > 10^{12}$ cm^{-3}, by Doschek, Feldman, & Cohen (1977). An important fact related to the abundance of C II is that the ionization potential is relatively high, 24.4 eV, more than twice the ionization potential of C I at 11.3 eV. Therefore C II may be abundant both in H I and H II regions, and the spectral analysis of C II lines may be used to determine both the electron density and neutral hydrogen density since both influence the level populations of the ground-state fine-structure states $^2P^o_{1/2}$ and $^2P^o_{3/2}$ corresponding to the 158 μm line in the IR (Keenan et al. 1986). The EUV spectra of N III is prominent in the observations of the Sun; the intercombination and allowed multiplets are observed at λ1749 and at λλ 686,764 and 772, respectively (Nussbaumer & Storey 1979). Recently, the N III] intercombination lines have been reported in the *IUE* observations from the nova RR Tel (P. G. Judge, private communication). Similarly, the O IV emission lines have been observed in novae, planetary nebulae, and the solar transition region (Hayes 1983), as well as other astrophysical sources.

Previous atomic calculations have been carried out, in various approximations, for the collisional data for the excitation of each of the three ions: Lennon et al. 1985 and Hayes & Nussbaumer 1984 for C II; Hayes (1983) for O IV and Nussbaumer & Storey (1979) for N III. In the present work we consider all three ions with similar close-coupling calculations for each ion (the close-coupling approximation is the most accurate method for low-energy electron-ion/atom impact excitation). The data set thus obtained should be consistent and accurate and more complete than previous works. While the calculations of Lennon et al. and Hayes & Nussbaumer for C II are also in the close coupling approximation, the present work includes more excited states and is more detailed. The present N III and O IV results are considerably more extensive than previously available data and should be much more accurate, in particular for N III where the Nussbaumer & Storey calculations employed the distorted wave approximation that neglects coupling and resonance effects; consequently the present values for N III differ considerably from the Nussbaumer & Storey results. Also, the present calculations were carried out using the newly developed Opacity Project codes (Seaton 1987; Berrington et al. 1987) where the *R*-matrix method is employed to treat the electron + ion processes in the close-coupling approximation. A new code is used to obtain the fine-structure collision strengths.

2. ATOMIC CALCULATIONS

Recently some new results have been reported by Luo and Pradhan (1990) for the collision strengths for electron impact excitation of C II, N III, and O IV, and for C II by Blum & Pradhan (1991), using the *R*-matrix method. The most important features of the close-coupling calculations are the inclusion of the often strong coupling between the low-lying states of atoms and ions and the autoionizing resonances that generally enhance the effective scattering cross section by a large amount, up to a factor of 2 or 3, or even more. However, the computations are very extensive and require the collision strengths to be evaluated at a large number of energies in order

to delineate the resonances in detail. The calculations by Luo & Pradhan (1990) have been repeated by the authors with a number of improvements, the primary ones being the extension of the collision strengths to the region of all channels open (Blum & Pradhan 1991) and more accurate treatment of the fine structure with a new code.

The calculations include 10 states with total LS symmetries: $2s^22p(^2P^o)$, $2s2p^2(^4P, {}^2D, {}^2S, {}^2P)$, $2s^23s(^2S)$, $2s^23p(^2P^o)$, $2p^3(^4S^o, {}^2D^o, {}^2P^o)$ for C II, and eight states, excluding the $n = 3$ states, for N III and O IV. Following the scattering calculations, carried out in LS coupling, the scattering matrices are transformed to a pair coupling representation to yield collision strengths for all fine-structure sublevels of the LS states included in the eigenfunction expansion for the target ion.

Previous calculations for the fine-structure collision strengths have usually relied on a code, used independently after the scattering calculations have been carried out, developed by Saraph (1972, 1978). We have developed a new code called STGFJ that is directly interfaced with the R-matrix package of codes and is more efficient in the calculations for large numbers of fine-structure collision strengths.

In the present report we discuss the new results, pointing out some important features that are likely to affect the density and temperature diagnostics of lines emanating from the excited states of C II, N III, and O IV.

3. DISCUSSION OF RESULTS

Table 1 lists the LS multiplet and the respective fine-structure component wavelengths for the important intercombination and dipole-allowed transitions in C II, N III, and O IV. As the spectral features cover a wide range in the EUV, the corresponding emission lines provide useful density and temperature diagnostics over extended ranges. The collision strengths presented are for the excitation of (1) the ground states' sublevels, (2) the metastable state ^4P, (3) the dipole allowed transitions for the ^2D, ^2S and the ^2P, and (4) a type of transition, within the ^4P_J for example, that will be affected by collisional mixing among excited levels.

TABLE 1

MULTIPLET AND COMPONENT WAVELENGTHS FOR INTERCOMBINATION AND ALLOWED TRANSITIONS

Multiplet	J	J'	C II	N III	O IV
$^2P^o$–^4P	...	...	2327.0	1749.0	1402.0
	1/2	1/2	2326.8	1749.4	1405.7
	1/2	3/2	2325.7	1747.6	1403.1
	1/2	5/2	2324.1	1745.1	1399.5
	3/2	1/2	2330.3	1754.8	1413.4
	3/2	3/2	2329.1	1753.0	1410.8
	3/2	5/2	2327.6	1750.6	1407.1
$^2P^o$–^2D	...	...	1336.0	991.0	788.0
	1/2	3/2	1335.2	990.4	788.2
	1/2	5/2	1335.3	990.3	788.1
	3/2	3/2	1336.4	992.1	790.6
	3/2	5/2	1336.4	992.0	790.5
$^2P^o$–^2S	...	...	1047.0	764.0	609.0
	1/2	1/2	1036.9	763.8	608.7
	3/2	1/2	1037.6	764.8	610.2
$^2P^o$–^2P	...	...	905.0	686.0	554.0
	1/2	1/2	904.4	685.9	554.4
	1/2	3/2	904.1	685.4	553.6
	3/2	1/2	905.0	686.7	555.6
	3/2	3/2	904.6	686.2	554.8

3.1. *Ground-State Fine Structure*

The $^2P^o_{1/2}$–$^2P^o_{3/2}$ transition in C II, N III, and O IV corresponds to the forbidden IR lines at 158, 57, and 26 μm, respectively. The collision strengths for the three ions are presented in Figure 1, showing the detailed resonance structures that are the dominant factor in the excitation of this forbidden transition. In particular, the near-threshold resonance in C II, corresponding to the autoionizing state $2s2p^3(^1D^o)$, has been the subject of two previous calculations (Lennon et al. 1985; Hayes & Nussbaumer 1984). The previous works recommended that the resonance position be shifted downward, closer to the threshold of excitation, in order to coincide with the position extrapolated by Edlen (1934). We have further analyzed the resonance position (Blum & Pradhan 1991) and conclude that in light of the uncertainty in the extrapolated value, which has not yet been confirmed by direct spectroscopic observation, the calculated position should be retained and the rate coefficient be so obtained (L. J. Curtis, L. Johansson, & I. Martinson, private communication).

The broad feature corresponding to the $2s^22p^3(^1D^o)$ resonance in C II is no longer present in N III and O IV collision strengths as it moves downward as z^2 with increasing ion charge and becomes a pure bound state. The energy levels calculated by Luo & Pradhan (1989) for this state are in very good agreement with the experimentally observed positions in N II and O III, thus lending confidence to the suggestion herein that the calculated position of the *autoionizing* state in C II may be correct. The rate coefficient at 1000 K is ~30% lower if the calculated, as opposed to the shifted, resonance position is used (23% lower at 10,000 K).

It is seen in Figure 1 that if one considers the same transition along an isoelectronic sequence then the resonance structures in the near-threshold region correspond to successively higher members of the Rydberg series of resonances converging on to the excited thresholds; the lower members become bound states of the electron + ion system. The near-threshold region in the collision strength is dominated by large resonances in both C II and O IV, consequently enhancing the effective collision strength averaged over a typical Maxwellian distribution at ~10,000 K. For N III the resonance contributions are relatively small for this transition.

3.2. *Intercombination Transition*

The excitation of the metastable state ^4P from the ground state $^2P^o$ involves change of spin and parity; thus the downward transition is allowed by angular momentum selection rules but is spin forbidden, i.e., an intercombination transition. As the transition probability of the metastable state is considerably lower than fully dipole-allowed transitions, it may be collisionally excited as the electron density increases, affecting the upper state level population and consequently the intercombination line intensity. The $\lambda\lambda$ 2327, 1749, and 1402 multiplets in C II, N III, and O IV, respectively, correspond to

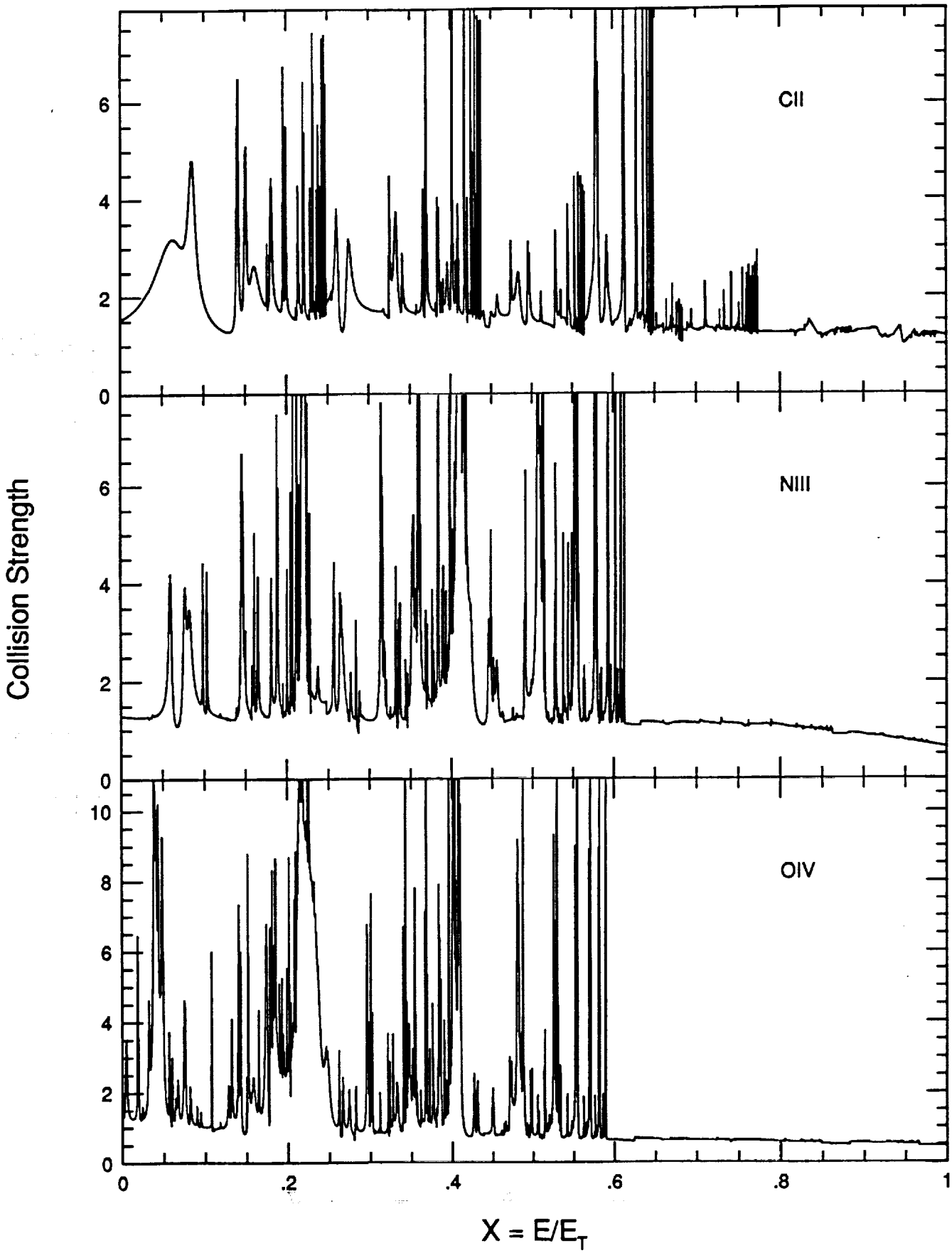

FIG. 1.—The collision strengths for the ground state fine-structure transition $^2P^o_{1/2}$–$^2P^o_{3/2}$ in C II, N III, and O IV. The X units are excitation energies divided by the threshold energy for the transition.

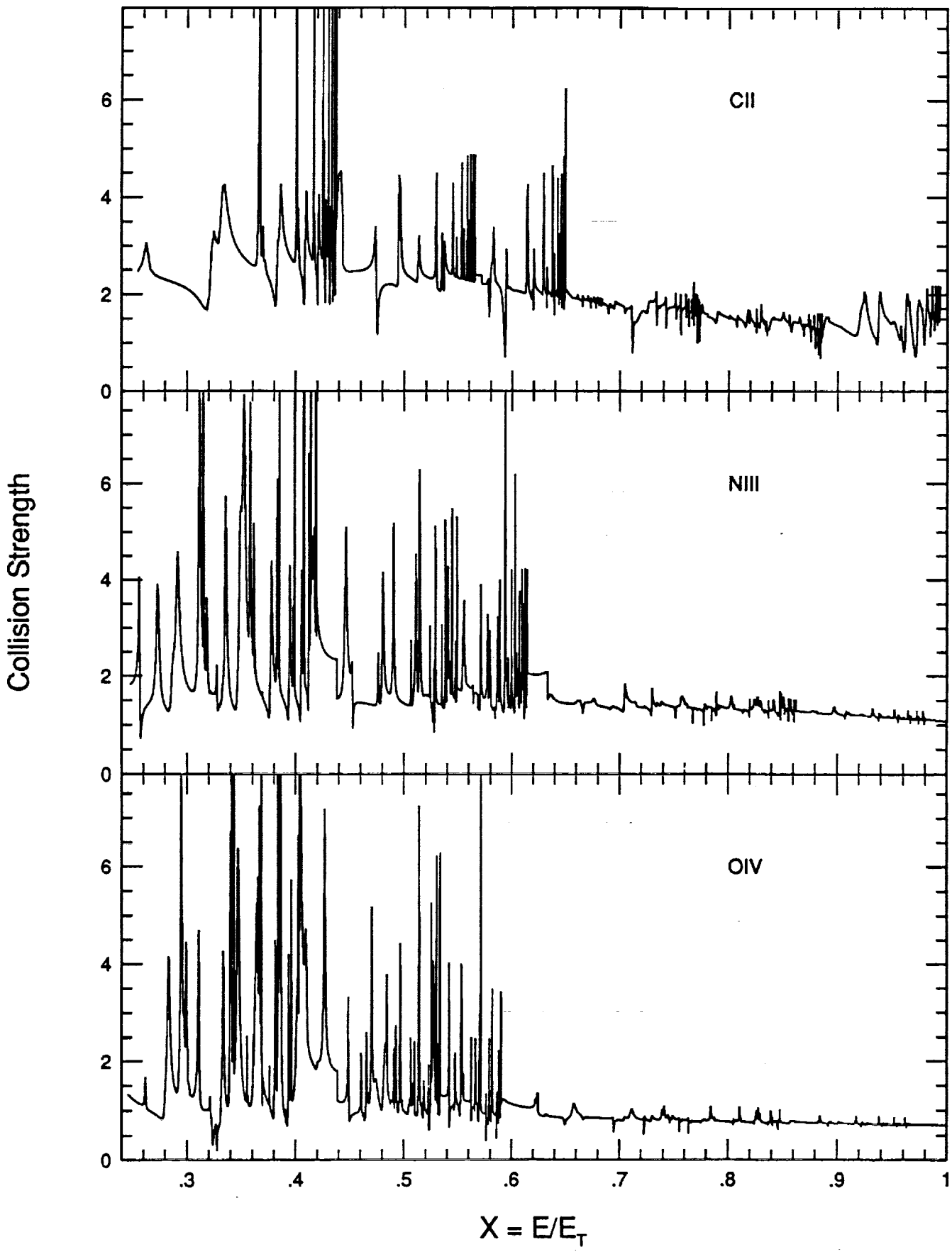

FIG. 2.—Collision strength for the excitation of the metastable state ^4P, from the ground state $^2P^o$, in C II, N III, and O IV

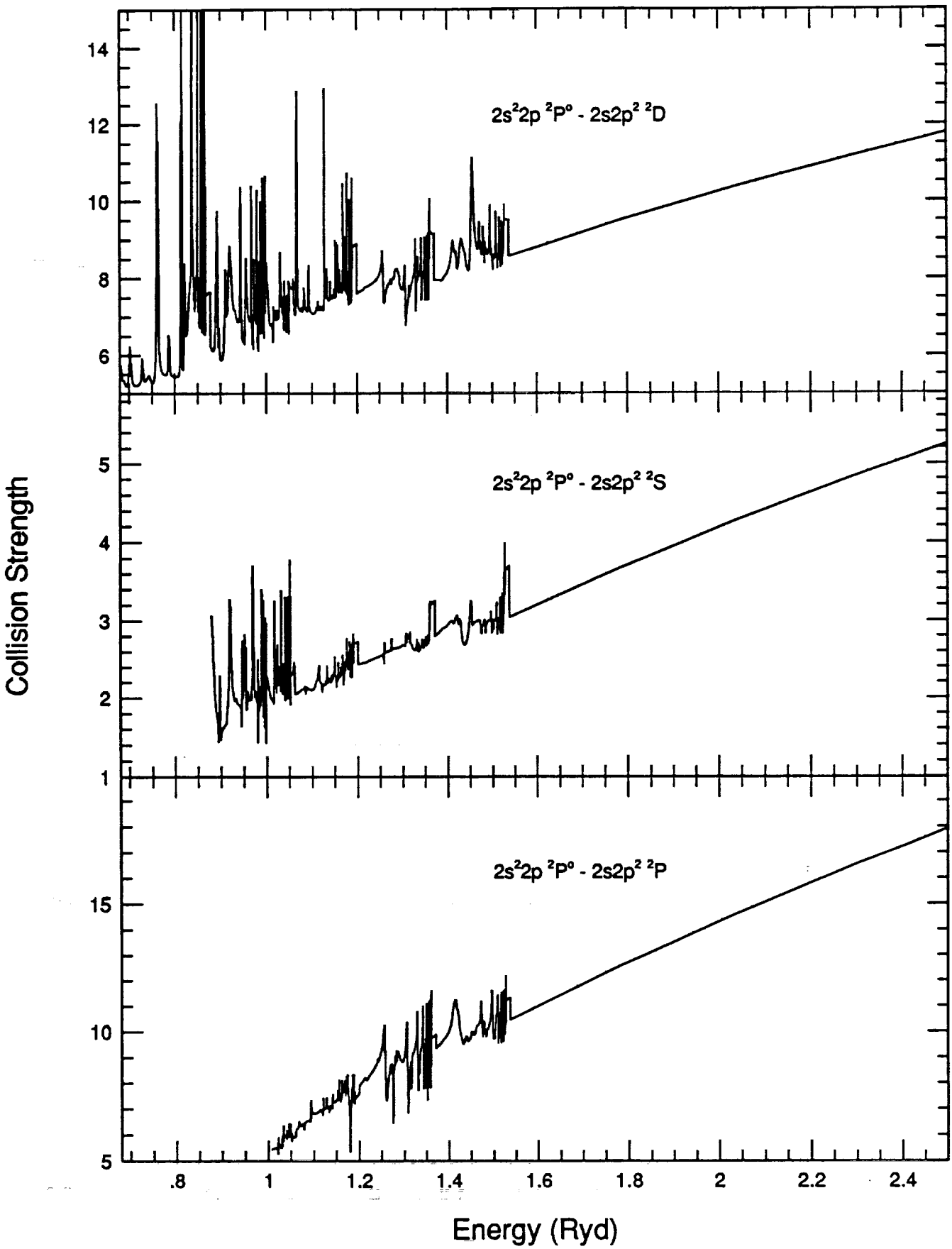

FIG. 3.—Collision strengths for the dipole-allowed transitions in C II from the ground state $^2P^o$

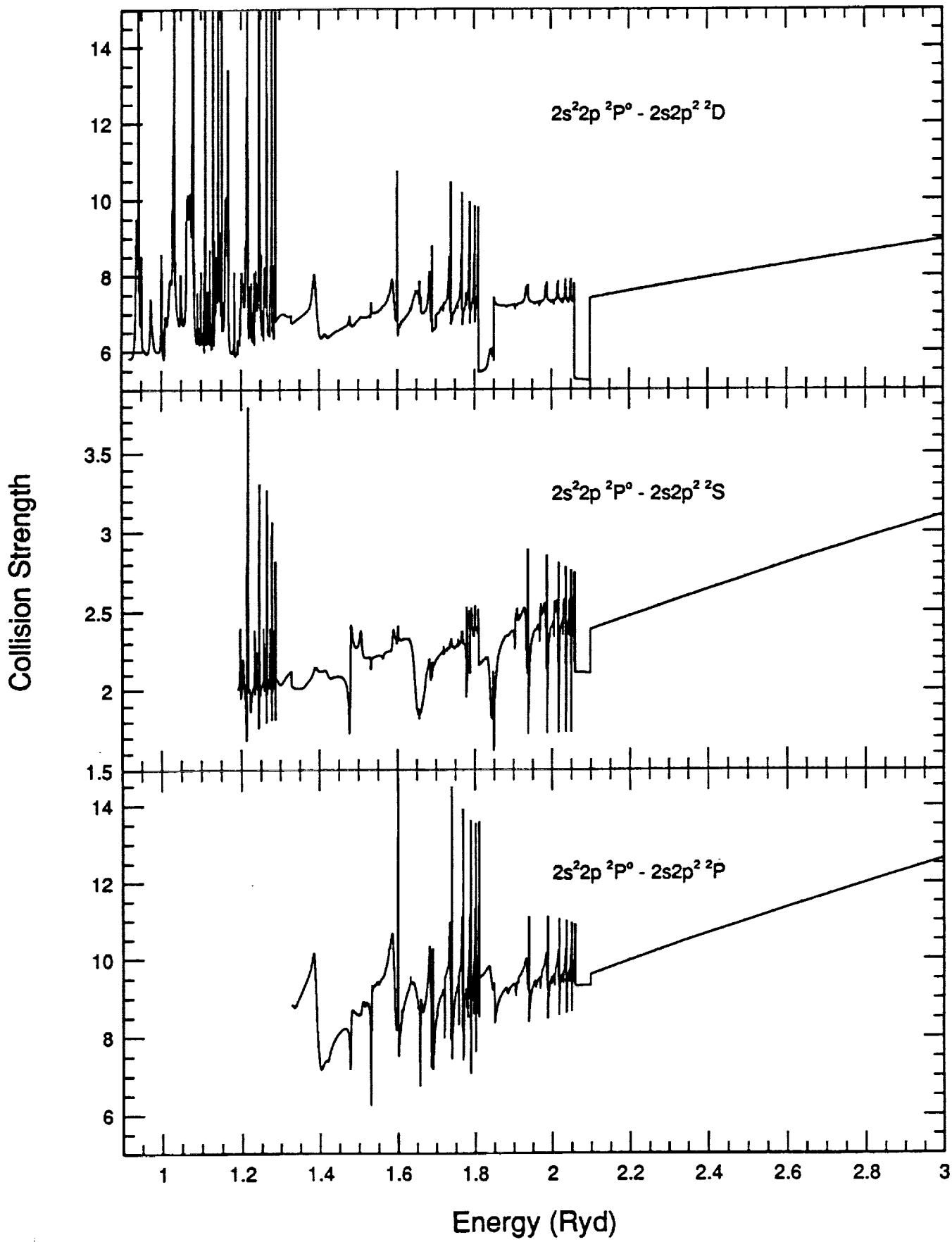

FIG. 4.—Collision strengths for the dipole-allowed transitions, from the ground state, in N III. The rectangular features are artificial and the collision strengths should be continuous across these features.

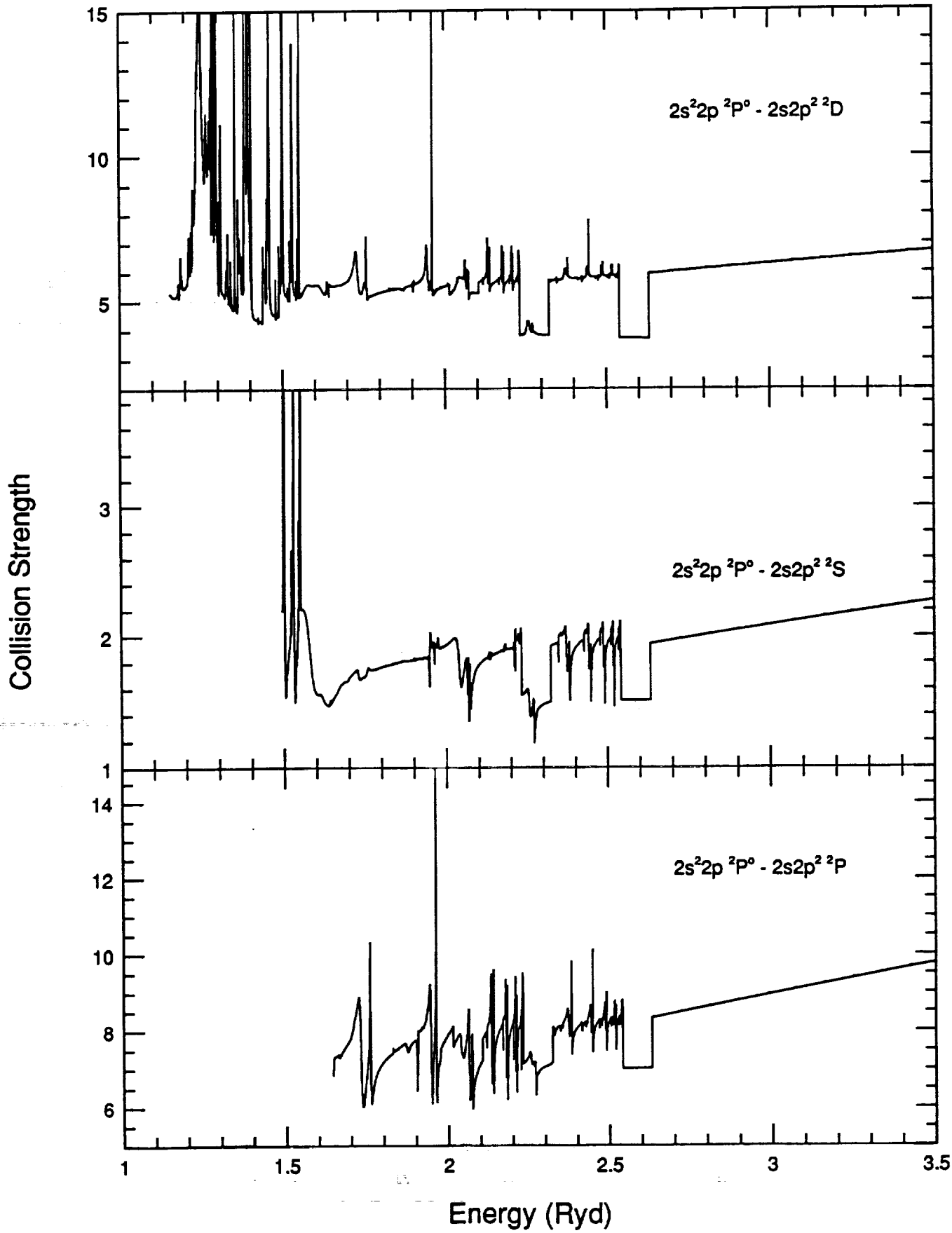

FIG. 5.—Collision strengths for the dipole-allowed transitions in O IV from the ground state

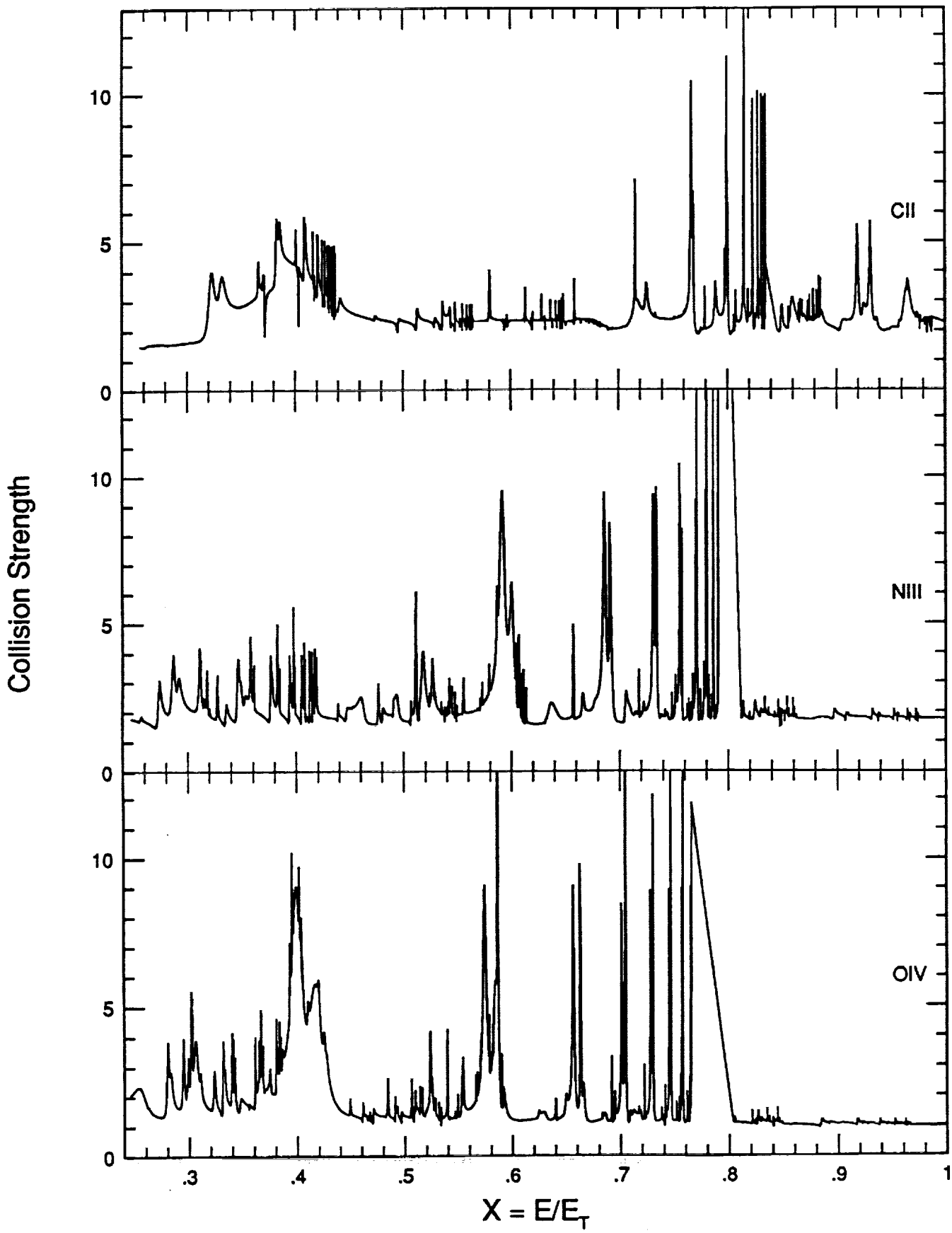

FIG. 6.—Collision strengths for collisional mixing among the fine-structure sublevels of the metastable state: $^4P_{3/2}$–$^4P_{5/2}$, in C II, N III, and O IV (the large feature in N III and O IV at approximately $X = 0.8$ is spurious and is due to certain missing points).

TABLE 2

MAXWELLIAN-AVERAGED COLLISION STRENGTHS FOR C II

Temp (K)	TRANSITION KEY							
	1 2	1 3	1 4	1 5	1 6	1 7	1 8	1 9	1 10
	1 11	1 12	1 13	1 14	1 15	1 16	1 17	1 18	2 3
	2 4	2 5	2 6	2 7	2 8	2 9	2 10	2 11	2 12
	2 13	2 14	2 15	2 16	2 17	2 18	3 4	3 5	3 6
	3 7	3 8	3 9	3 10	3 11	3 12	3 13	3 14	3 15
	3 16	3 17	3 18	4 5	4 6	4 7	4 8	4 9	4 10
	4 11	4 12	4 13	4 14	4 15	4 16	4 17	4 18	5 6
	5 7	5 8	5 9	5 10	5 11	5 12	5 13	5 14	5 15
	5 16	5 17	5 18	6 7	6 8	6 9	6 10	6 11	6 12
	6 13	6 14	6 15	6 16	6 17	6 18	7 8	7 9	7 10
	7 11	7 12	7 13	7 14	7 15	7 16	7 17	7 18	8 9
	8 10	8 11	8 12	8 13	8 14	8 15	8 16	8 17	8 18
	9 10	9 11	9 12	9 13	9 14	9 15	9 16	9 17	9 18
	10 11	10 12	10 13	10 14	10 15	10 16	10 17	10 18	11 12
	11 13	11 14	11 15	11 16	11 17	11 18	12 13	12 14	12 15
	12 16	12 17	12 18	13 14	13 15	13 16	13 17	13 18	14 15
	14 16	14 17	14 18	15 16	15 17	15 18	16 17	16 18	17 18
1000.	1.5763	0.2653	0.3925	0.2435	1.2826	0.5206	0.7915	1.1607	0.6689
	0.2056	0.2114	0.1175	0.0050	0.1153	0.0837	0.1811	0.1066	0.1853
	0.5088	1.1084	0.8812	2.7251	1.5831	0.6689	2.9904	0.4113	0.1175
	0.5403	0.0101	0.1235	0.2746	0.1066	0.4687	0.6119	0.6588	0.4189
	0.2302	0.0642	0.0742	0.0798	0.0238	0.0075	0.0080	0.8802	0.2660
	0.1275	0.1234	0.1937	1.5041	0.6467	0.6516	0.1284	0.1209	0.1871
	0.0476	0.0122	0.0187	1.7604	0.4017	0.3854	0.2256	0.4087	0.4923
	1.4552	0.1926	0.1129	0.3491	0.0714	0.0112	0.0352	2.6406	0.2768
	0.9038	0.2853	0.6661	2.1560	0.5786	0.2364	0.6387	0.2486	0.1628
	0.1724	0.1156	2.2686	0.7841	1.2182	0.5284	0.8679	0.4929	0.8198
	0.3729	0.1165	0.3863	0.1734	0.7841	3.7946	0.2373	2.3823	0.0917
	0.1834	3.4386	0.6610	1.3220	0.0000	0.0268	0.0402	0.5244	1.0490
	0.7652	0.0257	0.0281	0.0400	0.2958	2.6477	0.1387	1.6166	0.8818
	0.0514	0.0400	0.0962	0.5916	0.6960	4.8767	0.8818	4.1154	9.5962
	19.1924	0.0000	0.0299	0.0448	0.1545	0.3090	8.7134	0.0062	0.0407
	0.0474	0.2226	0.5301	0.0124	0.0651	0.1113	0.5301	0.9752	0.9026
	1.3538	0.1657	0.3314	1.4527	0.5521	0.7312	0.5173	1.4078	0.9318
2000.	1.6361	0.2577	0.3821	0.2397	1.2879	0.5136	0.7146	1.1782	0.6800
	0.2227	0.2145	0.1184	0.0065	0.1222	0.0911	0.1784	0.1067	0.1820
	0.4974	1.0796	0.8739	2.7291	1.4292	0.6800	3.0363	0.4454	0.1184
	0.5474	0.0130	0.1337	0.2929	0.1067	0.4634	0.6137	0.6748	0.4279
	0.2379	0.0629	0.0815	0.0974	0.0230	0.0082	0.0088	0.8879	0.2769
	0.1227	0.1152	0.1813	1.5265	0.6619	0.6697	0.1259	0.1367	0.2210
	0.0460	0.0134	0.0206	1.7759	0.4134	0.3859	0.2108	0.3823	0.5081
	1.4892	0.1888	0.1395	0.3971	0.0690	0.0124	0.0385	2.6638	0.2688
	0.9301	0.2671	0.6225	2.0820	0.5692	0.2406	0.6431	0.2759	0.1667
	0.1726	0.1090	2.3232	0.8241	1.1994	0.5129	0.8538	0.4958	0.8297
	0.4139	0.1160	0.3929	0.1635	0.8241	3.8966	0.2275	2.3406	0.0929
	0.1857	3.5355	0.6798	1.3595	0.0000	0.0404	0.0606	0.5634	1.1270
	0.7932	0.0268	0.0322	0.0462	0.3077	2.6714	0.1934	1.6341	0.8868
	0.0535	0.0462	0.1105	0.6154	0.7663	4.9632	0.8868	4.1553	9.8055
	19.6095	0.0000	0.0425	0.0637	0.1605	0.3210	8.7615	0.0123	0.0582
	0.0659	0.2008	0.4961	0.0246	0.0907	0.1575	0.4961	0.8977	0.8771
	1.3155	0.1614	0.3228	1.4713	0.5381	0.7187	0.5093	1.3760	0.9841
3000.	1.7157	0.2507	0.3719	0.2340	1.2975	0.5122	0.6915	1.1968	0.6916
	0.2309	0.2186	0.1215	0.0074	0.1325	0.1009	0.1765	0.1062	0.1776
	0.4847	1.0508	0.8741	2.7453	1.3830	0.6916	3.0851	0.4617	0.1215
	0.5587	0.0149	0.1476	0.3193	0.1062	0.4591	0.6200	0.6895	0.4346
	0.2440	0.0642	0.0917	0.1165	0.0233	0.0094	0.0097	0.8997	0.2858
	0.1214	0.1086	0.1691	1.5521	0.6734	0.6838	0.1283	0.1567	0.2598
	0.0465	0.0152	0.0231	1.7994	0.4241	0.3903	0.1980	0.3574	0.5207
	1.5151	0.1925	0.1680	0.4566	0.0698	0.0137	0.0438	2.6992	0.2673
	0.9543	0.2488	0.5843	2.0259	0.5904	0.2452	0.6498	0.2860	0.1747
	0.1764	0.1023	2.3804	0.8600	1.1976	0.5062	0.8856	0.5007	0.8418
	0.4291	0.1179	0.4087	0.1534	0.8600	4.0004	0.2223	2.3333	0.0928
	0.1857	3.5786	0.6984	1.3967	0.0000	0.0504	0.0756	0.5715	1.1431
	0.8275	0.0303	0.0407	0.0596	0.3091	2.7350	0.2539	1.6452	0.8902
	0.0607	0.0596	0.1411	0.6182	0.8516	5.1260	0.8902	4.1809	10.0274
	20.0477	0.0000	0.0470	0.0705	0.1603	0.3205	8.8098	0.0144	0.0750
	0.0842	0.1845	0.4579	0.0287	0.1161	0.2023	0.4579	0.8270	0.8617
	1.2925	0.1577	0.3154	1.4840	0.5274	0.7100	0.5037	1.3525	1.0071

TABLE 2—*Continued*

Temp (K)									
4000.	1.8034	0.2459	0.3650	0.2304	1.3094	0.5145	0.6844	1.2157	0.7029
	0.2354	0.2235	0.1270	0.0080	0.1419	0.1094	0.1761	0.1057	0.1748
	0.4763	1.0315	0.8793	2.7685	1.3689	0.7029	3.1343	0.4708	0.1270
	0.5741	0.0160	0.1597	0.3430	0.1057	0.4578	0.6358	0.7078	0.4404
	0.2495	0.0660	0.1029	0.1322	0.0238	0.0110	0.0111	0.9103	0.2912
	0.1210	0.1035	0.1582	1.5926	0.6835	0.6963	0.1320	0.1764	0.2939
	0.0477	0.0177	0.0265	1.8206	0.4308	0.3936	0.1875	0.3359	0.5318
	1.5379	0.1979	0.1910	0.5144	0.0715	0.0155	0.0508	2.7310	0.2673
	0.9693	0.2324	0.5526	1.9846	0.6122	0.2497	0.6548	0.2905	0.1870
	0.1833	0.0969	2.4334	0.8877	1.2025	0.5033	0.9183	0.5040	0.8526
	0.4358	0.1216	0.4338	0.1453	0.8877	4.0938	0.2190	2.3396	0.0925
	0.1850	3.6144	0.7172	1.4342	0.0000	0.0574	0.0861	0.5674	1.1351
	0.8561	0.0364	0.0512	0.0758	0.3060	2.8076	0.2973	1.6526	0.8926
	0.0729	0.0758	0.1782	0.6120	0.9183	5.2914	0.8926	4.1981	10.2527
	20.4893	0.0000	0.0489	0.0734	0.1570	0.3141	8.8487	0.0149	0.0884
	0.1001	0.1715	0.4230	0.0298	0.1378	0.2392	0.4230	0.7661	0.8515
	1.2772	0.1544	0.3089	1.4912	0.5197	0.7032	0.4994	1.3351	1.0170
5000.	1.8874	0.2430	0.3610	0.2290	1.3228	0.5187	0.6830	1.2346	0.7138
	0.2386	0.2288	0.1338	0.0083	0.1494	0.1160	0.1774	0.1052	0.1735
	0.4720	1.0206	0.8870	2.7961	1.3660	0.7138	3.1830	0.4773	0.1338
	0.5913	0.0166	0.1691	0.3617	0.1052	0.4599	0.6599	0.7302	0.4459
	0.2544	0.0677	0.1129	0.1443	0.0245	0.0126	0.0125	0.9197	0.2939
	0.1207	0.0995	0.1490	1.6474	0.6929	0.7078	0.1355	0.1932	0.3212
	0.0489	0.0202	0.0301	1.8395	0.4341	0.3951	0.1790	0.3179	0.5419
	1.5591	0.2032	0.2082	0.5634	0.0734	0.0174	0.0579	2.7592	0.2671
	0.9768	0.2184	0.5270	1.9552	0.6298	0.2545	0.6585	0.2930	0.2014
	0.1914	0.0921	2.4802	0.9078	1.2098	0.5020	0.9447	0.5064	0.8631
	0.4395	0.1260	0.4633	0.1382	0.9078	4.1740	0.2167	2.3510	0.0922
	0.1844	3.6432	0.7363	1.4724	0.0000	0.0622	0.0933	0.5588	1.1177
	0.8779	0.0437	0.0609	0.0906	0.3013	2.8763	0.3250	1.6574	0.8940
	0.0874	0.0907	0.2124	0.6027	0.9653	5.4371	0.8941	4.2091	10.4718
	20.9160	0.0000	0.0498	0.0747	0.1528	0.3056	8.8759	0.0149	0.0984
	0.1127	0.1608	0.3928	0.0299	0.1549	0.2673	0.3928	0.7144	0.8447
	1.2669	0.1515	0.3030	1.4958	0.5143	0.6975	0.4955	1.3221	1.0222
6000.	1.9615	0.2416	0.3593	0.2291	1.3372	0.5238	0.6837	1.2533	0.7244
	0.2411	0.2340	0.1410	0.0085	0.1552	0.1210	0.1801	0.1050	0.1734
	0.4707	1.0159	0.8959	2.8260	1.3674	0.7244	3.2309	0.4822	0.1410
	0.6090	0.0170	0.1762	0.3761	0.1050	0.4652	0.6896	0.7554	0.4513
	0.2589	0.0693	0.1212	0.1532	0.0250	0.0141	0.0138	0.9284	0.2950
	0.1203	0.0966	0.1413	1.7117	0.7019	0.7184	0.1385	0.2067	0.3421
	0.0500	0.0225	0.0333	1.8568	0.4353	0.3953	0.1725	0.3034	0.5512
	1.5793	0.2078	0.2209	0.6023	0.0750	0.0192	0.0645	2.7853	0.2664
	0.9795	0.2068	0.5071	1.9344	0.6432	0.2600	0.6622	0.2943	0.2161
	0.1998	0.0879	2.5211	0.9221	1.2180	0.5018	0.9648	0.5085	0.8747
	0.4415	0.1305	0.4933	0.1319	0.9221	4.2426	0.2152	2.3645	0.0921
	0.1841	3.6627	0.7557	1.5110	0.0000	0.0653	0.0980	0.5486	1.0974
	0.8946	0.0509	0.0688	0.1029	0.2965	2.9380	0.3417	1.6603	0.8951
	0.1018	0.1029	0.2405	0.5929	0.9977	5.5614	0.8951	4.2158	10.6809
	21.3205	0.0000	0.0500	0.0750	0.1484	0.2967	8.8936	0.0149	0.1054
	0.1221	0.1519	0.3671	0.0298	0.1677	0.2875	0.3671	0.6708	0.8401
	1.2602	0.1489	0.2978	1.4993	0.5106	0.6929	0.4923	1.3128	1.0272
7000.	2.0240	0.2412	0.3590	0.2300	1.3520	0.5290	0.6853	1.2716	0.7347
	0.2429	0.2391	0.1481	0.0087	0.1596	0.1247	0.1842	0.1051	0.1739
	0.4712	1.0152	0.9052	2.8568	1.3706	0.7347	3.2779	0.4858	0.1481
	0.6263	0.0174	0.1816	0.3871	0.1051	0.4734	0.7224	0.7815	0.4564
	0.2630	0.0705	0.1277	0.1599	0.0255	0.0155	0.0150	0.9367	0.2950
	0.1198	0.0947	0.1353	1.7804	0.7105	0.7285	0.1411	0.2171	0.3579
	0.0510	0.0246	0.0364	1.8735	0.4351	0.3945	0.1677	0.2921	0.5598
	1.5986	0.2116	0.2303	0.6324	0.0764	0.0209	0.0705	2.8102	0.2654
	0.9791	0.1975	0.4922	1.9195	0.6531	0.2664	0.6664	0.2948	0.2302
	0.2078	0.0842	2.5574	0.9321	1.2267	0.5028	0.9797	0.5109	0.8883
	0.4423	0.1348	0.5222	0.1262	0.9321	4.3019	0.2145	2.3796	0.0920
	0.1841	3.6731	0.7750	1.5496	0.0000	0.0673	0.1010	0.5384	1.0771
	0.9081	0.0573	0.0751	0.1125	0.2920	2.9928	0.3511	1.6620	0.8961
	0.1145	0.1125	0.2627	0.5839	1.0199	5.6671	0.8962	4.2202	10.8792
	21.7021	0.0000	0.0498	0.0747	0.1442	0.2885	8.9047	0.0148	0.1101
	0.1289	0.1445	0.3454	0.0297	0.1767	0.3013	0.3454	0.6343	0.8373
	1.2559	0.1466	0.2932	1.5025	0.5085	0.6895	0.4898	1.3070	1.0337

TABLE 2—*Continued*

Temp (K)									
8000.	2.0756	0.2413	0.3595	0.2315	1.3669	0.5341	0.6873	1.2896	0.7448
	0.2442	0.2441	0.1550	0.0088	0.1631	0.1276	0.1892	0.1058	0.1749
	0.4728	1.0170	0.9143	2.8877	1.3746	0.7448	3.3240	0.4883	0.1550
	0.6431	0.0176	0.1858	0.3956	0.1058	0.4841	0.7564	0.8070	0.4614
	0.2669	0.0716	0.1327	0.1648	0.0259	0.0167	0.0162	0.9449	0.2945
	0.1191	0.0935	0.1306	1.8499	0.7187	0.7379	0.1432	0.2252	0.3699
	0.0517	0.0266	0.0393	1.8898	0.4341	0.3930	0.1644	0.2837	0.5678
	1.6171	0.2148	0.2372	0.6555	0.0776	0.0225	0.0762	2.8347	0.2640
	0.9767	0.1903	0.4820	1.9086	0.6604	0.2738	0.6713	0.2948	0.2434
	0.2153	0.0808	2.5899	0.9390	1.2360	0.5049	0.9906	0.5138	0.9040
	0.4422	0.1389	0.5492	0.1212	0.9390	4.3542	0.2147	2.3966	0.0921
	0.1843	3.6755	0.7942	1.5877	0.0000	0.0685	0.1028	0.5290	1.0583
	0.9195	0.0627	0.0800	0.1199	0.2880	3.0416	0.3557	1.6632	0.8976
	0.1254	0.1199	0.2799	0.5759	1.0351	5.7581	0.8976	4.2240	11.0672
	22.0619	0.0000	0.0493	0.0740	0.1406	0.2811	8.9112	0.0148	0.1130
	0.1335	0.1384	0.3270	0.0296	0.1828	0.3102	0.3270	0.6039	0.8356
	1.2534	0.1447	0.2894	1.5060	0.5078	0.6874	0.4882	1.3045	1.0424
9000.	2.1177	0.2418	0.3605	0.2332	1.3816	0.5388	0.6895	1.3073	0.7546
	0.2450	0.2489	0.1616	0.0090	0.1658	0.1299	0.1949	0.1070	0.1760
	0.4750	1.0201	0.9229	2.9180	1.3790	0.7546	3.3691	0.4900	0.1616
	0.6595	0.0179	0.1890	0.4024	0.1070	0.4968	0.7905	0.8311	0.4662
	0.2704	0.0725	0.1366	0.1686	0.0262	0.0179	0.0173	0.9530	0.2935
	0.1183	0.0930	0.1272	1.9176	0.7266	0.7468	0.1449	0.2314	0.3791
	0.0524	0.0285	0.0420	1.9060	0.4325	0.3912	0.1625	0.2779	0.5752
	1.6348	0.2174	0.2424	0.6732	0.0785	0.0241	0.0817	2.8591	0.2624
	0.9732	0.1849	0.4758	1.9004	0.6657	0.2822	0.6770	0.2944	0.2556
	0.2224	0.0778	2.6197	0.9437	1.2462	0.5082	0.9985	0.5171	0.9216
	0.4416	0.1427	0.5742	0.1168	0.9437	4.4012	0.2158	2.4157	0.0923
	0.1847	3.6717	0.8130	1.6251	0.0000	0.0692	0.1038	0.5208	1.0418
	0.9298	0.0671	0.0838	0.1257	0.2845	3.0853	0.3571	1.6645	0.8996
	0.1342	0.1257	0.2932	0.5691	1.0456	5.8375	0.8997	4.2286	11.2457
	22.4016	0.0000	0.0487	0.0731	0.1374	0.2748	8.9147	0.0148	0.1147
	0.1365	0.1335	0.3115	0.0297	0.1868	0.3156	0.3115	0.5786	0.8349
	1.2523	0.1432	0.2864	1.5099	0.5084	0.6867	0.4875	1.3050	1.0534
10000.	2.1519	0.2425	0.3618	0.2349	1.3961	0.5431	0.6918	1.3246	0.7642
	0.2455	0.2537	0.1680	0.0091	0.1681	0.1317	0.2010	0.1087	0.1771
	0.4774	1.0238	0.9309	2.9475	1.3836	0.7642	3.4134	0.4909	0.1680
	0.6754	0.0181	0.1917	0.4080	0.1087	0.5107	0.8237	0.8533	0.4708
	0.2738	0.0732	0.1396	0.1715	0.0264	0.0191	0.0184	0.9611	0.2924
	0.1175	0.0932	0.1249	1.9818	0.7341	0.7551	0.1464	0.2362	0.3861
	0.0529	0.0303	0.0448	1.9222	0.4307	0.3892	0.1618	0.2743	0.5821
	1.6516	0.2196	0.2464	0.6869	0.0793	0.0256	0.0869	2.8834	0.2608
	0.9691	0.1812	0.4730	1.8940	0.6694	0.2912	0.6832	0.2937	0.2668
	0.2289	0.0752	2.6473	0.9469	1.2573	0.5128	1.0041	0.5208	0.9408
	0.4406	0.1463	0.5973	0.1128	0.9469	4.4442	0.2178	2.4374	0.0926
	0.1852	3.6630	0.8314	1.6615	0.0000	0.0695	0.1043	0.5138	1.0278
	0.9393	0.0707	0.0867	0.1301	0.2816	3.1251	0.3565	1.6664	0.9025
	0.1413	0.1301	0.3035	0.5631	1.0529	5.9079	0.9026	4.2351	11.4153
	22.7228	0.0000	0.0480	0.0720	0.1348	0.2696	8.9162	0.0149	0.1154
	0.1383	0.1296	0.2985	0.0298	0.1890	0.3184	0.2985	0.5577	0.8349
	1.2523	0.1421	0.2842	1.5143	0.5100	0.6872	0.4877	1.3080	1.0664
11000.	2.1796	0.2432	0.3631	0.2366	1.4102	0.5468	0.6942	1.3416	0.7736
	0.2456	0.2585	0.1741	0.0092	0.1701	0.1333	0.2073	0.1109	0.1783
	0.4798	1.0278	0.9382	2.9759	1.3883	0.7736	3.4567	0.4913	0.1741
	0.6911	0.0184	0.1940	0.4128	0.1109	0.5255	0.8555	0.8733	0.4752
	0.2769	0.0738	0.1420	0.1737	0.0267	0.0202	0.0195	0.9692	0.2912
	0.1167	0.0938	0.1234	2.0417	0.7411	0.7630	0.1476	0.2398	0.3914
	0.0533	0.0321	0.0474	1.9385	0.4287	0.3871	0.1619	0.2725	0.5886
	1.6676	0.2214	0.2494	0.6975	0.0800	0.0272	0.0921	2.9077	0.2590
	0.9647	0.1787	0.4730	1.8889	0.6720	0.3007	0.6899	0.2929	0.2771
	0.2350	0.0728	2.6733	0.9491	1.2696	0.5183	1.0080	0.5248	0.9611
	0.4394	0.1497	0.6185	0.1093	0.9492	4.4842	0.2204	2.4616	0.0929
	0.1858	3.6506	0.8492	1.6968	0.0000	0.0696	0.1044	0.5080	1.0162
	0.9483	0.0734	0.0890	0.1336	0.2790	3.1615	0.3547	1.6691	0.9062
	0.1469	0.1336	0.3116	0.5581	1.0581	5.9712	0.9063	4.2441	11.5768
	23.0270	0.0000	0.0473	0.0709	0.1327	0.2654	8.9161	0.0150	0.1155
	0.1392	0.1266	0.2874	0.0299	0.1901	0.3193	0.2874	0.5406	0.8355
	1.2532	0.1413	0.2826	1.5191	0.5124	0.6888	0.4886	1.3130	1.0808

TABLE 2—*Continued*

Temp (K)									
12000.	2.2021	0.2439	0.3645	0.2382	1.4240	0.5501	0.6966	1.3582	0.7827
	0.2456	0.2632	0.1801	0.0093	0.1719	0.1347	0.2136	0.1135	0.1793
	0.4821	1.0317	0.9449	3.0032	1.3932	0.7827	3.4992	0.4912	0.1801
	0.7065	0.0186	0.1961	0.4171	0.1135	0.5406	0.8855	0.8910	0.4793
	0.2797	0.0743	0.1438	0.1753	0.0268	0.0213	0.0206	0.9774	0.2900
	0.1159	0.0949	0.1227	2.0969	0.7478	0.7703	0.1487	0.2427	0.3956
	0.0537	0.0338	0.0500	1.9548	0.4268	0.3850	0.1629	0.2722	0.5946
	1.6826	0.2230	0.2518	0.7056	0.0805	0.0287	0.0971	2.9322	0.2574
	0.9603	0.1773	0.4753	1.8848	0.6738	0.3104	0.6969	0.2921	0.2865
	0.2406	0.0707	2.6980	0.9507	1.2831	0.5248	1.0107	0.5290	0.9819
	0.4381	0.1528	0.6379	0.1061	0.9507	4.5220	0.2235	2.4883	0.0933
	0.1865	3.6354	0.8664	1.7308	0.0000	0.0696	0.1044	0.5034	1.0070
	0.9569	0.0756	0.0908	0.1362	0.2768	3.1953	0.3522	1.6728	0.9107
	0.1512	0.1362	0.3178	0.5537	1.0618	6.0290	0.9108	4.2560	11.7304
	23.3152	0.0000	0.0465	0.0697	0.1311	0.2621	8.9149	0.0150	0.1152
	0.1394	0.1243	0.2780	0.0300	0.1904	0.3189	0.2780	0.5267	0.8365
	1.2547	0.1409	0.2818	1.5244	0.5154	0.6913	0.4902	1.3197	1.0962
13000.	2.2203	0.2446	0.3657	0.2396	1.4373	0.5528	0.6991	1.3746	0.7917
	0.2454	0.2679	0.1860	0.0094	0.1735	0.1361	0.2197	0.1163	0.1803
	0.4842	1.0353	0.9509	3.0294	1.3983	0.7917	3.5409	0.4908	0.1860
	0.7219	0.0188	0.1980	0.4211	0.1163	0.5557	0.9137	0.9067	0.4832
	0.2824	0.0748	0.1452	0.1766	0.0270	0.0224	0.0216	0.9855	0.2888
	0.1152	0.0962	0.1225	2.1473	0.7541	0.7773	0.1495	0.2448	0.3988
	0.0540	0.0355	0.0525	1.9711	0.4249	0.3830	0.1644	0.2730	0.6003
	1.6968	0.2243	0.2536	0.7118	0.0810	0.0301	0.1019	2.9566	0.2558
	0.9561	0.1768	0.4793	1.8813	0.6750	0.3201	0.7040	0.2912	0.2951
	0.2458	0.0688	2.7216	0.9518	1.2976	0.5320	1.0125	0.5333	1.0028
	0.4367	0.1556	0.6558	0.1033	0.9519	4.5581	0.2271	2.5173	0.0937
	0.1873	3.6181	0.8829	1.7636	0.0000	0.0695	0.1043	0.4998	0.9998
	0.9652	0.0773	0.0922	0.1383	0.2749	3.2268	0.3492	1.6776	0.9160
	0.1545	0.1383	0.3228	0.5498	1.0646	6.0824	0.9161	4.2708	11.8767
	23.5883	0.0000	0.0457	0.0685	0.1299	0.2597	8.9129	0.0151	0.1146
	0.1392	0.1226	0.2701	0.0301	0.1900	0.3178	0.2701	0.5154	0.8378
	1.2567	0.1408	0.2816	1.5300	0.5189	0.6946	0.4923	1.3277	1.1123
14000.	2.2349	0.2453	0.3668	0.2408	1.4502	0.5551	0.7018	1.3906	0.8005
	0.2451	0.2727	0.1918	0.0095	0.1750	0.1373	0.2256	0.1194	0.1812
	0.4861	1.0386	0.9562	3.0545	1.4035	0.8005	3.5818	0.4902	0.1918
	0.7372	0.0190	0.1998	0.4248	0.1194	0.5705	0.9400	0.9203	0.4869
	0.2850	0.0751	0.1462	0.1776	0.0271	0.0234	0.0226	0.9937	0.2877
	0.1144	0.0977	0.1228	2.1932	0.7600	0.7837	0.1503	0.2465	0.4012
	0.0543	0.0371	0.0549	1.9874	0.4231	0.3811	0.1664	0.2747	0.6056
	1.7101	0.2254	0.2550	0.7165	0.0814	0.0316	0.1065	2.9812	0.2543
	0.9521	0.1770	0.4846	1.8784	0.6757	0.3298	0.7111	0.2903	0.3030
	0.2506	0.0671	2.7445	0.9526	1.3131	0.5398	1.0136	0.5376	1.0236
	0.4354	0.1583	0.6721	0.1007	0.9527	4.5928	0.2310	2.5483	0.0941
	0.1881	3.5992	0.8989	1.7950	0.0000	0.0694	0.1041	0.4971	0.9943
	0.9731	0.0785	0.0934	0.1399	0.2732	3.2565	0.3461	1.6834	0.9219
	0.1570	0.1399	0.3266	0.5465	1.0668	6.1322	0.9221	4.2883	12.0161
	23.8473	0.0000	0.0449	0.0674	0.1291	0.2581	8.9102	0.0151	0.1139
	0.1388	0.1214	0.2635	0.0302	0.1893	0.3160	0.2635	0.5063	0.8394
	1.2591	0.1409	0.2819	1.5359	0.5227	0.6983	0.4949	1.3365	1.1285
15000.	2.2467	0.2459	0.3678	0.2419	1.4628	0.5570	0.7045	1.4063	0.8092
	0.2447	0.2774	0.1976	0.0096	0.1765	0.1385	0.2311	0.1226	0.1820
	0.4878	1.0415	0.9610	3.0785	1.4089	0.8092	3.6218	0.4894	0.1976
	0.7525	0.0192	0.2015	0.4284	0.1226	0.5849	0.9644	0.9321	0.4904
	0.2873	0.0755	0.1469	0.1784	0.0273	0.0243	0.0236	1.0019	0.2866
	0.1138	0.0994	0.1234	2.2347	0.7656	0.7898	0.1510	0.2477	0.4029
	0.0545	0.0387	0.0573	2.0038	0.4215	0.3793	0.1686	0.2770	0.6105
	1.7226	0.2264	0.2560	0.7199	0.0818	0.0329	0.1110	3.0057	0.2529
	0.9484	0.1776	0.4909	1.8758	0.6761	0.3392	0.7181	0.2894	0.3103
	0.2549	0.0656	2.7668	0.9534	1.3295	0.5480	1.0142	0.5419	1.0440
	0.4341	0.1607	0.6870	0.0984	0.9535	4.6265	0.2351	2.5812	0.0945
	0.1890	3.5793	0.9143	1.8252	0.0000	0.0693	0.1039	0.4951	0.9904
	0.9808	0.0794	0.0943	0.1411	0.2718	3.2846	0.3429	1.6903	0.9284
	0.1588	0.1412	0.3297	0.5435	1.0686	6.1791	0.9287	4.3085	12.1488
	24.0928	0.0000	0.0442	0.0663	0.1286	0.2572	8.9069	0.0152	0.1130
	0.1381	0.1207	0.2578	0.0303	0.1883	0.3139	0.2578	0.4991	0.8412
	1.2618	0.1413	0.2826	1.5421	0.5267	0.7025	0.4977	1.3459	1.1446

TABLE 2—*Continued*

Temp (K)									
16000.	2.2562	0.2464	0.3687	0.2429	1.4749	0.5585	0.7072	1.4218	0.8176
	0.2443	0.2822	0.2033	0.0097	0.1779	0.1397	0.2364	0.1259	0.1826
	0.4893	1.0440	0.9652	3.1016	1.4144	0.8176	3.6611	0.4886	0.2033
	0.7678	0.0195	0.2032	0.4319	0.1259	0.5986	0.9869	0.9423	0.4936
	0.2896	0.0758	0.1475	0.1789	0.0274	0.0252	0.0246	1.0100	0.2857
	0.1132	0.1012	0.1243	2.2721	0.7708	0.7955	0.1515	0.2485	0.4042
	0.0547	0.0401	0.0595	2.0202	0.4200	0.3778	0.1711	0.2798	0.6152
	1.7343	0.2273	0.2568	0.7223	0.0821	0.0342	0.1152	3.0303	0.2516
	0.9451	0.1786	0.4978	1.8735	0.6764	0.3483	0.7250	0.2885	0.3169
	0.2589	0.0642	2.7885	0.9540	1.3467	0.5564	1.0145	0.5461	1.0638
	0.4328	0.1629	0.7007	0.0963	0.9541	4.6593	0.2393	2.6154	0.0950
	0.1899	3.5586	0.9291	1.8543	0.0000	0.0692	0.1038	0.4937	0.9877
	0.9882	0.0800	0.0950	0.1421	0.2704	3.3115	0.3397	1.6981	0.9354
	0.1600	0.1421	0.3321	0.5409	1.0702	6.2236	0.9357	4.3310	12.2751
	24.3256	0.0000	0.0435	0.0652	0.1284	0.2568	8.9032	0.0152	0.1122
	0.1373	0.1202	0.2530	0.0304	0.1872	0.3117	0.2530	0.4935	0.8432
	1.2647	0.1418	0.2837	1.5484	0.5307	0.7070	0.5007	1.3557	1.1605
18000.	2.2696	0.2471	0.3700	0.2443	1.4983	0.5605	0.7130	1.4518	0.8339
	0.2434	0.2919	0.2146	0.0100	0.1806	0.1420	0.2457	0.1326	0.1836
	0.4914	1.0477	0.9723	3.1451	1.4260	0.8339	3.7375	0.4869	0.2146
	0.7984	0.0199	0.2065	0.4387	0.1326	0.6240	1.0269	0.9586	0.4995
	0.2936	0.0762	0.1480	0.1795	0.0275	0.0269	0.0263	1.0264	0.2841
	0.1122	0.1049	0.1265	2.3361	0.7803	0.8059	0.1525	0.2494	0.4056
	0.0551	0.0428	0.0636	2.0528	0.4176	0.3751	0.1765	0 2863	0.6236
	1.7556	0.2287	0.2576	0.7248	0.0826	0.0367	0.1228	3.0793	0.2495
	0.9395	0.1814	0.5128	1.8696	0.6764	0.3654	0.7380	0.2869	0.3286
	0.2658	0.0618	2.8308	0.9554	1.3828	0.5737	1.0146	0.5541	1.1010
	0.4303	0.1667	0.7248	0.0927	0.9555	4.7231	0.2477	2.6872	0.0959
	0.1918	3.5159	0.9570	1.9089	0.0000	0.0691	0.1036	0.4925	0.9851
	1.0020	0.0806	0.0961	0.1434	0.2681	3.3619	0.3338	1.7161	0.9505
	0.1612	0.1434	0.3355	0.5363	1.0733	6.3068	0.9509	4.3820	12.5098
	24.7555	0.0000	0.0422	0.0633	0.1288	0.2575	8.8949	0.0152	0.1104
	0.1355	0.1202	0.2456	0.0305	0.1847	0.3071	0.2456	0.4859	0.8474
	1.2710	0.1433	0.2866	1.5614	0.5390	0.7164	0.5072	1.3757	1.1907
20000.	2.2776	0.2475	0.3707	0.2453	1.5204	0.5615	0.7191	1.4807	0.8496
	0.2426	0.3016	0.2257	0.0102	0.1833	0.1442	0.2537	0.1390	0.1842
	0.4928	1.0500	0.9778	3.1856	1.4381	0.8496	3.8110	0.4852	0.2257
	0.8289	0.0204	0.2097	0.4452	0.1390	0.6465	1.0609	0.9705	0.5046
	0.2971	0.0766	0.1479	0.1797	0.0277	0.0283	0.0278	1.0426	0.2830
	0.1115	0.1086	0.1290	2.3880	0.7885	0.8149	0.1533	0.2494	0.4058
	0.0553	0.0451	0.0672	2.0854	0.4157	0.3732	0.1819	0.2933	0.6310
	1.7741	0.2299	0.2579	0.7249	0.0830	0.0389	0.1295	3.1281	0.2480
	0.9354	0.1847	0.5282	1.8663	0.6762	0.3808	0.7500	0.2854	0.3386
	0.2716	0.0598	2.8717	0.9570	1.4206	0.5911	1.0143	0.5615	1.1346
	0.4281	0.1699	0.7453	0.0897	0.9572	4.7851	0.2558	2.7617	0.0969
	0.1937	3.4729	0.9829	1.9595	0.0000	0.0691	0.1037	0.4925	0.9851
	1.0146	0.0806	0.0968	0.1441	0.2662	3.4089	0.3285	1.7368	0.9666
	0.1612	0.1441	0.3376	0.5324	1.0764	6.3839	0.9670	4.4393	12.7226
	25.1418	0.0000	0.0411	0.0616	0.1300	0.2598	8.8860	0.0153	0.1088
	0.1338	0.1209	0.2404	0.0305	0.1823	0.3029	0.2404	0.4821	0.8517
	1.2775	0.1451	0.2903	1.5745	0.5470	0.7259	0.5138	1.3953	1.2183
22000.	2.2816	0.2476	0.3710	0.2457	1.5414	0.5616	0.7254	1.5087	0.8647
	0.2419	0.3112	0.2366	0.0104	0.1858	0.1463	0.2604	0.1451	0.1845
	0.4934	1.0508	0.9822	3.2234	1.4508	0.8647	3.8821	0.4837	0.2366
	0.8590	0.0208	0.2127	0.4515	0.1451	0.6659	1.0898	0.9789	0.5090
	0.3002	0.0770	0.1475	0.1795	0.0278	0.0295	0.0292	1.0587	0.2822
	0.1110	0.1121	0.1316	2.4300	0.7957	0.8228	0.1540	0.2488	0.4052
	0.0555	0.0471	0.0703	2.1177	0.4145	0.3719	0.1872	0.3003	0.6375
	1.7902	0.2310	0.2576	0.7233	0.0833	0.0408	0.1352	3.1767	0.2470
	0.9326	0.1882	0.5431	1.8633	0.6759	0.3944	0.7608	0.2840	0.3471
	0.2763	0.0581	2.9116	0.9589	1.4593	0.6079	1.0138	0.5683	1.1646
	0.4260	0.1724	0.7628	0.0872	0.9592	4.8458	0.2634	2.8374	0.0979
	0.1957	3.4304	1.0070	2.0064	0.0000	0.0693	0.1040	0.4933	0.9867
	1.0261	0.0802	0.0973	0.1445	0.2646	3.4530	0.3238	1.7594	0.9832
	0.1605	0.1445	0.3391	0.5291	1.0797	6.4563	0.9838	4.5009	12.9153
	25.4889	0.0000	0.0401	0.0602	0.1316	0.2631	8.8768	0.0153	0.1075
	0.1322	0.1221	0.2368	0.0305	0.1801	0.2992	0.2368	0.4809	0.8561
	1.2841	0.1472	0.2943	1.5875	0.5546	0.7351	0.5202	1.4141	1.2430

TABLE 2—*Continued*

Temp (K)									
24000.	2.2829	0.2475	0.3708	0.2458	1.5615	0.5610	0.7320	1.5358	0.8792.
	0.2413	0.3206	0.2472	0.0106	0.1882	0.1483	0.2660	0.1508	0.1846
	0.4933	1.0504	0.9856	3.2589	1.4639	0.8792	3.9507	0.4825	0.2472
	0.8885	0.0213	0.2157	0.4574	0.1508	0.6828	1.1143	0.9848	0.5129
	0.3029	0.0773	0.1468	0.1790	0.0278	0.0305	0.0304	1.0747	0.2818
	0.1107	0.1154	0.1341	2.4641	0.8019	0.8297	0.1546	0.2478	0.4039
	0.0557	0.0488	0.0730	2.1497	0.4138	0.3711	0.1921	0.3070	0.6431
	1.8042	0.2319	0.2571	0.7206	0.0835	0.0425	0.1402	3.2248	0.2464
	0.9310	0.1915	0.5571	1.8603	0.6756	0.4065	0.7705	0.2828	0.3546
	0.2803	0.0567	2.9508	0.9613	1.4983	0.6241	1.0133	0.5744	1.1911
	0.4241	0.1745	0.7778	0.0851	0.9617	4.9053	0.2704	2.9131	0.0989
	0.1978	3.3891	1.0296	2.0500	0.0000	0.0696	0.1045	0.4945	0.9891
	1.0365	0.0796	0.0977	0.1446	0.2631	3.4949	0.3198	1.7833	1.0000
	0.1593	0.1446	0.3401	0.5262	1.0833	6.5249	1.0008	4.5653	13.0898
	25.8007	0.0000	0.0394	0.0591	0.1337	0.2671	8.8678	0.0153	0.1064
	0.1309	0.1236	0.2344	0.0305	0.1784	0.2963	0.2344	0.4816	0.8604
	1.2905	0.1493	0.2985	1.6004	0.5616	0.7440	0.5264	1.4318	1.2649
26000.	2.2820	0.2472	0.3704	0.2456	1.5808	0.5600	0.7387	1.5621	0.8932
	0.2408	0.3298	0.2574	0.0109	0.1905	0.1503	0.2706	0.1560	0.1844
	0.4928	1.0491	0.9882	3.2925	1.4774	0.8932	4.0172	0.4816	0.2574
	0.9170	0.0217	0.2184	0.4630	0.1560	0.6972	1.1353	0.9888	0.5161
	0.3053	0.0776	0.1460	0.1784	0.0279	0.0314	0.0314	1.0906	0.2816
	0.1106	0.1184	0.1365	2.4918	0.8072	0.8357	0.1552	0.2466	0.4023
	0.0558	0.0502	0.0753	2.1815	0.4135	0.3709	0.1967	0.3131	0.6481
	1.8162	0.2327	0.2563	0.7170	0.0837	0.0440	0.1443	3.2724	0.2462
	0.9304	0.1947	0.5701	1.8574	0.6753	0.4170	0.7791	0.2816	0.3612
	0.2837	0.0556	2.9891	0.9640	1.5370	0.6395	1.0129	0.5798	1.2144
	0.4224	0.1762	0.7910	0.0834	0.9645	4.9639	0.2768	2.9879	0.1000
	0.2000	3.3494	1.0508	2.0908	0.0000	0.0701	0.1051	0.4960	0.9920
	1.0459	0.0789	0.0981	0.1447	0.2619	3.5347	0.3163	1.8080	1.0168
	0.1578	0.1447	0.3409	0.5237	1.0872	6.5900	1.0177	4.6313	13.2479
	26.0808	0.0000	0.0388	0.0582	0.1360	0.2717	8.8592	0.0152	0.1056
	0.1299	0.1253	0.2330	0.0305	0.1770	0.2941	0.2330	0.4835	0.8645
	1.2967	0.1513	0.3027	1.6129	0.5682	0.7523	0.5323	1.4481	1.2842
28000.	2.2795	0.2466	0.3696	0.2452	1.5993	0.5586	0.7456	1.5876	0.9067
	0.2405	0.3386	0.2672	0.0111	0.1926	0.1520	0.2744	0.1607	0.1841
	0.4918	1.0469	0.9902	3.3244	1.4912	0.9068	4.0816	0.4810	0.2672
	0.9444	0.0222	0.2210	0.4683	0.1607	0.7095	1.1533	0.9914	0.5190
	0.3074	0.0779	0.1450	0.1777	0.0280	0.0321	0.0323	1.1062	0.2816
	0.1107	0.1212	0.1386	2.5145	0.8118	0.8408	0.1557	0.2451	0.4004
	0.0559	0.0514	0.0773	2.2128	0.4136	0.3710	0.2008	0.3187	0.6524
	1.8266	0.2336	0.2551	0.7130	0.0839	0.0453	0.1478	3.3195	0.2463
	0.9306	0.1976	0.5818	1.8544	0.6751	0.4261	0.7868	0.2806	0.3670
	0.2865	0.0546	3.0268	0.9671	1.5752	0.6539	1.0127	0.5846	1.2347
	0.4209	0.1776	0.8026	0.0820	0.9677	5.0216	0.2825	3.0612	0.1011
	0.2022	3.3114	1.0706	2.1289	0.0000	0.0706	0.1059	0.4975	0.9950
	1.0545	0.0781	0.0985	0.1447	0.2607	3.5727	0.3133	1.8331	1.0334
	0.1561	0.1447	0.3416	0.5215	1.0913	6.6521	1.0345	4.6978	13.3911
	26.3322	0.0000	0.0383	0.0574	0.1384	0.2766	8.8511	0.0152	0.1051
	0.1291	0.1271	0.2323	0.0305	0.1760	0.2925	0.2323	0.4864	0.8684
	1.3026	0.1534	0.3068	1.6251	0.5741	0.7600	0.5377	1.4632	1.3010
30000.	2.2758	0.2460	0.3686	0.2445	1.6171	0.5569	0.7526	1.6123	0.9197
	0.2403	0.3470	0.2766	0.0113	0.1946	0.1537	0.2776	0.1650	0.1836
	0.4905	1.0441	0.9917	3.3547	1.5052	0.9199	4.1442	0.4807	0.2766
	0.9706	0.0226	0.2234	0.4732	0.1650	0.7201	1.1688	0.9929	0.5214
	0.3092	0.0781	0.1440	0.1769	0.0280	0.0326	0.0331	1.1216	0.2818
	0.1109	0.1236	0.1406	2.5332	0.8158	0.8453	0.1563	0.2436	0.3983
	0.0560	0.0524	0.0790	2.2437	0.4140	0.3714	0.2045	0.3238	0.6562
	1.8355	0.2344	0.2543	0.7086	0.0841	0.0464	0.1507	3.3659	0.2467
	0.9314	0.2002	0.5923	1.8513	0.6750	0.4341	0.7935	0.2798	0.3722
	0.2888	0.0539	3.0638	0.9705	1.6126	0.6674	1.0125	0.5889	1.2525
	0.4196	0.1787	0.8129	0.0808	0.9712	5.0783	0.2875	3.1325	0.1023
	0.2045	3.2753	1.0893	2.1647	0.0000	0.0712	0.1068	0.4989	0.9979
	1.0624	0.0772	0.0988	0.1447	0.2597	3.6090	0.3107	1.8583	1.0497
	0.1544	0.1447	0.3423	0.5195	1.0956	6.7115	1.0510	4.7641	13.5206
	26.5576	0.0000	0.0379	0.0569	0.1410	0.2816	8.8435	0.0152	0.1049
	0.1286	0.1289	0.2321	0.0304	0.1753	0.2916	0.2321	0.4898	0.8722
	1.3082	0.1553	0.3107	1.6369	0.5796	0.7671	0.5427	1.4770	1.3157

TABLE 2—*Continued*

Temp (K)									
32000.	2.2711	0.2452	0.3674	0.2437	1.6343	0.5550	0.7597	1.6364	0.9323
	0.2403	0.3550	0.2854	0.0115	0.1964	0.1552	0.2801	0.1689	0.1830
	0.4889	1.0407	0.9929	3.3837	1.5194	0.9326	4.2049	0.4805	0.2854
	0.9953	0.0230	0.2256	0.4777	0.1689	0.7292	1.1821	0.9937	0.5234
	0.3108	0.0784	0.1430	0.1761	0.0281	0.0331	0.0338	1.1368	0.2822
	0.1111	0.1258	0.1423	2.5486	0.8191	0.8492	0.1569	0.2420	0.3962
	0.0561	0.0532	0.0805	2.2741	0.4145	0.3721	0.2078	0.3282	0.6595
	1.8431	0.2353	0.2532	0.7041	0.0842	0.0474	0.1532	3.4116	0.2473
	0.9327	0.2025	0.6016	1.8481	0.6750	0.4410	0.7994	0.2790	0.3770
	0.2909	0.0533	3.1000	0.9741	1.6490	0.6801	1.0125	0.5927	1.2679
	0.4185	0.1796	0.8221	0.0799	0.9749	5.1339	0.2920	3.2015	0.1034
	0.2069	3.2410	1.1070	2.1984	0.0000	0.0718	0.1077	0.5003	1.0006
	1.0697	0.0764	0.0992	0.1447	0.2588	3.6437	0.3085	1.8832	1.0655
	0.1527	0.1447	0.3431	0.5177	1.1000	6.7681	1.0671	4.8295	13.6378
	26.7594	0.0000	0.0377	0.0565	0.1436	0.2867	8.8363	0.0152	0.1048
	0.1283	0.1307	0.2322	0.0304	0.1749	0.2913	0.2322	0.4936	0.8756
	1.3134	0.1572	0.3144	1.6483	0.5846	0.7736	0.5473	1.4896	1.3284
34000.	2.2657	0.2443	0.3660	0.2428	1.6510	0.5530	0.7668	1.6598	0.9446
	0.2403	0.3625	0.2937	0.0117	0.1981	0.1566	0.2823	0.1724	0.1823
	0.4871	1.0369	0.9938	3.4115	1.5337	0.9449	4.2639	0.4805	0.2937
	1.0186	0.0233	0.2276	0.4818	0.1724	0.7369	1.1938	0.9939	0.5251
	0.3122	0.0787	0.1419	0.1753	0.0281	0.0335	0.0343	1.1516	0.2826
	0.1115	0.1277	0.1438	2.5614	0.8220	0.8526	0.1575	0.2404	0.3940
	0.0562	0.0539	0.0817	2.3039	0.4153	0.3730	0.2107	0.3322	0.6624
	1.8496	0.2362	0.2520	0.6995	0.0843	0.0483	0.1552	3.4564	0.2480
	0.9344	0.2045	0.6098	1.8448	0.6750	0.4470	0.8046	0.2783	0.3813
	0.2926	0.0528	3.1353	0.9778	1.6841	0.6918	1.0125	0.5960	1.2814
	0.4175	0.1803	0.8304	0.0792	0.9788	5.1884	0.2959	3.2678	0.1047
	0.2093	3.2086	1.1237	2.2300	0.0000	0.0725	0.1087	0.5015	1.0030
	1.0764	0.0755	0.0996	0.1448	0.2580	3.6768	0.3066	1.9076	1.0809
	0.1511	0.1448	0.3439	0.5160	1.1045	6.8220	1.0826	4.8934	13.7434
	26.9397	0.0000	0.0375	0.0563	0.1461	0.2917	8.8295	0.0152	0.1049
	0.1282	0.1325	0.2326	0.0303	0.1749	0.2914	0.2326	0.4976	0.8788
	1.3182	0.1589	0.3179	1.6592	0.5891	0.7795	0.5515	1.5011	1.3394
36000.	2.2596	0.2433	0.3646	0.2418	1.6670	0.5509	0.7740	1.6826	0.9565
	0.2403	0.3695	0.3014	0.0118	0.1996	0.1579	0.2840	0.1756	0.1815
	0.4851	1.0327	0.9945	3.4381	1.5480	0.9568	4.3213	0.4806	0.3014
	1.0404	0.0237	0.2294	0.4856	0.1756	0.7436	1.2039	0.9936	0.5266
	0.3134	0.0791	0.1409	0.1744	0.0282	0.0337	0.0348	1.1662	0.2831
	0.1119	0.1293	0.1450	2.5721	0.8245	0.8556	0.1581	0.2388	0.3918
	0.0563	0.0544	0.0828	2.3331	0.4161	0.3740	0.2132	0.3355	0.6650
	1.8551	0.2372	0.2509	0.6950	0.0845	0.0490	0.1568	3.5002	0.2488
	0.9362	0.2062	0.6169	1.8415	0.6752	0.4522	0.8092	0.2778	0.3852
	0.2941	0.0524	3.1698	0.9817	1.7179	0.7027	1.0127	0.5989	1.2931
	0.4166	0.1809	0.8380	0.0786	0.9828	5.2416	0.2994	3.3314	0.1059
	0.2118	3.1779	1.1394	2.2597	0.0000	0.0732	0.1098	0.5025	1.0051
	1.0827	0.0747	0.1000	0.1448	0.2573	3.7083	0.3050	1.9314	1.0956
	0.1495	0.1449	0.3447	0.5146	1.1090	6.8733	1.0976	4.9554	13.8386
	27.1001	0.0000	0.0374	0.0562	0.1486	0.2967	8.8228	0.0151	0.1052
	0.1283	0.1343	0.2332	0.0303	0.1750	0.2919	0.2332	0.5017	0.8817
	1.3226	0.1606	0.3211	1.6697	0.5932	0.7849	0.5553	1.5115	1.3489
38000.	2.2530	0.2423	0.3630	0.2407	1.6826	0.5487	0.7812	1.7048	0.9679
	0.2404	0.3761	0.3087	0.0120	0.2010	0.1590	0.2854	0.1784	0.1807
	0.4830	1.0283	0.9950	3.4637	1.5624	0.9683	4.3770	0.4809	0.3087
	1.0608	0.0240	0.2311	0.4890	0.1784	0.7493	1.2128	0.9931	0.5278
	0.3145	0.0794	0.1399	0.1736	0.0282	0.0340	0.0353	1.1803	0.2836
	0.1123	0.1308	0.1461	2.5810	0.8265	0.8581	0.1588	0.2373	0.3896
	0.0564	0.0549	0.0836	2.3615	0.4170	0.3750	0.2154	0.3384	0.6673
	1.8597	0.2382	0.2497	0.6905	0.0846	0.0496	0.1581	3.5430	0.2497
	0.9382	0.2077	0.6231	1.8381	0.6753	0.4567	0.8132	0.2773	0.3888
	0.2954	0.0521	3.2033	0.9856	1.7503	0.7128	1.0129	0.6016	1.3033
	0.4159	0.1814	0.8448	0.0782	0.9868	5.2933	0.3024	3.3921	0.1072
	0.2143	3.1488	1.1542	2.2877	0.0000	0.0739	0.1109	0.5033	1.0067
	1.0886	0.0740	0.1004	0.1450	0.2566	3.7382	0.3036	1.9544	1.1098
	0.1480	0.1450	0.3456	0.5132	1.1134	6.9220	1.1120	5.0151	13.9240
	27.2424	0.0000	0.0374	0.0561	0.1511	0.3015	8.8162	0.0151	0.1055
	0.1285	0.1359	0.2340	0.0302	0.1754	0.2928	0.2340	0.5058	0.8844
	1.3265	0.1621	0.3242	1.6796	0.5969	0.7898	0.5587	1.5208	1.3571

TABLE 2—*Continued*

Temp (K)									
40000.	2.2460	0.2412	0.3614	0.2395	1.6976	0.5464	0.7884	1.7263	0.9791
	0.2406	0.3822	0.3154	0.0121	0.2023	0.1600	0.2866	0.1810	0.1799
	0.4807	1.0237	0.9953	3.4884	1.5767	0.9795	4.4311	0.4811	0.3154
	1.0797	0.0242	0.2326	0.4921	0.1810	0.7542	1.2207	0.9924	0.5288
	0.3155	0.0797	0.1389	0.1727	0.0283	0.0341	0.0356	1.1941	0.2842
	0.1128	0.1321	0.1470	2.5885	0.8283	0.8603	0.1595	0.2357	0.3875
	0.0565	0.0552	0.0843	2.3891	0.4179	0.3761	0.2173	0.3409	0.6693
	1.8636	0.2392	0.2486	0.6862	0.0848	0.0502	0.1591	3.5845	0.2507
	0.9403	0.2089	0.6284	1.8346	0.6755	0.4606	0.8167	0.2769	0.3922
	0.2964	0.0519	3.2358	0.9895	1.7812	0.7221	1.0133	0.6038	1.3122
	0.4153	0.1817	0.8511	0.0779	0.9909	5.3434	0.3050	3.4497	0.1084
	0.2169	3.1211	1.1682	2.3140	0.0000	0.0746	0.1119	0.5040	1.0080
	1.0941	0.0733	0.1007	0.1451	0.2560	3.7665	0.3024	1.9764	1.1232
	0.1466	0.1451	0.3466	0.5120	1.1178	6.9679	1.1257	5.0724	14.0004
	27.3679	0.0000	0.0375	0.0562	0.1534	0.3062	8.8094	0.0151	0.1060
	0.1289	0.1375	0.2348	0.0302	0.1758	0.2939	0.2348	0.5098	0.8868
	1.3301	0.1635	0.3270	1.6891	0.6002	0.7941	0.5618	1.5292	1.3641

the intercombination transitions and afford useful electron density diagnostics.

The collision strengths are shown in Figure 2. As the transition is spin forbidden its collision strength decreases with increasing electron energy owing to the fact that the incident electron must exchange with the bound ionic electron for the transition to take place; unlikely at large impact parameters associated with higher energies. It is this fact that also makes the line ratio of the intercombination to dipole-allowed transition, $I(^2P^o\text{–}^4P)/I(^2P^o\text{–}^2D)$, a useful temperature diagnostic since the collision strength for the dipole-allowed transition increases with incident electron energy (see next section). The effective collision strength for the ^4P state is also significantly enhanced by the autoionizing resonances.

3.3. *Dipole-allowed Transitions*

The boron-like ions have three dipole-allowed transitions lying energetically close together: $^2P^o\text{–}^2D$, $^2P^o\text{–}^2S$, and $^2P^o\text{–}^2P$. While the resonance transition, $2\,P^o\text{–}^2D$, is the more prominent, the excitation of the other two upper states is nonnegligible, and lines are often observed from all three allowed transitions. It has been shown by Luo & Pradhan (1990) that the coupling among the excited states needs to be included in order to obtain accurate cross sections for any one of them (the simple Gaunt Factor formula for the resonance transition gives a value about a factor of 2 lower).

Figures 3, 4, and 5 give the collision strengths for the three dipole transitions in C II, N III, and O IV, respectively. Characteristic of the allowed transition is the energy behavior of the collision strength which increases with electron energy in accordance with the Bethe form, $\Omega \sim a \ln E$. The $^2P^o\text{–}^2D$ transition in all three ions shows a rather large resonance structure due to a number of autoionizing resonances in the near threshold region, and we expect it to enhance the effective rate coefficient. The collision strengths for the $^2P^o\text{–}^2S$ and the $^2P^o\text{–}^2P$ transitions also show strong resonance features in the near-threshold region for N III and O IV (for C II the $^2P^o\text{–}^2P$ collision strength does not seem to be appreciably affected). The significant resonance enhancement of the dipole-allowed transitions is important since it is normally assumed that only the forbidden transitions are so affected. While that is generally the case, the boron-like ions are exceptional due to the strong coupling of several excited states to the ground state, which also accounts for the presence of strong resonance features.

3.4. *Collisional Mixing*

As mentioned earlier, collisions between excited fine-structure sublevels is likely to produce appreciable mixing of level populations. The collisional cross sections for fine-structure transitions among the excited states are thus needed to produce a full radiative-collisional model for the observed line intensities (e.g., Keenan et al. 1986). In the present work we have explicitly considered a relatively large number of excited states and the data should be sufficient for constructing such a model for all three ions.

One of the primary modes for collisional mixing will be among the three fine-structure levels of the metastable state, $^4P_{1/2,3/2,5/2}$. In Figure 6 we present the collision strength for the strongest of the three transitions, the $^4P_{3/2}\text{–}^4P_{5/2}$. Once again we observe significant resonance enhancement. We should also like to point out that the accuracy of the collision strengths for the fine-structure transitions is crucially dependent on the accuracy of the *LS* coupling calculations. The present calculations were carried out with a code that is directly interfaced with *R*-matrix scattering codes, and thus it was readily possible to obtain the fine-structure values at a fine mesh to delineate the extensive resonance structures.

4. RATE COEFFICIENTS

The Maxwellian-averaged collision strength, also known as the effective collision strength, is given by

$$\gamma_{ij} = \int_0^\infty \Omega_{ij} e^{-\epsilon_j/kT} d(\epsilon_j/kT)\,, \qquad (1)$$

where Ω_{ij} is the collision strength for excitation from level i to level j, averaged over a Maxwellian distribution of incident electron energies ϵ_j above the excitation threshold of the level j, at temperature T. This smoothly varying function of temperature can then be used to obtain the rate coefficient, q_{ij}, for

TABLE 3

MAXWELLIAN-AVERAGED COLLISION STRENGTHS FOR N III

Temp (K)	TRANSITION KEY								
	1 2	1 3	1 4	1 5	1 6	1 7	1 8	1 9	1 10
	1 11	1 12	1 13	1 14	1 15	2 3	2 4	2 5	2 6
	2 7	2 8	2 9	2 10	2 11	2 12	2 13	2 14	2 15
	3 4	3 5	3 6	3 7	3 8	3 9	3 10	3 11	3 12
	3 13	3 14	3 15	4 5	4 6	4 7	4 8	4 9	4 10
	4 11	4 12	4 13	4 14	4 15	5 6	5 7	5 8	5 9
	5 10	5 11	5 12	5 13	5 14	5 15	6 7	6 8	6 9
	6 10	6 11	6 12	6 13	6 14	6 15	7 8	7 9	7 10
	7 11	7 12	7 13	7 14	7 15	8 9	8 10	8 11	8 12
	8 13	8 14	8 15	9 10	9 11	9 12	9 13	9 14	9 15
	10 11	10 12	10 13	10 14	10 15	11 12	11 13	11 14	11 15
	12 13	12 14	12 15	13 14	13 15	14 15			
1000.	1.2896	0.1930	0.2835	0.1691	1.6362	0.4282	0.6885	1.8968	1.0463
	0.0036	0.1276	0.0901	0.0142	0.0781	0.1298	0.3621	0.7994	0.8411
	3.2877	1.3769	1.0463	4.8400	0.0073	0.1337	0.3017	0.0781	0.1064
	0.9613	0.5651	0.4942	0.3087	0.0908	0.3178	0.2604	1.2311	0.1934
	0.0524	0.0544	0.0393	1.7615	0.7807	0.8250	0.1815	0.4855	0.6708
	2.4621	0.2726	0.2188	0.0810	0.1065	0.6520	1.7566	0.2723	0.3531
	1.3815	3.6932	0.1237	0.6134	0.0520	0.2292	1.0962	0.5668	0.6782
	0.9067	0.0201	3.4628	0.8509	1.4319	0.4109	0.8503	0.6425	1.7348
	0.0302	0.8509	5.6194	0.1037	2.6603	0.1012	0.2023	0.0000	0.0432
	0.0648	0.6573	1.3147	1.7995	0.2036	3.8132	0.1710	1.8985	0.9793
	0.4072	0.9678	6.9982	0.9793	4.7758	0.8338	1.2506	0.1921	0.3842
	1.6170	0.5217	0.7315	0.5226	1.3569	0.5398			
2000.	1.2857	0.1909	0.2812	0.1705	1.7072	0.5357	0.6938	1.9133	1.0587
	0.0039	0.1257	0.0888	0.0140	0.0782	0.1304	0.3614	0.7933	0.9843
	3.5016	1.3877	1.0587	4.8854	0.0079	0.1317	0.2973	0.0782	0.1062
	0.9571	0.5678	0.4966	0.3122	0.0922	0.2555	0.2382	1.2409	0.1994
	0.0580	0.0545	0.0393	1.7604	0.7854	0.8320	0.1845	0.4018	0.5854
	2.4817	0.2831	0.2317	0.0811	0.1065	0.6590	1.7672	0.2767	0.3299
	1.1509	3.7225	0.1353	0.6369	0.0520	0.2293	1.1511	0.5626	0.8842
	0.9623	0.0489	3.4470	0.8412	1.4380	0.4122	0.8439	0.6545	2.1151
	0.0734	0.8412	5.5908	0.1038	2.6715	0.0931	0.1862	0.0000	0.0471
	0.0707	0.6601	1.3202	1.7154	0.2464	3.7964	0.1860	1.9056	0.9828
	0.4928	0.9824	6.9795	0.9828	4.7935	0.8450	1.2674	0.1927	0.3853
	1.6490	0.5219	0.7322	0.5232	1.3578	0.5417			
3000.	1.2871	0.1882	0.2781	0.1713	1.7445	0.5596	0.6962	1.9175	1.0685
	0.0040	0.1246	0.0885	0.0139	0.0782	0.1306	0.3596	0.7852	1.0204
	3.5878	1.3924	1.0685	4.9034	0.0081	0.1311	0.2951	0.0782	0.1060
	0.9687	0.5797	0.4964	0.3104	0.0920	0.2246	0.2242	1.2479	0.2021
	0.0606	0.0545	0.0393	1.7882	0.7844	0.8292	0.1840	0.3592	0.5384
	2.4957	0.2877	0.2375	0.0811	0.1065	0.6555	1.7649	0.2760	0.3138
	1.0325	3.7435	0.1405	0.6473	0.0520	0.2293	1.1872	0.5567	1.2085
	1.0897	0.0724	3.4483	0.8452	1.4432	0.4133	0.8351	0.7067	2.7407
	0.1085	0.8452	5.5948	0.1039	2.6808	0.0935	0.1869	0.0000	0.0525
	0.0787	0.6624	1.3248	1.7084	0.2722	3.7914	0.2024	1.9114	0.9857
	0.5445	1.0012	6.9833	0.9857	4.8080	0.8537	1.2805	0.1931	0.3861
	1.6760	0.5219	0.7324	0.5233	1.3578	0.5432			
4000.	1.2976	0.1879	0.2784	0.1741	1.7651	0.5593	0.6969	1.9108	1.0721
	0.0041	0.1239	0.0885	0.0138	0.0782	0.1323	0.3619	0.7864	1.0242
	3.6247	1.3939	1.0721	4.8937	0.0081	0.1310	0.2938	0.0782	0.1057
	0.9904	0.5959	0.4968	0.3085	0.0917	0.2072	0.2148	1.2529	0.2030
	0.0615	0.0544	0.0393	1.8323	0.7840	0.8267	0.1835	0.3346	0.5095
	2.5059	0.2894	0.2396	0.0811	0.1065	0.6520	1.7641	0.2752	0.3023
	0.9640	3.7588	0.1424	0.6512	0.0520	0.2293	1.2191	0.5540	1.4937
	1.2136	0.0872	3.4549	0.8538	1.4481	0.4143	0.8310	0.7624	3.2985
	0.1308	0.8538	5.6090	0.1039	2.6896	0.0962	0.1925	0.0000	0.0575
	0.0862	0.6645	1.3291	1.7248	0.2883	3.7897	0.2189	1.9167	0.9884
	0.5765	1.0206	6.9929	0.9884	4.8215	0.8602	1.2902	0.1935	0.3869
	1.6938	0.5217	0.7324	0.5234	1.3576	0.5446			
5000.	1.3163	0.1889	0.2806	0.1780	1.7791	0.5551	0.6968	1.8999	1.0716
	0.0041	0.1233	0.0887	0.0136	0.0782	0.1349	0.3669	0.7933	1.0219
	3.6464	1.3936	1.0716	4.8715	0.0082	0.1311	0.2929	0.0782	0.1054
	1.0145	0.6121	0.4979	0.3073	0.0915	0.1965	0.2081	1.2569	0.2033
	0.0617	0.0544	0.0393	1.8791	0.7848	0.8255	0.1831	0.3191	0.4903
	2.5138	0.2899	0.2402	0.0810	0.1065	0.6497	1.7658	0.2746	0.2937
	0.9203	3.7707	0.1429	0.6523	0.0520	0.2292	1.2510	0.5537	1.6956
	1.3062	0.0964	3.4632	0.8631	1.4527	0.4153	0.8306	0.8059	3.6968
	0.1447	0.8631	5.6261	0.1040	2.6981	0.0995	0.1990	0.0000	0.0617
	0.0926	0.6666	1.3332	1.7381	0.2987	3.7906	0.2336	1.9218	0.9910
	0.5973	1.0385	7.0056	0.9910	4.8343	0.8648	1.2972	0.1938	0.3876
	1.7054	0.5215	0.7324	0.5235	1.3572	0.5460			

TABLE 3—*Continued*

Temp (K)									
6000.	1.3403	0.1905	0.2838	0.1826	1.7899	0.5516	0.6963	1.8888	1.0690
	0.0041	0.1229	0.0888	0.0135	0.0782	0.1380	0.3732	0.8029	1.0199
	3.6630	1.3926	1.0690	4.8467	0.0082	0.1312	0.2923	0.0782	0.1051
	1.0372	0.6267	0.4991	0.3065	0.0914	0.1894	0.2032	1.2601	0.2033
	0.0616	0.0544	0.0393	1.9223	0.7860	0.8253	0.1828	0.3086	0.4767
	2.5203	0.2899	0.2401	0.0810	0.1064	0.6485	1.7685	0.2742	0.2873
	0.8907	3.7804	0.1427	0.6522	0.0520	0.2291	1.2831	0.5551	1.8249
	1.3684	0.1021	3.4720	0.8716	1.4573	0.4162	0.8326	0.8362	3.9537
	0.1531	0.8717	5.6436	0.1040	2.7063	0.1029	0.2059	0.0000	0.0651
	0.0977	0.6686	1.3372	1.7433	0.3053	3.7933	0.2458	1.9268	0.9934
	0.6107	1.0537	7.0196	0.9934	4.8467	0.8682	1.3023	0.1942	0.3883
	1.7131	0.5212	0.7324	0.5234	1.3567	0.5472			
7000.	1.3667	0.1924	0.2874	0.1875	1.7988	0.5495	0.6957	1.8790	1.0658
	0.0041	0.1226	0.0889	0.0133	0.0782	0.1412	0.3799	0.8135	1.0191
	3.6773	1.3913	1.0658	4.8239	0.0082	0.1312	0.2918	0.0782	0.1048
	1.0572	0.6394	0.5002	0.3061	0.0914	0.1845	0.1996	1.2629	0.2032
	0.0614	0.0544	0.0393	1.9602	0.7872	0.8255	0.1827	0.3012	0.4669
	2.5258	0.2896	0.2396	0.0809	0.1063	0.6478	1.7712	0.2741	0.2824
	0.8698	3.7888	0.1423	0.6515	0.0519	0.2290	1.3147	0.5573	1.9019
	1.4077	0.1054	3.4808	0.8790	1.4618	0.4172	0.8360	0.8561	4.1083
	0.1581	0.8790	5.6604	0.1040	2.7144	0.1066	0.2132	0.0000	0.0677
	0.1016	0.6705	1.3411	1.7422	0.3095	3.7974	0.2554	1.9316	0.9958
	0.6189	1.0660	7.0338	0.9958	4.8589	0.8707	1.3060	0.1945	0.3890
	1.7182	0.5210	0.7323	0.5234	1.3562	0.5484			
8000.	1.3937	0.1944	0.2910	0.1923	1.8062	0.5485	0.6950	1.8710	1.0627
	0.0041	0.1223	0.0890	0.0131	0.0783	0.1445	0.3866	0.8242	1.0194
	3.6900	1.3900	1.0627	4.8046	0.0082	0.1312	0.2913	0.0783	0.1045
	1.0745	0.6502	0.5010	0.3059	0.0913	0.1810	0.1968	1.2654	0.2030
	0.0611	0.0543	0.0392	1.9927	0.7882	0.8257	0.1827	0.2959	0.4597
	2.5308	0.2891	0.2390	0.0809	0.1063	0.6475	1.7734	0.2740	0.2787
	0.8547	3.7963	0.1417	0.6506	0.0519	0.2288	1.3452	0.5599	1.9439
	1.4312	0.1073	3.4893	0.8851	1.4662	0.4180	0.8399	0.8687	4.1939
	0.1609	0.8851	5.6762	0.1040	2.7223	0.1106	0.2213	0.0000	0.0697
	0.1045	0.6725	1.3449	1.7372	0.3118	3.8022	0.2627	1.9364	0.9982
	0.6236	1.0758	7.0476	0.9982	4.8708	0.8724	1.3086	0.1948	0.3896
	1.7214	0.5207	0.7322	0.5234	1.3557	0.5495			
9000.	1.4200	0.1962	0.2945	0.1969	1.8125	0.5481	0.6945	1.8647	1.0598
	0.0041	0.1220	0.0890	0.0130	0.0783	0.1476	0.3931	0.8346	1.0203
	3.7010	1.3889	1.0598	4.7891	0.0082	0.1311	0.2908	0.0783	0.1042
	1.0891	0.6595	0.5016	0.3058	0.0913	0.1783	0.1948	1.2677	0.2027
	0.0607	0.0543	0.0392	2.0204	0.7889	0.8260	0.1827	0.2919	0.4544
	2.5355	0.2886	0.2383	0.0808	0.1062	0.6473	1.7750	0.2740	0.2760
	0.8434	3.8032	0.1410	0.6494	0.0518	0.2286	1.3739	0.5626	1.9630
	1.4442	0.1081	3.4974	0.8900	1.4705	0.4189	0.8439	0.8763	4.2344
	0.1622	0.8901	5.6908	0.1040	2.7301	0.1152	0.2303	0.0000	0.0710
	0.1065	0.6744	1.3487	1.7304	0.3129	3.8075	0.2680	1.9411	1.0005
	0.6259	1.0832	7.0606	1.0005	4.8825	0.8737	1.3105	0.1951	0.3902
	1.7232	0.5204	0.7320	0.5233	1.3551	0.5505			
10000.	1.4454	0.1979	0.2978	0.2013	1.8179	0.5481	0.6940	1.8599	1.0574
	0.0041	0.1218	0.0889	0.0128	0.0783	0.1506	0.3992	0.8442	1.0213
	3.7107	1.3880	1.0574	4.7771	0.0081	0.1310	0.2903	0.0783	0.1039
	1.1015	0.6675	0.5020	0.3057	0.0914	0.1763	0.1933	1.2699	0.2024
	0.0604	0.0542	0.0391	2.0440	0.7893	0.8261	0.1828	0.2889	0.4504
	2.5399	0.2880	0.2375	0.0807	0.1061	0.6472	1.7760	0.2741	0.2740
	0.8349	3.8099	0.1402	0.6481	0.0518	0.2284	1.4006	0.5652	1.9674
	1.4503	0.1083	3.5052	0.8939	1.4748	0.4198	0.8478	0.8807	4.2460
	0.1624	0.8940	5.7044	0.1040	2.7378	0.1201	0.2402	0.0000	0.0718
	0.1077	0.6762	1.3524	1.7231	0.3132	3.8132	0.2716	1.9457	1.0028
	0.6264	1.0887	7.0727	1.0028	4.8940	0.8746	1.3119	0.1954	0.3907
	1.7240	0.5202	0.7319	0.5232	1.3546	0.5516			
11000.	1.4694	0.1995	0.3007	0.2054	1.8224	0.5482	0.6937	1.8563	1.0554
	0.0041	0.1215	0.0888	0.0127	0.0783	0.1533	0.4049	0.8530	1.0223
	3.7189	1.3874	1.0554	4.7680	0.0081	0.1309	0.2898	0.0783	0.1037
	1.1119	0.6744	0.5022	0.3056	0.0914	0.1747	0.1922	1.2721	0.2021
	0.0600	0.0542	0.0391	2.0641	0.7896	0.8262	0.1829	0.2866	0.4473
	2.5442	0.2874	0.2367	0.0807	0.1059	0.6471	1.7765	0.2743	0.2726
	0.8283	3.8164	0.1394	0.6468	0.0517	0.2281	1.4251	0.5676	1.9626
	1.4520	0.1080	3.5127	0.8970	1.4790	0.4206	0.8514	0.8829	4.2391
	0.1620	0.8971	5.7171	0.1040	2.7454	0.1254	0.2509	0.0000	0.0723
	0.1084	0.6781	1.3561	1.7160	0.3128	3.8190	0.2739	1.9503	1.0050
	0.6257	1.0926	7.0840	1.0051	4.9055	0.8752	1.3128	0.1957	0.3913
	1.7241	0.5199	0.7317	0.5231	1.3541	0.5525			

TABLE 3—*Continued*

Temp (K)									
12000.	1.4922	0.2009	0.3034	0.2091	1.8263	0.5483	0.6935	1.8539	1.0538
	0.0040	0.1213	0.0887	0.0126	0.0783	0.1558	0.4100	0.8610	1.0232
	3.7260	1.3869	1.0538	4.7615	0.0081	0.1307	0.2893	0.0783	0.1035
	1.1207	0.6804	0.5023	0.3056	0.0915	0.1735	0.1914	1.2742	0.2017
	0.0596	0.0541	0.0391	2.0813	0.7896	0.8261	0.1830	0.2847	0.4450
	2.5485	0.2868	0.2358	0.0806	0.1058	0.6470	1.7766	0.2745	0.2716
	0.8230	3.8228	0.1386	0.6454	0.0517	0.2278	1.4475	0.5699	1.9520
	1.4508	0.1073	3.5199	0.8994	1.4832	0.4214	0.8548	0.8837	4.2206
	0.1610	0.8995	5.7290	0.1040	2.7529	0.1311	0.2621	0.0000	0.0724
	0.1086	0.6799	1.3598	1.7095	0.3121	3.8248	0.2751	1.9548	1.0073
	0.6241	1.0953	7.0946	1.0074	4.9168	0.8756	1.3134	0.1959	0.3918
	1.7235	0.5196	0.7316	0.5231	1.3536	0.5534			
13000.	1.5139	0.2021	0.3058	0.2126	1.8296	0.5482	0.6934	1.8522	1.0526
	0.0040	0.1211	0.0886	0.0125	0.0783	0.1581	0.4147	0.8681	1.0238
	3.7319	1.3867	1.0526	4.7571	0.0080	0.1305	0.2887	0.0783	0.1033
	1.1282	0.6857	0.5022	0.3055	0.0916	0.1724	0.1908	1.2763	0.2014
	0.0592	0.0540	0.0390	2.0961	0.7895	0.8260	0.1832	0.2832	0.4432
	2.5528	0.2862	0.2350	0.0804	0.1057	0.6469	1.7764	0.2748	0.2708
	0.8188	3.8291	0.1378	0.6439	0.0516	0.2275	1.4678	0.5719	1.9378
	1.4478	0.1065	3.5268	0.9011	1.4873	0.4222	0.8579	0.8835	4.1949
	0.1597	0.9013	5.7402	0.1040	2.7603	0.1369	0.2738	0.0000	0.0723
	0.1085	0.6817	1.3634	1.7036	0.3109	3.8308	0.2754	1.9593	1.0095
	0.6219	1.0969	7.1045	1.0096	4.9280	0.8759	1.3138	0.1962	0.3923
	1.7225	0.5194	0.7315	0.5230	1.3531	0.5543			
14000.	1.5345	0.2032	0.3079	0.2157	1.8325	0.5480	0.6934	1.8513	1.0518
	0.0040	0.1208	0.0884	0.0125	0.0784	0.1602	0.4189	0.8745	1.0241
	3.7368	1.3867	1.0518	4.7544	0.0080	0.1303	0.2882	0.0784	0.1032
	1.1346	0.6904	0.5021	0.3055	0.0917	0.1715	0.1904	1.2785	0.2010
	0.0588	0.0540	0.0389	2.1090	0.7893	0.8258	0.1834	0.2819	0.4418
	2.5570	0.2855	0.2341	0.0803	0.1055	0.6467	1.7759	0.2751	0.2703
	0.8152	3.8355	0.1370	0.6425	0.0515	0.2272	1.4863	0.5738	1.9215
	1.4435	0.1055	3.5336	0.9024	1.4914	0.4230	0.8607	0.8827	4.1649
	0.1582	0.9026	5.7509	0.1040	2.7677	0.1428	0.2856	0.0000	0.0720
	0.1080	0.6835	1.3669	1.6984	0.3096	3.8367	0.2751	1.9638	1.0117
	0.6192	1.0977	7.1138	1.0118	4.9392	0.8760	1.3140	0.1964	0.3928
	1.7212	0.5192	0.7313	0.5229	1.3526	0.5552			
15000.	1.5541	0.2041	0.3098	0.2185	1.8349	0.5475	0.6935	1.8510	1.0511
	0.0040	0.1206	0.0882	0.0124	0.0784	0.1621	0.4226	0.8800	1.0240
	3.7409	1.3869	1.0511	4.7531	0.0080	0.1300	0.2876	0.0784	0.1032
	1.1400	0.6946	0.5018	0.3054	0.0918	0.1706	0.1900	1.2806	0.2007
	0.0584	0.0539	0.0389	2.1202	0.7890	0.8256	0.1836	0.2808	0.4405
	2.5613	0.2849	0.2332	0.0802	0.1053	0.6466	1.7752	0.2754	0.2699
	0.8120	3.8419	0.1362	0.6410	0.0514	0.2268	1.5031	0.5755	1.9040
	1.4384	0.1044	3.5401	0.9034	1.4955	0.4238	0.8633	0.8814	4.1323
	0.1565	0.9035	5.7611	0.1039	2.7749	0.1488	0.2975	0.0000	0.0716
	0.1074	0.6853	1.3705	1.6938	0.3081	3.8426	0.2743	1.9682	1.0139
	0.6162	1.0979	7.1226	1.0140	4.9502	0.8760	1.3140	0.1967	0.3933
	1.7196	0.5190	0.7312	0.5228	1.3522	0.5560			
16000.	1.5729	0.2049	0.3114	0.2210	1.8371	0.5469	0.6936	1.8511	1.0507
	0.0040	0.1204	0.0880	0.0124	0.0784	0.1637	0.4259	0.8848	1.0237
	3.7442	1.3872	1.0508	4.7529	0.0079	0.1297	0.2871	0.0784	0.1032
	1.1446	0.6983	0.5016	0.3053	0.0919	0.1699	0.1897	1.2827	0.2003
	0.0580	0.0538	0.0388	2.1301	0.7886	0.8253	0.1838	0.2797	0.4395
	2.5655	0.2842	0.2324	0.0801	0.1051	0.6465	1.7743	0.2757	0.2696
	0.8092	3.8484	0.1354	0.6396	0.0513	0.2264	1.5183	0.5771	1.8859
	1.4329	0.1032	3.5466	0.9040	1.4995	0.4246	0.8656	0.8798	4.0984
	0.1548	0.9042	5.7710	0.1039	2.7821	0.1547	0.3094	0.0000	0.0710
	0.1065	0.6871	1.3740	1.6896	0.3065	3.8484	0.2730	1.9726	1.0160
	0.6130	1.0976	7.1310	1.0162	4.9612	0.8760	1.3139	0.1969	0.3937
	1.7178	0.5188	0.7311	0.5228	1.3518	0.5568			
18000.	1.6086	0.2061	0.3139	0.2252	1.8406	0.5451	0.6941	1.8524	1.0505
	0.0039	0.1199	0.0877	0.0124	0.0785	0.1665	0.4313	0.8926	1.0222
	3.7490	1.3883	1.0505	4.7552	0.0078	0.1292	0.2860	0.0785	0.1033
	1.1522	0.7050	0.5009	0.3052	0.0921	0.1684	0.1892	1.2870	0.1996
	0.0572	0.0536	0.0387	2.1468	0.7877	0.8246	0.1843	0.2778	0.4375
	2.5742	0.2829	0.2307	0.0797	0.1047	0.6461	1.7723	0.2764	0.2691
	0.8040	3.8614	0.1339	0.6366	0.0511	0.2256	1.5446	0.5798	1.8492
	1.4210	0.1007	3.5591	0.9045	1.5074	0.4260	0.8698	0.8760	4.0293
	0.1511	0.9047	5.7899	0.1038	2.7963	0.1662	0.3323	0.0000	0.0696
	0.1045	0.6905	1.3809	1.6823	0.3031	3.8601	0.2696	1.9814	1.0203
	0.6061	1.0959	7.1468	1.0206	4.9829	0.8757	1.3136	0.1973	0.3946
	1.7140	0.5184	0.7308	0.5226	1.3510	0.5583			

TABLE 3—*Continued*

Temp (K)									
20000.	1.6421	0.2068	0.3157	0.2285	1.8433	0.5426	0.6949	1.8547	1.0507
	0.0039	0.1195	0.0873	0.0125	0.0786	0.1687	0.4353	0.8980	1.0198
	3.7520	1.3898	1.0507	4.7601	0.0077	0.1286	0.2850	0.0786	0.1036
	1.1581	0.7108	0.5002	0.3051	0.0924	0.1671	0.1887	1.2914	0.1988
	0.0565	0.0533	0.0385	2.1605	0.7867	0.8238	0.1847	0.2760	0.4356
	2.5830	0.2816	0.2291	0.0794	0.1043	0.6457	1.7700	0.2771	0.2686
	0.7988	3.8745	0.1324	0.6337	0.0509	0.2246	1.5663	0.5822	1.8130
	1.4087	0.0982	3.5714	0.9043	1.5152	0.4275	0.8733	0.8717	3.9609
	0.1473	0.9046	5.8080	0.1037	2.8102	0.1770	0.3539	0.0000	0.0681
	0.1021	0.6940	1.3877	1.6758	0.2995	3.8715	0.2655	1.9900	1.0246
	0.5990	1.0933	7.1615	1.0249	5.0043	0.8753	1.3130	0.1978	0.3955
	1.7100	0.5181	0.7306	0.5225	1.3504	0.5597			
22000.	1.6740	0.2073	0.3168	0.2310	1.8456	0.5396	0.6958	1.8578	1.0513
	0.0038	0.1191	0.0869	0.0127	0.0786	0.1703	0.4383	0.9017	1.0166
	3.7536	1.3915	1.0513	4.7667	0.0076	0.1281	0.2840	0.0786	0.1041
	1.1629	0.7161	0.4994	0.3049	0.0926	0.1657	0.1882	1.2958	0.1981
	0.0558	0.0531	0.0383	2.1725	0.7856	0.8231	0.1852	0.2741	0.4336
	2.5918	0.2803	0.2275	0.0790	0.1038	0.6454	1.7676	0.2778	0.2679
	0.7936	3.8878	0.1310	0.6307	0.0507	0.2235	1.5843	0.5842	1.7781
	1.3962	0.0957	3.5834	0.9037	1.5227	0.4288	0.8762	0.8671	3.8943
	0.1436	0.9041	5.8256	0.1036	2.8237	0.1869	0.3739	0.0000	0.0664
	0.0996	0.6973	1.3943	1.6695	0.2959	3.8827	0.2610	1.9984	1.0287
	0.5918	1.0902	7.1755	1.0291	5.0252	0.8749	1.3123	0.1982	0.3963
	1.7059	0.5179	0.7305	0.5224	1.3498	0.5610			
24000.	1.7045	0.2074	0.3175	0.2328	1.8475	0.5362	0.6968	1.8613	1.0521
	0.0037	0.1188	0.0865	0.0130	0.0787	0.1715	0.4403	0.9038	1.0129
	3.7542	1.3936	1.0521	4.7746	0.0075	0.1276	0.2830	0.0787	0.1046
	1.1670	0.7210	0.4986	0.3048	0.0928	0.1642	0.1875	1.3003	0.1973
	0.0552	0.0528	0.0381	2.1833	0.7845	0.8223	0.1856	0.2720	0.4313
	2.6007	0.2790	0.2259	0.0786	0.1033	0.6450	1.7652	0.2784	0.2671
	0.7879	3.9012	0.1296	0.6278	0.0504	0.2223	1.5992	0.5858	1.7445
	1.3838	0.0933	3.5953	0.9028	1.5301	0.4301	0.8787	0.8624	3.8300
	0.1400	0.9033	5.8427	0.1034	2.8368	0.1960	0.3920	0.0000	0.0647
	0.0971	0.7006	1.4008	1.6631	0.2923	3.8937	0.2563	2.0066	1.0328
	0.5847	1.0868	7.1888	1.0332	5.0456	0.8744	1.3116	0.1985	0.3970
	1.7019	0.5176	0.7303	0.5223	1.3493	0.5623			
26000.	1.7339	0.2074	0.3177	0.2341	1.8493	0.5324	0.6979	1.8652	1.0530
	0.0037	0.1184	0.0861	0.0132	0.0788	0.1723	0.4415	0.9047	1.0087
	3.7543	1.3958	1.0531	4.7834	0.0074	0.1271	0.2821	0.0788	0.1053
	1.1708	0.7257	0.4978	0.3046	0.0930	0.1627	0.1867	1.3047	0.1965
	0.0546	0.0525	0.0379	2.1934	0.7834	0.8215	0.1860	0.2699	0.4288
	2.6097	0.2777	0.2244	0.0782	0.1027	0.6446	1.7627	0.2790	0.2661
	0.7820	3.9147	0.1283	0.6248	0.0502	0.2211	1.6115	0.5872	1.7122
	1.3715	0.0910	3.6070	0.9018	1.5372	0.4313	0.8808	0.8575	3.7681
	0.1365	0.9023	5.8595	0.1032	2.8494	0.2042	0.4084	0.0000	0.0630
	0.0946	0.7037	1.4069	1.6564	0.2889	3.9044	0.2515	2.0145	1.0366
	0.5778	1.0834	7.2016	1.0372	5.0652	0.8739	1.3108	0.1989	0.3977
	1.6981	0.5174	0.7301	0.5222	1.3489	0.5634			
28000.	1.7622	0.2071	0.3176	0.2350	1.8509	0.5284	0.6991	1.8694	1.0541
	0.0036	0.1181	0.0858	0.0136	0.0789	0.1727	0.4421	0.9046	1.0043
	3.7539	1.3981	1.0542	4.7928	0.0073	0.1266	0.2813	0.0789	0.1060
	1.1744	0.7304	0.4970	0.3045	0.0932	0.1611	0.1858	1.3091	0.1957
	0.0540	0.0522	0.0377	2.2032	0.7824	0.8207	0.1864	0.2676	0.4261
	2.6186	0.2763	0.2229	0.0777	0.1021	0.6443	1.7603	0.2796	0.2650
	0.7756	3.9281	0.1271	0.6218	0.0499	0.2198	1.6216	0.5884	1.6813
	1.3593	0.0888	3.6185	0.9006	1.5439	0.4324	0.8825	0.8526	3.7084
	0.1331	0.9012	5.8758	0.1030	2.8614	0.2115	0.4230	0.0000	0.0614
	0.0921	0.7067	1.4128	1.6494	0.2855	3.9148	0.2469	2.0221	1.0404
	0.5711	1.0799	7.2137	1.0410	5.0839	0.8734	1.3100	0.1992	0.3984
	1.6944	0.5172	0.7299	0.5221	1.3484	0.5644			
30000.	1.7895	0.2067	0.3172	0.2354	1.8525	0.5242	0.7003	1.8737	1.0553
	0.0036	0.1178	0.0855	0.0139	0.0790	0.1730	0.4421	0.9036	0.9996
	3.7532	1.4006	1.0553	4.8026	0.0072	0.1262	0.2805	0.0790	0.1067
	1.1779	0.7350	0.4962	0.3044	0.0934	0.1595	0.1847	1.3136	0.1948
	0.0534	0.0519	0.0375	2.2129	0.7813	0.8199	0.1867	0.2653	0.4232
	2.6275	0.2750	0.2214	0.0772	0.1015	0.6439	1.7579	0.2801	0.2637
	0.7690	3.9415	0.1259	0.6187	0.0496	0.2184	1.6297	0.5893	1.6515
	1.3473	0.0866	3.6297	0.8993	1.5503	0.4334	0.8839	0.8475	3.6508
	0.1300	0.8999	5.8917	0.1028	2.8726	0.2180	0.4360	0.0000	0.0598
	0.0897	0.7095	1.4183	1.6420	0.2823	3.9247	0.2423	2.0292	1.0438
	0.5646	1.0765	7.2250	1.0446	5.1015	0.8728	1.3092	0.1995	0.3989
	1.6908	0.5170	0.7297	0.5219	1.3478	0.5653			

TABLE 3—*Continued*

Temp (K)									
32000.	1.8156	0.2062	0.3166	0.2356	1.8541	0.5200	0.7016	1.8783	1.0565
	0.0036	0.1176	0.0852	0.0142	0.0791	0.1730	0.4418	0.9020	0.9948
	3.7524	1.4032	1.0566	4.8129	0.0071	0.1257	0.2798	0.0791	0.1075
	1.1814	0.7395	0.4955	0.3042	0.0935	0.1578	0.1836	1.3179	0.1940
	0.0529	0.0515	0.0372	2.2225	0.7802	0.8191	0.1871	0.2628	0.4200
	2.6362	0.2736	0.2200	0.0767	0.1008	0.6435	1.7555	0.2806	0.2622
	0.7621	3.9546	0.1247	0.6157	0.0493	0.2170	1.6362	0.5900	1.6229
	1.3355	0.0846	3.6405	0.8979	1.5562	0.4342	0.8850	0.8425	3.5952
	0.1269	0.8986	5.9069	0.1025	2.8831	0.2238	0.4475	0.0000	0.0583
	0.0874	0.7121	1.4235	1.6342	0.2792	3.9342	0.2379	2.0358	1.0471
	0.5584	1.0732	7.2356	1.0479	5.1179	0.8723	1.3084	0.1997	0.3994
	1.6874	0.5167	0.7293	0.5217	1.3471	0.5661			
34000.	1.8407	0.2056	0.3158	0.2354	1.8556	0.5156	0.7030	1.8829	1.0578
	0.0035	0.1173	0.0849	0.0146	0.0791	0.1728	0.4410	0.8999	0.9899
	3.7515	1.4059	1.0579	4.8234	0.0070	0.1253	0.2791	0.0791	0.1082
	1.1850	0.7441	0.4947	0.3040	0.0937	0.1561	0.1824	1.3222	0.1931
	0.0523	0.0512	0.0370	2.2322	0.7791	0.8183	0.1873	0.2603	0.4168
	2.6448	0.2722	0.2186	0.0762	0.1002	0.6431	1.7531	0.2810	0.2607
	0.7549	3.9675	0.1236	0.6126	0.0490	0.2156	1.6412	0.5905	1.5953
	1.3239	0.0827	3.6509	0.8965	1.5617	0.4350	0.8858	0.8374	3.5415
	0.1240	0.8973	5.9214	0.1022	2.8926	0.2288	0.4577	0.0000	0.0568
	0.0852	0.7145	1.4282	1.6260	0.2762	3.9430	0.2336	2.0419	1.0500
	0.5524	1.0700	7.2453	1.0509	5.1327	0.8717	1.3075	0.1999	0.3998
	1.6841	0.5164	0.7289	0.5214	1.3462	0.5668			
36000.	1.8646	0.2049	0.3149	0.2351	1.8572	0.5112	0.7043	1.8876	1.0591
	0.0035	0.1171	0.0846	0.0149	0.0792	0.1725	0.4400	0.8973	0.9849
	3.7506	1.4086	1.0592	4.8341	0.0069	0.1250	0.2784	0.0792	0.1089
	1.1885	0.7485	0.4939	0.3039	0.0938	0.1544	0.1812	1.3263	0.1922
	0.0518	0.0508	0.0368	2.2418	0.7781	0.8175	0.1876	0.2577	0.4134
	2.6531	0.2709	0.2171	0.0757	0.0995	0.6427	1.7506	0.2813	0.2590
	0.7477	3.9801	0.1226	0.6094	0.0486	0.2141	1.6449	0.5909	1.5687
	1.3125	0.0808	3.6608	0.8949	1.5666	0.4356	0.8863	0.8323	3.4895
	0.1213	0.8958	5.9350	0.1019	2.9012	0.2333	0.4665	0.0000	0.0554
	0.0831	0.7166	1.4324	1.6176	0.2733	3.9512	0.2296	2.0473	1.0526
	0.5467	1.0668	7.2539	1.0537	5.1460	0.8710	1.3065	0.2001	0.4001
	1.6808	0.5160	0.7283	0.5210	1.3451	0.5672			
38000.	1.8874	0.2042	0.3139	0.2346	1.8589	0.5068	0.7057	1.8924	1.0604
	0.0034	0.1168	0.0843	0.0152	0.0792	0.1721	0.4387	0.8943	0.9800
	3.7497	1.4114	1.0606	4.8449	0.0068	0.1246	0.2777	0.0792	0.1096
	1.1921	0.7530	0.4931	0.3037	0.0939	0.1526	0.1799	1.3303	0.1913
	0.0513	0.0505	0.0365	2.2513	0.7770	0.8166	0.1878	0.2551	0.4099
	2.6612	0.2694	0.2157	0.0751	0.0988	0.6422	1.7482	0.2816	0.2572
	0.7402	3.9923	0.1215	0.6063	0.0483	0.2126	1.6474	0.5911	1.5430
	1.3012	0.0791	3.6700	0.8933	1.5709	0.4360	0.8866	0.8272	3.4391
	0.1186	0.8943	5.9477	0.1016	2.9087	0.2371	0.4743	0.0000	0.0540
	0.0811	0.7185	1.4360	1.6088	0.2706	3.9587	0.2256	2.0520	1.0549
	0.5412	1.0637	7.2614	1.0560	5.1576	0.8703	1.3055	0.2002	0.4003
	1.6776	0.5155	0.7277	0.5205	1.3438	0.5676			
40000.	1.9090	0.2034	0.3127	0.2339	1.8605	0.5024	0.7071	1.8972	1.0617
	0.0034	0.1166	0.0841	0.0155	0.0792	0.1716	0.4373	0.8911	0.9751
	3.7488	1.4142	1.0620	4.8558	0.0068	0.1242	0.2771	0.0792	0.1102
	1.1957	0.7573	0.4923	0.3034	0.0940	0.1509	0.1785	1.3342	0.1903
	0.0509	0.0501	0.0363	2.2608	0.7758	0.8157	0.1879	0.2525	0.4063
	2.6689	0.2680	0.2143	0.0746	0.0981	0.6417	1.7456	0.2819	0.2554
	0.7328	4.0040	0.1205	0.6030	0.0480	0.2110	1.6488	0.5911	1.5182
	1.2901	0.0774	3.6785	0.8916	1.5747	0.4363	0.8866	0.8220	3.3904
	0.1161	0.8927	5.9593	0.1012	2.9152	0.2405	0.4810	0.0000	0.0528
	0.0792	0.7201	1.4392	1.5998	0.2679	3.9653	0.2219	2.0560	1.0568
	0.5359	1.0606	7.2676	1.0580	5.1673	0.8695	1.3043	0.2002	0.4003
	1.6744	0.5148	0.7268	0.5199	1.3422	0.5677			

TABLE 4

MAXWELLIAN-AVERAGED COLLISION STRENGTHS FOR O IV

Temp (K)	TRANSITION KEY								
	1 2	1 3	1 4	1 5	1 6	1 7	1 8	1 9	1 10
	1 11	1 12	1 13	1 14	1 15	2 3	2 4	2 5	2 6
	2 7	2 8	2 9	2 10	2 11	2 12	2 13	2 14	2 15
	3 4	3 5	3 6	3 7	3 8	3 9	3 10	3 11	3 12
	3 13	3 14	3 15	4 5	4 6	4 7	4 8	4 9	4 10
	4 11	4 12	4 13	4 14	4 15	5 6	5 7	5 8	5 9
	5 10	5 11	5 12	5 13	5 14	5 15	6 7	6 8	6 9
	6 10	6 11	6 12	6 13	6 14	6 15	7 8	7 9	7 10
	7 11	7 12	7 13	7 14	7 15	8 9	8 10	8 11	8 12
	8 13	8 14	8 15	9 10	9 11	9 12	9 13	9 14	9 15
	10 11	10 12	10 13	10 14	10 15	11 12	11 13	11 14	11 15
	12 13	12 14	12 15	13 14	13 15	14 15			
1000.	1.6411	0.1238	0.1837	0.1158	1.5676	0.1762	1.0990	1.5518	0.8686
	0.0053	0.0716	0.0504	0.0170	0.0521	0.0879	0.2396	0.5192	0.5250
	2.9627	2.1980	0.8686	3.9723	0.0105	0.0748	0.1692	0.0521	0.0860
	1.0175	0.8275	0.3590	0.2050	0.0813	0.1141	0.1098	1.1501	0.1402
	0.0497	0.0309	0.0223	2.1583	0.5580	0.5701	0.1625	0.1809	0.2670
	2.2997	0.2033	0.1765	0.0460	0.0605	0.4367	1.2554	0.2438	0.1528
	0.5189	3.4498	0.1122	0.4575	0.0296	0.1301	3.4061	0.6802	0.9861
	1.0840	0.0646	3.1212	0.6552	1.3362	0.3447	1.0202	0.7390	2.3660
	0.0969	0.6552	5.0093	0.0646	2.4569	0.6570	1.3139	0.0000	0.0408
	0.0613	0.6248	1.2493	2.3023	0.3634	3.3015	0.2113	1.7310	0.8850
	0.7267	0.9140	6.1105	0.8851	4.3474	0.7016	1.0526	0.1763	0.3527
	1.4162	0.3596	0.5411	0.3910	0.9601	0.4857			
2000.	1.7575	0.1208	0.1791	0.1124	1.5797	0.1828	1.0259	1.5719	0.8726
	0.0048	0.0720	0.0515	0.0170	0.0522	0.0854	0.2332	0.5061	0.5353
	2.9898	2.0518	0.8726	4.0165	0.0097	0.0761	0.1707	0.0522	0.0862
	1.0398	0.8050	0.3615	0.2081	0.0821	0.1005	0.1389	1.1575	0.1339
	0.0438	0.0309	0.0224	2.1535	0.5626	0.5767	0.1642	0.1761	0.3026
	2.3148	0.1924	0.1630	0.0460	0.0605	0.4430	1.2659	0.2463	0.2021
	0.5160	3.4723	0.1002	0.4329	0.0296	0.1302	3.2003	0.6868	0.8827
	0.9822	0.1175	3.1498	0.6724	1.3408	0.3457	1.0302	0.6713	2.1259
	0.1762	0.6724	5.0610	0.0647	2.4652	0.5598	1.1196	0.0000	0.0467
	0.0700	0.6269	1.2535	2.0344	0.3849	3.3166	0.2053	1.7369	0.8879
	0.7697	0.9098	6.1326	0.8881	4.3621	0.7058	1.0589	0.1766	0.3533
	1.4313	0.3603	0.5422	0.3917	0.9620	0.4867			
3000.	1.8181	0.1193	0.1768	0.1110	1.6086	0.2115	0.9578	1.5871	0.8778
	0.0045	0.0722	0.0526	0.0170	0.0522	0.0843	0.2302	0.4996	0.5755
	3.0648	1.9157	0.8778	4.0520	0.0090	0.0775	0.1720	0.0522	0.0862
	1.0419	0.7669	0.3668	0.2126	0.0827	0.0955	0.1482	1.1593	0.1301
	0.0403	0.0309	0.0224	2.1070	0.5716	0.5872	0.1654	0.1739	0.3135
	2.3185	0.1858	0.1550	0.0460	0.0605	0.4522	1.2860	0.2481	0.2181
	0.5130	3.4778	0.0931	0.4181	0.0296	0.1301	3.0228	0.7123	0.8962
	0.9526	0.1317	3.1729	0.6977	1.3435	0.3463	1.0684	0.6444	2.1287
	0.1975	0.6977	5.1082	0.0646	2.4701	0.4936	0.9873	0.0000	0.0555
	0.0832	0.6281	1.2560	1.8771	0.3687	3.3240	0.2274	1.7404	0.8896
	0.7374	0.9378	6.1632	0.8898	4.3707	0.7082	1.0623	0.1767	0.3534
	1.4381	0.3606	0.5424	0.3919	0.9626	0.4871			
4000.	1.9103	0.1195	0.1774	0.1119	1.6472	0.2586	0.9051	1.5974	0.8820
	0.0043	0.0724	0.0534	0.0170	0.0522	0.0849	0.2314	0.5012	0.6397
	3.1719	1.8103	0.8820	4.0769	0.0085	0.0786	0.1730	0.0522	0.0863
	1.0418	0.7359	0.3747	0.2178	0.0831	0.0954	0.1522	1.1599	0.1277
	0.0382	0.0309	0.0223	2.0672	0.5841	0.6008	0.1663	0.1753	0.3198
	2.3197	0.1818	0.1500	0.0460	0.0604	0.4631	1.3142	0.2494	0.2244
	0.5182	3.4796	0.0886	0.4091	0.0296	0.1300	2.9983	0.7396	0.9874
	0.9694	0.1345	3.1906	0.7198	1.3458	0.3467	1.1095	0.6433	2.2919
	0.2018	0.7199	5.1459	0.0646	2.4741	0.4448	0.8897	0.0000	0.0634
	0.0952	0.6291	1.2580	1.7810	0.3544	3.3326	0.2509	1.7433	0.8910
	0.7087	0.9678	6.1974	0.8912	4.3779	0.7090	1.0635	0.1767	0.3534
	1.4407	0.3607	0.5425	0.3920	0.9628	0.4873			
5000.	2.0214	0.1211	0.1800	0.1146	1.6861	0.3134	0.8624	1.6035	0.8847
	0.0041	0.0725	0.0540	0.0171	0.0521	0.0868	0.2357	0.5090	0.7133
	3.2858	1.7248	0.8847	4.0918	0.0083	0.0793	0.1737	0.0521	0.0863
	1.0448	0.7147	0.3836	0.2233	0.0834	0.0971	0.1543	1.1598	0.1262
	0.0367	0.0308	0.0223	2.0433	0.5982	0.6156	0.1668	0.1783	0.3246
	2.3195	0.1791	0.1466	0.0459	0.0604	0.4747	1.3459	0.2501	0.2274
	0.5269	3.4793	0.0856	0.4030	0.0295	0.1299	3.0864	0.7615	1.1050
	1.0049	0.1340	3.2037	0.7363	1.3479	0.3470	1.1423	0.6532	2.5115
	0.2010	0.7363	5.1737	0.0645	2.4778	0.4073	0.8145	0.0000	0.0694
	0.1041	0.6300	1.2598	1.7185	0.3443	3.3398	0.2691	1.7459	0.8923
	0.6885	0.9911	6.2247	0.8925	4.3844	0.7090	1.0635	0.1766	0.3534
	1.4413	0.3608	0.5425	0.3920	0.9629	0.4874			

TABLE 4—*Continued*

Temp (K)									
6000.	2.1308	0.1234	0.1838	0.1185	1.7214	0.3678	0.8270	1.6069	0.8860
	0.0041	0.0726	0.0543	0.0171	0.0521	0.0895	0.2419	0.5200	0.7856
	3.3927	1.6540	0.8860	4.0998	0.0081	0.0797	0.1741	0.0521	0.0863
	1.0510	0.7011	0.3925	0.2286	0.0835	0.0994	0.1555	1.1593	0.1251
	0.0357	0.0308	0.0223	2.0326	0.6121	0.6300	0.1669	0.1815	0.3283
	2.3185	0.1772	0.1443	0.0459	0.0603	0.4860	1.3772	0.2504	0.2289
	0.5358	3.4777	0.0835	0.3987	0.0295	0.1297	3.2309	0.7761	1.2181
	1.0426	0.1323	3.2127	0.7479	1.3499	0.3473	1.1642	0.6658	2.7252
	0.1985	0.7479	5.1929	0.0645	2.4813	0.3774	0.7547	0.0000	0.0736
	0.1104	0.6309	1.2615	1.6739	0.3370	3.3440	0.2818	1.7484	0.8935
	0.6739	1.0072	6.2421	0.8937	4.3906	0.7087	1.0631	0.1766	0.3533
	1.4408	0.3608	0.5425	0.3919	0.9630	0.4875			
7000.	2.2273	0.1259	0.1881	0.1229	1.7526	0.4181	0.7973	1.6087	0.8864
	0.0040	0.0725	0.0545	0.0171	0.0521	0.0926	0.2488	0.5324	0.8522
	3.4892	1.5947	0.8864	4.1039	0.0081	0.0800	0.1742	0.0521	0.0862
	1.0592	0.6928	0.4007	0.2334	0.0834	0.1016	0.1561	1.1585	0.1242
	0.0349	0.0308	0.0223	2.0308	0.6249	0.6432	0.1668	0.1843	0.3311
	2.3170	0.1758	0.1425	0.0458	0.0602	0.4962	1.4060	0.2502	0.2295
	0.5436	3.4755	0.0819	0.3955	0.0295	0.1296	3.3914	0.7840	1.3146
	1.0757	0.1302	3.2181	0.7556	1.3518	0.3476	1.1760	0.6773	2.9081
	0.1953	0.7557	5.2049	0.0644	2.4847	0.3530	0.7059	0.0000	0.0765
	0.1147	0.6317	1.2632	1.6391	0.3313	3.3446	0.2902	1.7509	0.8947
	0.6626	1.0174	6.2497	0.8949	4.3966	0.7082	1.0623	0.1765	0.3532
	1.4397	0.3608	0.5425	0.3919	0.9630	0.4875			
8000.	2.3072	0.1284	0.1924	0.1275	1.7811	0.4634	0.7724	1.6098	0.8863
	0.0040	0.0724	0.0546	0.0171	0.0520	0.0958	0.2560	0.5451	0.9123
	3.5768	1.5449	0.8863	4.1059	0.0081	0.0800	0.1741	0.0520	0.0862
	1.0684	0.6883	0.4078	0.2376	0.0833	0.1036	0.1563	1.1577	0.1236
	0.0343	0.0307	0.0222	2.0349	0.6360	0.6548	0.1665	0.1868	0.3330
	2.3154	0.1747	0.1411	0.0458	0.0601	0.5052	1.4311	0.2498	0.2294
	0.5503	3.4732	0.0807	0.3930	0.0294	0.1294	3.5450	0.7864	1.3922
	1.1025	0.1279	3.2206	0.7606	1.3537	0.3479	1.1797	0.6867	3.0552
	0.1919	0.7606	5.2112	0.0643	2.4881	0.3326	0.6653	0.0000	0.0783
	0.1174	0.6326	1.2649	1.6103	0.3265	3.3419	0.2953	1.7532	0.8959
	0.6530	1.0230	6.2486	0.8961	4.4024	0.7076	1.0614	0.1765	0.3531
	1.4381	0.3608	0.5424	0.3918	0.9630	0.4876			
9000.	2.3707	0.1309	0.1967	0.1322	1.8085	0.5038	0.7514	1.6105	0.8860
	0.0040	0.0723	0.0546	0.0171	0.0520	0.0990	0.2631	0.5574	0.9663
	3.6584	1.5029	0.8860	4.1071	0.0081	0.0800	0.1738	0.0520	0.0862
	1.0780	0.6865	0.4138	0.2413	0.0831	0.1053	0.1563	1.1570	0.1231
	0.0338	0.0307	0.0222	2.0429	0.6455	0.6647	0.1661	0.1889	0.3343
	2.3140	0.1737	0.1399	0.0457	0.0601	0.5129	1.4523	0.2492	0.2290
	0.5558	3.4710	0.0796	0.3909	0.0294	0.1293	3.6805	0.7848	1.4526
	1.1231	0.1256	3.2208	0.7635	1.3556	0.3482	1.1772	0.6938	3.1696
	0.1884	0.7636	5.2129	0.0643	2.4914	0.3154	0.6309	0.0000	0.0793
	0.1190	0.6334	1.2665	1.5853	0.3222	3.3364	0.2981	1.7556	0.8970
	0.6444	1.0252	6.2406	0.8972	4.4082	0.7069	1.0604	0.1764	0.3529
	1.4362	0.3609	0.5423	0.3918	0.9629	0.4876			
10000.	2.4199	0.1332	0.2007	0.1367	1.8357	0.5401	0.7336	1.6112	0.8856
	0.0041	0.0721	0.0545	0.0171	0.0520	0.1021	0.2700	0.5693	1.0152
	3.7363	1.4672	0.8856	4.1080	0.0081	0.0799	0.1734	0.0520	0.0862
	1.0876	0.6869	0.4188	0.2443	0.0828	0.1068	0.1560	1.1564	0.1226
	0.0333	0.0306	0.0222	2.0539	0.6533	0.6729	0.1656	0.1906	0.3351
	2.3128	0.1729	0.1390	0.0457	0.0600	0.5194	1.4699	0.2484	0.2283
	0.5604	3.4692	0.0787	0.3891	0.0294	0.1291	3.7943	0.7803	1.4985
	1.1385	0.1232	3.2193	0.7649	1.3574	0.3485	1.1705	0.6990	3.2564
	0.1849	0.7649	5.2113	0.0642	2.4946	0.3007	0.6015	0.0000	0.0798
	0.1197	0.6342	1.2681	1.5632	0.3183	3.3288	0.2990	1.7579	0.8981
	0.6365	1.0248	6.2273	0.8983	4.4139	0.7062	1.0593	0.1764	0.3528
	1.4339	0.3609	0.5422	0.3917	0.9629	0.4876			
11000.	2.4576	0.1354	0.2046	0.1411	1.8632	0.5727	0.7184	1.6119	0.8852
	0.0041	0.0719	0.0544	0.0171	0.0519	0.1051	0.2765	0.5805	1.0599
	3.8121	1.4368	0.8852	4.1091	0.0081	0.0797	0.1729	0.0519	0.0862
	1.0972	0.6889	0.4228	0.2469	0.0825	0.1082	0.1557	1.1559	0.1222
	0.0330	0.0306	0.0221	2.0668	0.6596	0.6797	0.1651	0.1921	0.3356
	2.3118	0.1723	0.1381	0.0456	0.0599	0.5248	1.4841	0.2476	0.2274
	0.5641	3.4678	0.0779	0.3876	0.0293	0.1290	3.8861	0.7738	1.5328
	1.1496	0.1209	3.2167	0.7651	1.3592	0.3488	1.1607	0.7025	3.3210
	0.1814	0.7652	5.2074	0.0641	2.4978	0.2880	0.5760	0.0000	0.0798
	0.1197	0.6350	1.2696	1.5433	0.3145	3.3199	0.2986	1.7601	0.8992
	0.6291	1.0226	6.2105	0.8994	4.4195	0.7055	1.0582	0.1763	0.3526
	1.4315	0.3609	0.5421	0.3916	0.9628	0.4876			

TABLE 4—*Continued*

Temp (K)									
12000.	2.4862	0.1375	0.2082	0.1453	1.8913	0.6021	0.7054	1.6127	0.8849
	0.0041	0.0717	0.0542	0.0171	0.0519	0.1080	0.2827	0.5911	1.1009
	3.8862	1.4108	0.8849	4.1104	0.0081	0.0794	0.1724	0.0519	0.0862
	1.1067	0.6923	0.4259	0.2490	0.0823	0.1093	0.1552	1.1556	0.1219
	0.0326	0.0306	0.0221	2.0813	0.6647	0.6852	0.1645	0.1932	0.3357
	2.3112	0.1716	0.1373	0.0455	0.0599	0.5293	1.4955	0.2468	0.2264
	0.5671	3.4668	0.0772	0.3862	0.0293	0.1288	3.9576	0.7660	1.5580
	1.1573	0.1186	3.2133	0.7645	1.3610	0.3491	1.1490	0.7048	3.3682
	0.1779	0.7646	5.2020	0.0641	2.5010	0.2769	0.5538	0.0000	0.0795
	0.1192	0.6357	1.2712	1.5252	0.3110	3.3103	0.2972	1.7624	0.9003
	0.6219	1.0190	6.1915	0.9005	4.4250	0.7047	1.0571	0.1762	0.3525
	1.4289	0.3609	0.5420	0.3915	0.9627	0.4876			
13000.	2.5080	0.1394	0.2115	0.1492	1.9198	0.6288	0.6942	1.6137	0.8846
	0.0041	0.0714	0.0540	0.0172	0.0519	0.1107	0.2886	0.6009	1.1386
	3.9588	1.3883	0.8846	4.1120	0.0082	0.0791	0.1718	0.0519	0.0862
	1.1159	0.6967	0.4284	0.2508	0.0820	0.1103	0.1546	1.1554	0.1215
	0.0323	0.0305	0.0221	2.0969	0.6687	0.6896	0.1640	0.1942	0.3356
	2.3108	0.1711	0.1366	0.0455	0.0598	0.5329	1.5045	0.2459	0.2253
	0.5694	3.4663	0.0766	0.3849	0.0292	0.1287	4.0113	0.7574	1.5760
	1.1625	0.1164	3.2095	0.7634	1.3628	0.3494	1.1361	0.7060	3.4016
	0.1746	0.7634	5.1956	0.0640	2.5041	0.2672	0.5344	0.0000	0.0789
	0.1184	0.6365	1.2727	1.5087	0.3075	3.3004	0.2950	1.7646	0.9013
	0.6150	1.0144	6.1713	0.9016	4.4305	0.7040	1.0560	0.1761	0.3523
	1.4262	0.3609	0.5419	0.3914	0.9627	0.4876			
14000.	2.5247	0.1411	0.2146	0.1530	1.9484	0.6531	0.6845	1.6147	0.8845
	0.0041	0.0712	0.0538	0.0172	0.0518	0.1132	0.2941	0.6101	1.1734
	4.0296	1.3689	0.8845	4.1140	0.0082	0.0788	0.1712	0.0518	0.0862
	1.1248	0.7019	0.4302	0.2523	0.0817	0.1111	0.1540	1.1553	0.1212
	0.0320	0.0305	0.0221	2.1132	0.6717	0.6932	0.1634	0.1950	0.3353
	2.3107	0.1706	0.1359	0.0454	0.0597	0.5359	1.5114	0.2451	0.2241
	0.5712	3.4662	0.0760	0.3837	0.0292	0.1285	4.0496	0.7484	1.5884
	1.1656	0.1142	3.2055	0.7617	1.3646	0.3496	1.1226	0.7066	3.4243
	0.1713	0.7618	5.1888	0.0639	2.5072	0.2586	0.5172	0.0000	0.0782
	0.1173	0.6373	1.2742	1.4935	0.3042	3.2906	0.2923	1.7668	0.9024
	0.6083	1.0093	6.1508	0.9027	4.4358	0.7032	1.0548	0.1761	0.3522
	1.4234	0.3609	0.5418	0.3913	0.9626	0.4875			
15000.	2.5377	0.1427	0.2175	0.1565	1.9767	0.6751	0.6760	1.6159	0.8844
	0.0041	0.0709	0.0536	0.0172	0.0518	0.1156	0.2992	0.6186	1.2055
	4.0982	1.3521	0.8844	4.1162	0.0082	0.0785	0.1706	0.0518	0.0862
	1.1334	0.7076	0.4315	0.2534	0.0814	0.1118	0.1533	1.1554	0.1210
	0.0317	0.0305	0.0220	2.1299	0.6740	0.6959	0.1628	0.1955	0.3348
	2.3109	0.1701	0.1353	0.0454	0.0596	0.5384	1.5165	0.2442	0.2229
	0.5725	3.4664	0.0754	0.3826	0.0292	0.1283	4.0749	0.7391	1.5963
	1.1671	0.1121	3.2016	0.7598	1.3663	0.3499	1.1087	0.7065	3.4385
	0.1682	0.7599	5.1819	0.0639	2.5103	0.2510	0.5021	0.0000	0.0774
	0.1160	0.6380	1.2757	1.4795	0.3009	3.2811	0.2893	1.7690	0.9034
	0.6018	1.0037	6.1305	0.9037	4.4411	0.7024	1.0537	0.1760	0.3520
	1.4206	0.3609	0.5417	0.3912	0.9625	0.4875			
16000.	2.5482	0.1442	0.2202	0.1597	2.0046	0.6950	0.6687	1.6171	0.8844
	0.0041	0.0707	0.0534	0.0172	0.0518	0.1179	0.3039	0.6264	1.2349
	4.1643	1.3374	0.8844	4.1186	0.0082	0.0782	0.1700	0.0518	0.0861
	1.1417	0.7138	0.4325	0.2544	0.0811	0.1124	0.1526	1.1556	0.1207
	0.0315	0.0304	0.0220	2.1467	0.6757	0.6981	0.1623	0.1960	0.3341
	2.3113	0.1696	0.1347	0.0453	0.0595	0.5404	1.5203	0.2434	0.2217
	0.5734	3.4669	0.0749	0.3816	0.0291	0.1282	4.0895	0.7299	1.6008
	1.1673	0.1101	3.1979	0.7577	1.3680	0.3501	1.0948	0.7060	3.4461
	0.1651	0.7578	5.1752	0.0638	2.5133	0.2443	0.4887	0.0000	0.0764
	0.1146	0.6388	1.2772	1.4664	0.2977	3.2721	0.2859	1.7711	0.9044
	0.5955	0.9979	6.1108	0.9048	4.4463	0.7017	1.0525	0.1759	0.3518
	1.4177	0.3608	0.5415	0.3911	0.9623	0.4874			
18000.	2.5650	0.1468	0.2249	0.1656	2.0578	0.7292	0.6566	1.6198	0.8845
	0.0041	0.0702	0.0530	0.0172	0.0517	0.1218	0.3124	0.6403	1.2867
	4.2874	1.3132	0.8845	4.1241	0.0081	0.0776	0.1688	0.0517	0.0861
	1.1571	0.7267	0.4333	0.2558	0.0806	0.1133	0.1511	1.1562	0.1202
	0.0310	0.0303	0.0219	2.1799	0.6775	0.7009	0.1612	0.1964	0.3324
	2.3126	0.1687	0.1337	0.0452	0.0594	0.5432	1.5243	0.2417	0.2191
	0.5740	3.4689	0.0740	0.3796	0.0290	0.1278	4.0934	0.7118	1.6020
	1.1651	0.1062	3.1912	0.7531	1.3713	0.3506	1.0677	0.7039	3.4466
	0.1593	0.7532	5.1628	0.0636	2.5191	0.2331	0.4661	0.0000	0.0743
	0.1115	0.6402	1.2799	1.4430	0.2917	3.2560	0.2787	1.7751	0.9063
	0.5833	0.9860	6.0743	0.9067	4.4561	0.7001	1.0502	0.1757	0.3514
	1.4120	0.3608	0.5412	0.3909	0.9620	0.4873			

TABLE 4—*Continued*

Temp (K)									
20000.	2.5795	0.1489	0.2288	0.1706	2.1065	0.7568	0.6471	1.6226	0.8848
	0.0041	0.0698	0.0526	0.0172	0.0516	0.1252	0.3195	0.6519	1.3296
	4.3971	1.2943	0.8848	4.1299	0.0081	0.0771	0.1677	0.0516	0.0861
	1.1709	0.7397	0.4333	0.2567	0.0801	0.1138	0.1496	1.1572	0.1197
	0.0306	0.0303	0.0219	2.2114	0.6778	0.7021	0.1601	0.1963	0.3303
	2.3145	0.1679	0.1327	0.0451	0.0592	0.5449	1.5250	0.2402	0.2165
	0.5734	3.4718	0.0731	0.3778	0.0290	0.1275	4.0731	0.6947	1.5960
	1.1605	0.1026	3.1859	0.7482	1.3743	0.3510	1.0421	0.7010	3.4335
	0.1539	0.7485	5.1522	0.0635	2.5244	0.2241	0.4482	0.0000	0.0721
	0.1081	0.6414	1.2824	1.4225	0.2859	3.2427	0.2711	1.7787	0.9080
	0.5718	0.9744	6.0424	0.9085	4.4651	0.6986	1.0480	0.1754	0.3509
	1.4064	0.3607	0.5408	0.3906	0.9616	0.4870			
22000.	2.5948	0.1507	0.2320	0.1748	2.1499	0.7787	0.6397	1.6254	0.8852
	0.0040	0.0694	0.0522	0.0173	0.0515	0.1281	0.3255	0.6615	1.3645
	4.4926	1.2794	0.8852	4.1360	0.0081	0.0765	0.1667	0.0515	0.0860
	1.1831	0.7522	0.4325	0.2572	0.0796	0.1139	0.1480	1.1584	0.1192
	0.0302	0.0302	0.0218	2.2406	0.6770	0.7023	0.1591	0.1959	0.3279
	2.3169	0.1671	0.1317	0.0449	0.0590	0.5457	1.5233	0.2387	0.2140
	0.5718	3.4755	0.0723	0.3760	0.0289	0.1271	4.0369	0.6789	1.5854
	1.1542	0.0993	3.1819	0.7434	1.3770	0.3514	1.0183	0.6976	3.4118
	0.1489	0.7437	5.1436	0.0633	2.5290	0.2170	0.4340	0.0000	0.0698
	0.1048	0.6425	1.2846	1.4044	0.2804	3.2320	0.2636	1.7819	0.9095
	0.5608	0.9632	6.0151	0.9100	4.4729	0.6971	1.0457	0.1752	0.3504
	1.4008	0.3605	0.5403	0.3902	0.9609	0.4866			
24000.	2.6130	0.1521	0.2347	0.1783	2.1878	0.7958	0.6338	1.6283	0.8857
	0.0040	0.0690	0.0518	0.0173	0.0514	0.1305	0.3304	0.6693	1.3925
	4.5743	1.2675	0.8857	4.1422	0.0080	0.0760	0.1657	0.0514	0.0859
	1.1937	0.7639	0.4313	0.2574	0.0791	0.1139	0.1464	1.1597	0.1188
	0.0298	0.0301	0.0217	2.2670	0.6756	0.7018	0.1582	0.1952	0.3253
	2.3197	0.1664	0.1309	0.0448	0.0588	0.5460	1.5201	0.2373	0.2114
	0.5693	3.4797	0.0715	0.3743	0.0288	0.1267	3.9905	0.6643	1.5718
	1.1470	0.0961	3.1791	0.7388	1.3792	0.3516	0.9964	0.6939	3.3843
	0.1442	0.7391	5.1368	0.0631	2.5328	0.2114	0.4227	0.0000	0.0676
	0.1015	0.6434	1.2863	1.3882	0.2752	3.2236	0.2562	1.7845	0.9107
	0.5504	0.9527	5.9920	0.9113	4.4790	0.6956	1.0434	0.1748	0.3497
	1.3954	0.3602	0.5396	0.3897	0.9599	0.4861			
26000.	2.6359	0.1532	0.2368	0.1812	2.2203	0.8086	0.6290	1.6311	0.8862
	0.0040	0.0687	0.0515	0.0173	0.0513	0.1324	0.3344	0.6755	1.4145
	4.6429	1.2579	0.8862	4.1483	0.0079	0.0755	0.1649	0.0513	0.0858
	1.2029	0.7746	0.4297	0.2574	0.0787	0.1136	0.1447	1.1612	0.1183
	0.0295	0.0300	0.0217	2.2906	0.6736	0.7007	0.1573	0.1942	0.3225
	2.3227	0.1656	0.1300	0.0446	0.0586	0.5458	1.5157	0.2360	0.2088
	0.5662	3.4843	0.0708	0.3727	0.0287	0.1263	3.9376	0.6509	1.5562
	1.1392	0.0932	3.1772	0.7342	1.3808	0.3517	0.9763	0.6899	3.3531
	0.1398	0.7346	5.1315	0.0629	2.5356	0.2069	0.4138	0.0000	0.0655
	0.0982	0.6440	1.2875	1.3735	0.2702	3.2172	0.2491	1.7863	0.9114
	0.5404	0.9430	5.9725	0.9121	4.4834	0.6940	1.0411	0.1744	0.3489
	1.3900	0.3598	0.5388	0.3890	0.9587	0.4854			
28000.	2.6652	0.1540	0.2384	0.1836	2.2477	0.8179	0.6250	1.6338	0.8868
	0.0039	0.0684	0.0512	0.0173	0.0512	0.1340	0.3376	0.6803	1.4311
	4.6995	1.2501	0.8868	4.1543	0.0079	0.0751	0.1641	0.0512	0.0857
	1.2107	0.7843	0.4280	0.2573	0.0783	0.1132	0.1431	1.1628	0.1179
	0.0292	0.0299	0.0216	2.3114	0.6713	0.6992	0.1565	0.1931	0.3195
	2.3259	0.1649	0.1292	0.0445	0.0584	0.5453	1.5104	0.2348	0.2063
	0.5625	3.4891	0.0702	0.3710	0.0286	0.1258	3.8810	0.6386	1.5393
	1.1309	0.0904	3.1761	0.7299	1.3818	0.3516	0.9578	0.6859	3.3194
	0.1357	0.7304	5.1273	0.0627	2.5372	0.2033	0.4067	0.0000	0.0634
	0.0952	0.6443	1.2880	1.3601	0.2655	3.2123	0.2422	1.7873	0.9118
	0.5310	0.9338	5.9559	0.9125	4.4856	0.6924	1.0387	0.1740	0.3480
	1.3847	0.3592	0.5378	0.3883	0.9571	0.4845			
30000.	2.7022	0.1546	0.2396	0.1854	2.2706	0.8243	0.6218	1.6364	0.8874
	0.0039	0.0681	0.0508	0.0172	0.0510	0.1352	0.3400	0.6840	1.4433
	4.7455	1.2436	0.8874	4.1602	0.0078	0.0746	0.1633	0.0510	0.0855
	1.2172	0.7929	0.4261	0.2570	0.0779	0.1126	0.1415	1.1644	0.1174
	0.0289	0.0297	0.0215	2.3296	0.6688	0.6974	0.1557	0.1917	0.3165
	2.3292	0.1642	0.1285	0.0443	0.0582	0.5445	1.5047	0.2336	0.2039
	0.5584	3.4940	0.0696	0.3694	0.0284	0.1253	3.8225	0.6273	1.5216
	1.1224	0.0879	3.1753	0.7257	1.3821	0.3514	0.9409	0.6818	3.2842
	0.1318	0.7262	5.1239	0.0625	2.5375	0.2005	0.4010	0.0000	0.0615
	0.0922	0.6443	1.2880	1.3478	0.2610	3.2085	0.2357	1.7874	0.9117
	0.5219	0.9253	5.9415	0.9125	4.4856	0.6908	1.0362	0.1735	0.3470
	1.3794	0.3585	0.5365	0.3873	0.9551	0.4834			

TABLE 4—*Continued*

Temp (K)									
32000.	2.7481	0.1550	0.2405	0.1869	2.2893	0.8281	0.6191	1.6390	0.8880
	0.0039	0.0679	0.0506	0.0172	0.0508	0.1362	0.3419	0.6866	1.4517
	4.7820	1.2383	0.8880	4.1659	0.0077	0.0742	0.1626	0.0508	0.0853
	1.2227	0.8006	0.4241	0.2566	0.0775	0.1119	0.1399	1.1660	0.1170
	0.0286	0.0296	0.0214	2.3454	0.6660	0.6953	0.1549	0.1902	0.3134
	2.3324	0.1635	0.1277	0.0441	0.0579	0.5435	1.4985	0.2324	0.2014
	0.5540	3.4989	0.0690	0.3678	0.0283	0.1247	3.7633	0.6169	1.5033
	1.1138	0.0854	3.1748	0.7217	1.3816	0.3510	0.9253	0.6776	3.2480
	0.1282	0.7223	5.1207	0.0622	2.5365	0.1983	0.3966	0.0000	0.0596
	0.0894	0.6440	1.2872	1.3363	0.2567	3.2054	0.2295	1.7865	0.9111
	0.5133	0.9173	5.9288	0.9120	4.4833	0.6890	1.0335	0.1729	0.3458
	1.3741	0.3577	0.5350	0.3862	0.9526	0.4820			
34000.	2.8041	0.1552	0.2410	0.1880	2.3044	0.8298	0.6169	1.6415	0.8886
	0.0038	0.0676	0.0503	0.0172	0.0506	0.1369	0.3433	0.6884	1.4568
	4.8103	1.2338	0.8886	4.1714	0.0077	0.0738	0.1619	0.0506	0.0850
	1.2273	0.8074	0.4221	0.2561	0.0771	0.1111	0.1383	1.1675	0.1165
	0.0283	0.0295	0.0213	2.3590	0.6631	0.6931	0.1542	0.1887	0.3102
	2.3355	0.1628	0.1270	0.0439	0.0576	0.5423	1.4921	0.2313	0.1991
	0.5492	3.5036	0.0684	0.3662	0.0282	0.1241	3.7043	0.6073	1.4848
	1.1050	0.0832	3.1742	0.7177	1.3804	0.3504	0.9110	0.6734	3.2114
	0.1247	0.7184	5.1176	0.0619	2.5341	0.1965	0.3930	0.0000	0.0578
	0.0867	0.6433	1.2858	1.3255	0.2525	3.2027	0.2236	1.7847	0.9101
	0.5051	0.9097	5.9170	0.9110	4.4785	0.6872	1.0308	0.1722	0.3445
	1.3687	0.3567	0.5333	0.3850	0.9498	0.4805			
36000.	2.8705	0.1553	0.2414	0.1888	2.3162	0.8298	0.6150	1.6439	0.8891
	0.0038	0.0673	0.0500	0.0172	0.0504	0.1374	0.3441	0.6894	1.4591
	4.8314	1.2301	0.8892	4.1767	0.0076	0.0735	0.1612	0.0504	0.0848
	1.2310	0.8134	0.4200	0.2555	0.0768	0.1103	0.1368	1.1690	0.1161
	0.0281	0.0293	0.0212	2.3707	0.6602	0.6907	0.1535	0.1870	0.3070
	2.3384	0.1620	0.1262	0.0437	0.0573	0.5410	1.4854	0.2303	0.1968
	0.5443	3.5079	0.0678	0.3646	0.0280	0.1235	3.6459	0.5985	1.4662
	1.0963	0.0810	3.1734	0.7139	1.3785	0.3496	0.8977	0.6692	3.1745
	0.1215	0.7146	5.1142	0.0616	2.5304	0.1951	0.3902	0.0000	0.0561
	0.0842	0.6422	1.2837	1.3152	0.2486	3.2002	0.2180	1.7820	0.9086
	0.4972	0.9026	5.9058	0.9095	4.4714	0.6852	1.0279	0.1715	0.3430
	1.3633	0.3555	0.5314	0.3836	0.9466	0.4788			
38000.	2.9479	0.1553	0.2414	0.1893	2.3253	0.8284	0.6135	1.6461	0.8897
	0.0038	0.0671	0.0497	0.0171	0.0502	0.1378	0.3446	0.6898	1.4592
	4.8463	1.2269	0.8897	4.1818	0.0075	0.0731	0.1605	0.0502	0.0844
	1.2341	0.8186	0.4179	0.2549	0.0764	0.1094	0.1352	1.1702	0.1156
	0.0278	0.0292	0.0211	2.3806	0.6572	0.6883	0.1528	0.1853	0.3039
	2.3410	0.1613	0.1255	0.0434	0.0570	0.5395	1.4787	0.2292	0.1945
	0.5393	3.5119	0.0673	0.3629	0.0279	0.1228	3.5886	0.5902	1.4476
	1.0875	0.0790	3.1722	0.7101	1.3759	0.3487	0.8854	0.6650	3.1376
	0.1185	0.7109	5.1103	0.0613	2.5253	0.1939	0.3879	0.0000	0.0545
	0.0818	0.6409	1.2809	1.3054	0.2448	3.1976	0.2127	1.7783	0.9066
	0.4897	0.8957	5.8948	0.9076	4.4619	0.6832	1.0248	0.1707	0.3414
	1.3577	0.3542	0.5292	0.3820	0.9429	0.4769			
40000.	3.0361	0.1551	0.2413	0.1896	2.3319	0.8258	0.6121	1.6483	0.8902
	0.0037	0.0668	0.0495	0.0171	0.0500	0.1379	0.3448	0.6895	1.4574
	4.8559	1.2242	0.8902	4.1866	0.0074	0.0727	0.1599	0.0500	0.0841
	1.2364	0.8231	0.4157	0.2542	0.0761	0.1084	0.1337	1.1713	0.1151
	0.0276	0.0290	0.0209	2.3890	0.6542	0.6857	0.1522	0.1836	0.3007
	2.3432	0.1605	0.1248	0.0432	0.0567	0.5380	1.4719	0.2282	0.1923
	0.5341	3.5153	0.0668	0.3612	0.0277	0.1221	3.5325	0.5826	1.4291
	1.0787	0.0771	3.1705	0.7063	1.3725	0.3476	0.8739	0.6607	3.1009
	0.1156	0.7072	5.1056	0.0610	2.5190	0.1930	0.3861	0.0000	0.0530
	0.0795	0.6392	1.2775	1.2959	0.2412	3.1947	0.2077	1.7737	0.9041
	0.4824	0.8892	5.8835	0.9052	4.4502	0.6810	1.0215	0.1698	0.3397
	1.3520	0.3528	0.5269	0.3803	0.9389	0.4747			

electron impact excitation,

$$q_{ij} = \frac{8.63 \times 10^{-6}}{\sqrt{T} g_i} e^{-E_{ij}/kT} \gamma_{ij} \quad \text{cm}^3\ \text{s}^{-1}\ , \qquad (2)$$

where E_{ij} is the energy difference between levels i and j and g_i is the statistical weight of level i.

The importance of the position of low-lying autoionizing resonances, as pointed out in §3.1, can be seen in equation (1) where values of the collision strength for low energies contribute significantly due to the exponential term; the values for high energies are attenuated in the average. This effect can be especially important at lower temperatures.

In Tables 2, 3, and 4, we present the Maxwellian averaged collision strengths, γ_{ij}, for C II, N III, and O IV, respectively. The key to the level numbers, which appear in the Transition Keys of Tables 2, 3, and 4, is found in Table 5. The corresponding observed energies (Moore 1949) of the levels are also given in Table 5.

It is convenient to divide the effective collision strength into two components, one from contributions of collision strengths at energies below the highest target threshold where autoionizing resonances are present and one above this threshold where they are not. The close-coupling method is highly accurate for this first component but sometimes becomes less so for the second where pseudo-resonances (nonphysical features) may appear in the collision strengths at higher energies and may thus serve to overestimate the average collision strength. For low-lying transitions and lower temperatures, the effect of the pseudoresonances will be negligible on the rate coefficient. However, for transitions among high-lying states, especially those to the highest target threshold where the collision strength is due entirely to the component without autoionizing resonances, the effect of the pseudo-resonances can be significant (see Luo & Pradhan 1990).

By accounting for these two components, it is possible to place the following approximate error estimates on the Maxwellian-averaged collision strengths in Tables 2, 3, and 4. For the important IR and UV transitions listed in Table 1, among levels that lie fairly low in the close-coupling expansion, the collision strengths and, consequently, the rate coefficients should be accurate to ~10%, with the possible exception of the $^2P^o_{1/2}$–$^2P^o_{3/2}$ transition in C II (see the discussion in § 3.1) where the uncertainty may be up to 30%. For excitations to levels lying higher than the $2s2p^2(^4P)$ state, the uncertainties in the rate coefficients could be from 20% up to a factor of 2; the degradation in accuracy generally follows the excitation energy of the upper level.

5. CONCLUSION

New results are presented for the collision strengths and Maxwellian-averaged collision strengths for electron impact excitation of a number of states of C II, N III, and O IV, including fine structure, and astrophysically important features are pointed out. The levels considered are $2s^22p(^2P^o_{1/2,3/2})$, $2s2p^2(^4P_{1/2,3/2,5/2}, {}^2D_{3/2,5/2}, {}^2S_{1/2}, {}^2P_{1/2,3/2})$, $2s^23s(^2S_{1/2})$, $2s^23p(^2P^o_{1/2,3/2})$, $2p^3(^4S^o_{3/2}, {}^2D^o_{3/2,5/2}, {}^2P^o_{1/2,3/2})$ for C II, and all except the $n = 3$ levels for N III and O IV.

Work is in progress on the emissivities of the IR and the UV lines of the three ions under varying conditions of temperature and density. Other processes of importance in these calculations may be proton impact excitation of closely spaced fine-structure levels and excitation by neutral hydrogen of the $^2P^o_{1/2}$–$^2P^o_{3/2}$ transition in C II.

The present calculations are an extension of the work carried out for the Opacity Project (Seaton 1987; Pradhan 1987; Nahar & Pradhan 1991). A similar target representation has been developed for the other ions of the boron-isoelectronic sequence: Ne VI, Na VII, Mg VIII, Al IX, Si X, S XII, Ar XIV, Ca XVI, and Fe XXII. Further calculations for the highly charged ions of the B-sequence are in progress.

TABLE 5

LEVEL NUMBERS AND ENERGIES

LEVEL DESIGNATION	C II		N III		O IV	
	Number	Energy (Ryd)	Number	Energy (Ryd)	Number	Energy (Ryd)
$2s^22p(^2P^o_{1/2})$	1	0.0	1	0.0	1	0.0
$2s^22p(^2P^o_{3/2})$	2	0.000583	2	0.001590	2	0.003522
$2s2p^2(^4P_{1/2})$	3	0.391847	3	0.521173	3	0.648613
$2s2p^2(^4P_{3/2})$	4	0.392044	4	0.521719	4	0.649810
$2s2p^2(^4P_{5/2})$	5	0.392307	5	0.522459	5	1.156729
$2s2p^2(^2D_{3/2})$	6	0.682842	6	0.920667	6	0.651491
$2s2p^2(^2D_{5/2})$	7	0.682821	7	0.920597	7	1.156856
$2s2p^2(^2S_{1/2})$	8	0.879319	8	1.193792	8	1.497822
$2s2p^2(^2P_{1/2})$	9	1.008090	9	1.329321	9	1.644667
$2s2p^2(^2P_{3/2})$	10	1.008466	10	1.330327	10	1.646884
$2s^23s(^2S_{1/2})$	11	1.061971				
$2s^23p(^2P^o_{1/2})$	12	1.200364				
$2s^23p(^2P^o_{3/2})$	13	1.200465				
$2p^3(^4S^o_{3/2})$	14	1.294222	11	1.702268	11	2.107534
$2p^3(^2D^o_{3/2})$	15	1.371165	12	1.850682	12	2.325426
$2p^3(^2D^o_{5/2})$	16	1.371118	13	1.850530	13	2.325159
$2p^3(^2P^o_{1/2})$	17	1.537596	14	2.099601	14	2.633709
$2p^3(^2P^o_{3/2})$	18	1.537765	15	2.099638	15	2.633781

This work was supported in part by a grant from NASA (NAG 5-1644). The computational work was carried out on the Cray Y-MP at the Ohio Supercomputer Center in Columbus, Ohio.

REFERENCES

Berrington, K. A., Burke, P. G., Butler K., Seaton, M. J., Storey, P. J., Taylor, K. T., & Yu, Y. 1987, J. Phys., B 20, 6379
Blum, R. D., & Pradhan, A. K. 1991, Phys. Rev. A, submitted
Doschek, G., Feldman, U., & Cohen, L. 1977, ApJ, 33, 101
Edlen, B. 1934, Nova Acta R. Soc. Sci. Uppsala, 9, 103
Hayes, M. A. 1983, J. Phys. B, 16, 285
Hayes, M. A., & Nussbaumer, H. 1984, A & A, 134, 193
Keenan, F. P., Lennon, D. J., Johnson, C. T., & Kingston, A. E. 1986, MNRAS, 220, 571
Lennon, D. J., Dufton, P. L., Hibbert, A., & Kingston, A. E. 1985, ApJ, 294, 200
Luo, D., & Pradhan, A. K. 1990, Phys. Rev., A41, 165
Moore, C. E. 1949, Atomic Energy Levels, I
Nussbaumer, H., & Storey, P. J. 1979, A & A, 71, L5
Pwa, T. H., Mo, J. E., & Pottasch, S. R., 1984, A & A, 139, L1
Saraph, M. E. 1972, Comput. Phys. Comm., 3, 256
——— 1978, Comput. Phys. Comm., 15, 247
Seaton, M. J. 1987, J. Phys., B 20, 6363
Stencel, R. E., Linsky, J. L., Brown, A., Jordan, C., Carpenter, K. G., Wing, R. F., & Czyzak, S. 1981, MNRAS, 196, 4P

Fine structure and resonance transitions in C^+

Robert D. Blum and Anil K. Pradhan
Department of Astronomy, Ohio State University, Columbus, Ohio 43210
(Received 3 June 1991; revised manuscript received 15 July 1991)

Certain significant features in the collision strengths for electron-impact excitation of the fine-structure transition $^2P^\circ_{1/2}$-$^2P^\circ_{3/2}$ and the resonance transition $^2P^\circ$-^2D in C^+ are discussed based on improved calculations.

PACS number(s): 34.80.Kw

I. INTRODUCTION

R-matrix calculations in the close-coupling approximation have been reported earlier by Luo and Pradhan [1] for electron-impact excitation of a number of transitions in C^+, N^{2+}, and O^{3+} including fine structure. Of particular interest is the fine-structure transition within the ground state, $^2P^\circ_{1/2}$-$^2P^\circ_{3/2}$, and the first dipole-allowed (resonance) transition $^2P^\circ$-^2D. The former transition gives rise to a well-known [2,3] line in the infrared spectra of many astrophysical sources and it is important to determine the excitation cross section and rate coefficient accurately. The resonance transition in C^+ is currently the subject of experimental investigations using the crossed-beam [4] and the merged-beam techniques [5] for electron-ion scattering. Owing to the importance of these transitions we have entirely repeated the calculations of Luo and Pradhan, improving upon them in a number of respects.

The fine-structure transition $^2P^\circ_{1/2}$-$^2P^\circ_{3/2}$ has been considered by a number of previous studies, both in electron-C^+ scattering [2,3] and photoionization calculations [6,7] for C°. The cross sections are seen to be dominated by an autoionizing state, $2s2p^3(^1D^\circ)$, that lies just above the excitation threshold. Two of the previous calculations, by Luo and Pradhan [1] and Lennon *et al.* [3], obtained the resonance shape and position in substantial agreement with each other, and in disagreement with that of Hayes and Nussbaumer [2]. Although the $2s2p^3(^1D^\circ)$ level has not been observed, it was suggested by both Lennon *et al.* and Hayes and Nussbaumer that in calculating the rate coefficients the resonance position should be shifted closer to the excitation threshold to coincide with the value predicted by Edlen [8] in 1934. In the present study we extend the work of Luo and Pradhan to analyze the $^2P^\circ_{1/2}$-$^2P^\circ_{3/2}$ collision strength in terms of the individual angular momentum contributions with respect to the position and the shape of the resonance structures.

For the dipole transition, $^2P^\circ$-^2D, the work of Luo and Pradhan is also extended to include more partial waves explicitly in the close-coupling calculations and collision strengths in the region above all excitation thresholds are obtained (the earlier work did not consider this region due to the presence of pseudoresonances).

II. CALCULATIONS

Some of the improvements made over the previous Luo and Pradhan calculations are as follows.

(i) Observed target energies were substituted for calculated ones in the eigenfunction expansion, thus giving a more precise scale for the positions of autoionizing resonances. The ten target states included in the calculations are as follows: $2s^22p(^2P^\circ)$, $2s2p^2(^4P,^2D,^2S,^2P)$, $2s^23s(^2S)$, $2s^23p(^2P^\circ)$, $2p^3(^4S^\circ,^2D^\circ,^2P^\circ)$. Although the experimental and the calculated target energies are very close with the maximum discrepancy of 3% for the ^4P state [1], the small corrections to the eigenvalues of the diagonal elements of the Hamiltonian for the target ion give a slightly better representation of the positions of the Rydberg series of resonances that might affect the calculation of Maxwellian averaged rate coefficients. Given the extensive resonance structures present, and the sensitivity of the rate coefficients to these, the present calculations should yield better accuracy.

(ii) A more complete partial-wave expansion is employed for enhanced accuracy in the collision strengths for dipole-allowed transition; in the present work we employ partial waves up to $l \leq 10$, whereas the earlier work used $l \leq 4$, along with a Coulomb-Bethe-type method for "topping-up" or completing the partial-wave summation. Also, in the present work we have obviated the problem of pseudoresonances, in the region of all channels open, which did not enable the previous work to obtain accurate collision strengths in this region. The close-coupling calculations for $l \leq 10$ are carried up to the highest threshold of excitation of C^+ (with the top-up procedure as before). However, in the region of all channels open, we carry out separate Coulomb-Bethe calculations and *normalize* the results at the highest threshold, $2p^3(^2P^\circ)$, to the ten-state close-coupling (hereafter 10CC) calculations. It is known that the Coulomb-Bethe (hereafter CBe) approximation overestimates the collision strengths due to low partial waves describing close encounters [9]. This, for example, was found to be the case for all dipole transitions considered in the present work. The normalized results are labeled as 10CC+CBe and show a smooth variation with energy, consistent with the theoretical Bethe form $\Omega \sim \ln E$, free of pseudoresonances

that appear in many close-coupling calculations (due to correlation-type functions often represented by pseudo-orbitals [10]).

(iii) The calculations of Luo and Pradhan [1] were carried out using the R-matrix package of codes developed for the Opacity Project [11]. The fine-structure collision strengths were calculated using a new code, STGFJ, that separately transformed the reactance matrices obtained from the R-matrix codes from LS to a pair-coupling representation.

Some errors in the earlier work have been corrected. Although these are minor, mostly related to incomplete summation over some contributing channels of high-symmetry states ($J\pi$) in pair coupling, the final results for some of the transitions are affected; the $^2P^o_{1/2}$-$^2P^o_{3/2}$ collision strength changes by a few percent over the energy range considered. The procedure has also been improved by incorporating STGFJ directly into the R-matrix package of codes [11], thus enabling more detailed calculations to be carried out in a flexible manner, in particular by varying energy meshes and by delineating the individual contributions from the various total $J\pi$ states to the fine-structure collision strengths.

III. DISCUSSION OF RESULTS

A. Ground-state fine-structure transition

In Fig. 1 we present the total and the individual $J\pi$ contributions to the collision strength for the fine-structure transition $^2P^o_{1/2}$-$^2P^o_{3/2}$. It has been pointed out by Keenan *et al.* [12] that the collision strength exhibits a near-threshold resonance, due to the autoionizing state $2s2p^3(^1D^o)$, with a broad shoulder on the low-energy side. The calculations by Hayes and Nussbaumer [3], on the other hand, showed the shoulder to be on the high-energy side. Our results, and the results of Keenan *et al.*, show that the low-energy rise is due to the contribution to the collision strength by the total $J\pi$ symmetry $J=2$, odd parity. Our further analysis for other $J\pi$ symmetries, $J=0,1,2,3$ even and odd parities, shows all of those to contribute in the higher-energy region.

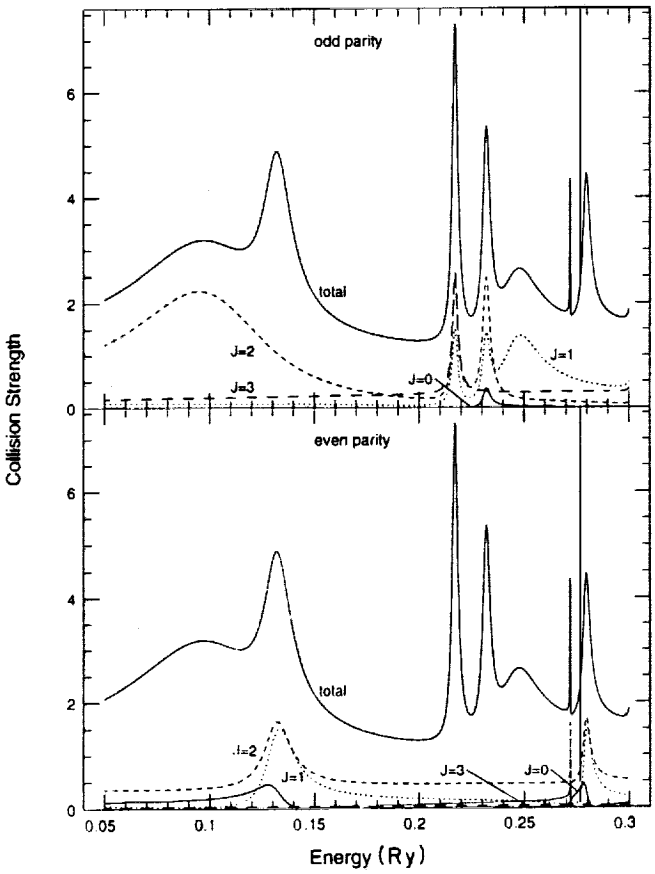

FIG. 1. Individual and total $J\pi$ contributions to the collision strength for the $2s^22p(^2P^o_{1/2}$-$^2P^o_{3/2})$ fine-structure transition.

It is important to determine, as precisely as possible, the detailed shape and position of this resonance as it influences the Maxwellian averaged rate coefficient for this transition to a great degree. The present results in Fig. 1 show the resonance to be at an energy somewhat lower than that of Keenan *et al.*, but essentially confirming the position and the shape that they obtain, and in disagreement with that of Hayes and Nussbaumer. However, both the previous calculations recommended that the calculated position of this resonance should be shifted by -0.06 Ry to coincide with the apparently observed position by Edlen (1934) [8]. An investigation of the work by Edlen shows that the position of the $2s2p^3(^1D^o)$ resonance was not in fact observed but rather extrapolated from the observed positions of the *bound* state in N^+ and O^{2+}. As such, the extrapolated position may not be highly reliable [13].

Nussbaumer and Storey [14] have carried out extensive configuration-interaction-type bound-state calculations for a large number of bound states of C°, including low-lying autoionizing states, to obtain recombination rate coefficients. However, for the $2s2p^3(^1D^o)$ state they quote only the extrapolated value by Edlen. In an effort to determine the position from bound-state atomic structure calculations we employed the SUPERSTRUCTURE program [15] with an even more extended basis set than Nussbaumer and Storey consisting of 66 configurations. However, the resulting value was much higher, 0.15 Ry above the C^+ ionization threshold, than the close-coupling calculations which yield the resonance position to be at 0.09 Ry. The photoionization calculations by Burke and Taylor [6] and Hofmann, Saha, and Trefftz [7] also report higher values, 0.12 and 0.14 Ry, respectively. In any case, a detailed comparison by Luo and Pradhan [16] with the work of Nussbaumer and Storey and other workers shows that the close-coupling results for the bound states of C° and N^+ are at least as accurate as the large configuration-interaction-type calculations. This is also reflected in the close agreement with experiment for the radiative transition probabilities for all transitions considered, a reliable indicator of the accuracy of the wave functions calculated [16]. We therefore suggest that the present resonance position and the collision strength in the near-threshold region is accurate and may not require a shift to lower energies.

The precise effect on the rate coefficients is shown in Table I, where the two sets of values under "Keenan *et al.*" are the Maxwellian averaged collision strengths by Keenan *et al.* with and without the shift of the

TABLE I. Maxwellian averaged collision strengths for the $2s^22p(^2P^o_{1/2}$-$^2P^o_{3/2})$ transition. The two columns under "Keenan *et al.*" are the rate coefficients by Keenan *et al.* with and without the shift of the $2s2p^3(^1D^o)$ resonance to the lower energy.

	Keenan *et al.* [12]		
$\log_{10}T$ (K)	Without shift	With shift	Present
3.0	1.60	2.16	1.58
4.0	2.11	2.76	2.15

$2s2p^3(^1D^o)$ resonance to the lower energy, compared with the present values at two temperatures that mark the range of interest in practical applications. While we reconfirm the unshifted values of Keenan *et al.*, the maximum difference between the two sets of rate coefficients is approximately 30% at the temperature of 1000 K. It is possible that with the lower value for electron-impact excitation some other process may be more important in the excitation of the ground-state fine-structure transition, e.g., H impact on C^+. Perhaps the final resolution of the discrepancy appears to be an experimental reexamination of the resonance position; we hope that the present work will provide an incentive for such a study.

B. Resonance transition

The collision strength for the $^2P^o$-^2D transition is presented in Fig. 2, showing the combined 10CC+CBe calculations. The present results are slightly higher than those of Luo and Pradhan [1] at threshold. The rich resonance structure in the region covered by the ten states included in the eigenfunction expansion has been delineated and shows a significant enhancement in the energy range 0.8–0.9 Ry (the excitation threshold energy is 0.6824 Ry). The enhancement, relative to the background, appears to be sufficiently large to be observed experimentally. The present collision strengths, with more partial waves included, are 5–10 % higher than the values of Luo and Pradhan [1] in the energy range considered.

At the energy of the highest threshold, $2p^3(^2P^o)$, the CBe collision strengths were scaled uniformly to the 10CC collision strengths (including the high-l top-up), by an amount equal to the difference between the 10CC and the CBe values *at only this energy*. No other adjustment was made to the CBe values. A very satisfactory energy behavior appears to have been thus obtained as one can readily discern that the *background* collision strength, from the excitation threshold onwards, shows a fairly smooth and monotonic increase all throughout the energy range characteristic of an optically allowed transition. This relatively simple method appears to effectively treat the high-energy region where pseudoresonances often plague the otherwise highly accurate close-coupling calculations. Of course in this particular case the energy range above the $2s2p^3(^2P^o)$ threshold is not likely to affect the rate coefficient for this transition as the Maxwellian at typical temperatures of around 10 000 K for the abundance of C^+ assumes extremely small values.

C. Comparison of *LS* multiplet to fine-structure collision strengths

The collision strengths for fine-structure transitions are calculated through an algebraic transformation of the reactance matrices (i.e., the K matrices) to a pair-

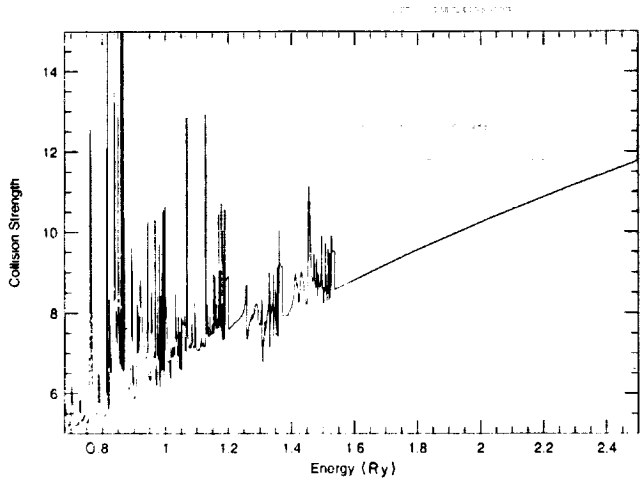

FIG. 2. Collision strength for the $^2P^o$-^2D resonance transition showing the combined 10CC+CBe results, where the CBe value is matched to the CC value at the highest target threshold in the CC expansion.

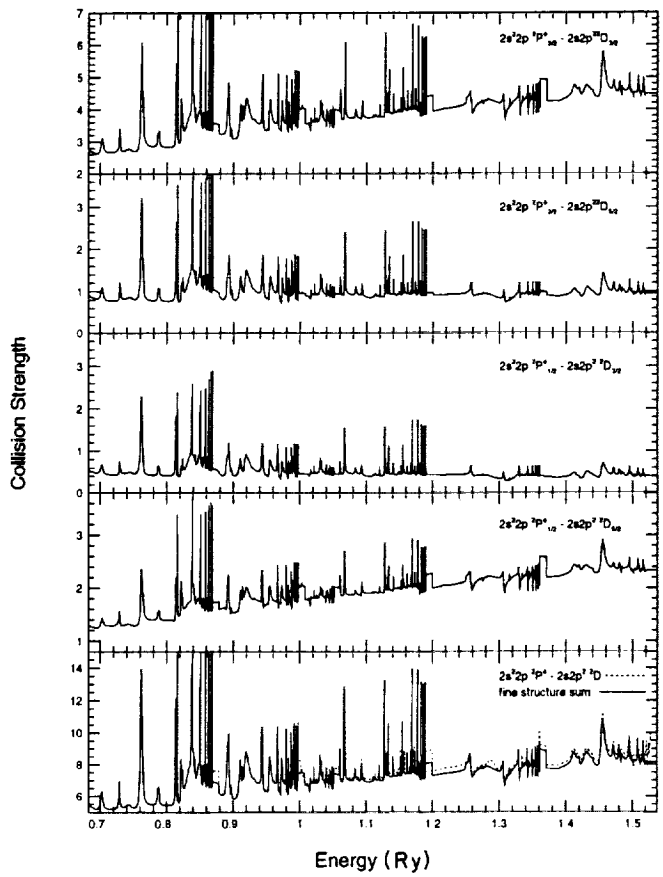

FIG. 3. Comparison of the *LS* multiplet and the sum of the fine-structure collision strengths for the $^2P^o$-^2D transition. The individual fine-structure components of the *LS* multiplet collision strength are also shown.

coupling representation. While the collision strengths for the multiplet transitions in LS coupling enable a top-up procedure to be employed based on the CBe approximation [17], no such procedure has been developed for the fine-structure transitions. Furthermore, the fine-structure collision strengths are calculated by transforming the K matrices for all the contributing total $SL\pi$ symmetries to the total $J\pi$ states for the $e+$ion system and the two sets of total symmetries (in LS and pair-coupling representations) do not precisely match in terms of individual contributions. Therefore in order to ensure that the fine-structure collision strengths are complete, particularly for the allowed transitions where a relatively large number of partial waves may contribute, it is necessary to include a sufficient number of $SL\pi$ states in the LS coupling calculations to attain convergence.

A useful check on the individual fine-structure collision strengths is provided by comparing the *sum* of the fine-structure components with the LS coupling values for the whole multiplet, i.e., $\sum_{J_i,J_{i'}} \Omega(S_iL_iJ_i - S_{i'}L_{i'}J_{i'})$ with $\Omega(S_iL_i - S_{i'}L_{i'})$. In Fig. 3 we show the collision strengths for the fine-structure components ${}^2P^o_J$-${}^2D_{J'}$ of the ${}^2P^o$-${}^2D$ multiplet and compare with the total. The close agreement between the two is an indication of the fact that the fine-structure collision strengths have converged in the same way as the total multiplet collision strength in terms of the contributing partial waves. Owing to some errors in the work of Luo and Pradhan [1], the individual fine-structure collision strengths did not add up to the total LS values, although the discrepancies were no more than 20% in the worst case.

In addition to the theoretical requirement that the sum of fine-structure components should add up to the LS value if only an algebraic transformation is carried out, it is also of practical importance in that we can now determine the rate coefficients for the individual components for the optically allowed fine-structure transitions; this has not been done before to our knowledge. Often the observed spectra consist of lines corresponding to the transitions within the fine-structure components rather than the whole multiplet. This is increasingly the case as the resolution of the spectroscopic instruments improves.

Further extending the work of Luo and Pradhan, rate coefficients have been computed for a large number of transitions, including all the fine-structure sublevels, at a range of temperatures for C^+, N^{2+}, and O^{3+}. The data involve 153 transitions in C^+ and 105 transitions in N^{2+} and O^{3+} corresponding to 18 and 15 states, including fine structure, respectively. Rate coefficients for each transition are planned to be tabulated at approximately ten temperatures close to the maximum abundance of each ion in ionization equilibrium [18].

ACKNOWLEDGMENTS

This work was supported in part by NASA Grant No. NAG 5-1644. The computational work was carried out on the Cray-YMP at the Ohio Supercomputer Center in Columbus, Ohio.

[1] D. Luo and A. K. Pradhan, Phys. Rev. A **41**, 165 (1990).
[2] M. A. Hayes and H. Nussbaumer, Astron. Astrophys. **134**, 193 (1984).
[3] D. J. Lennon, P. L. Dufton, A. Hibbert, and A. E. Kingston, Astrophys. J. **294**, 200 (1985).
[4] L. D. Gardner, J. L. Kohl, D. B. Reisenfeld, D. W. Savin, and A. R. Young, Bull. Am. Phys. Soc. **36**, 1251 (1991).
[5] G. H. Dunn, Bull Am. Phys. Soc. **36**, 1327 (1991).
[6] P. G. Burke and K. T. Taylor, J. Phys. B **12**, 2971 (1979).
[7] H. Hofmann, H. P. Saha, and E. Trefftz, Astron. Astrophys. **126**, 415 (1983).
[8] B. Edlen, Nova Acta Reg. Soc. Sci. Uppsala **9**, 103 (1934).
[9] Alan Burgess and John A. Tully, J. Phys. B **11**, 4271 (1978).
[10] R. B. Christensen, D. W. Norcross, and A. K. Pradhan, Phys. Rev. A **34**, 4704 (1986).
[11] K. A. Berrington, P. G. Burke, K. Butler, M. J. Seaton, P. J. Storey, K. T. Taylor, and Y. Yu, J. Phys. B **20**, 6379 (1987).
[12] F. P. Kennan, D. J. Lennon, C. T. Johnson, and A. E. Kingston, Mon. Not. R. Astron. Soc. **220**, 571 (1986).
[13] L. J. Curtis, L. Johansson, and I. Martinson (private communication).
[14] H. Nussbaumer and P. J. Storey, Astron. Astrophys. **134**, 193 (1984).
[15] W. Eissner, H. Nussbaumer, and M. Jones, Comput. Phys. Commun. **8**, 270 (1974).
[16] D. Luo and A. K. Pradhan, J. Phys. B **22**, 3377 (1989).
[17] V. M. Burke and M. J. Seaton, J. Phys. B **19**, L527 (1986).
[18] R. D. Blum and A. K. Pradhan (unpublished).

25/11/92

N93-14762

ELECTRON DENSITY DIAGNOSTICS FOR GASEOUS NEBULAE INVOLVING THE O IV INTERCOMBINATION LINES NEAR 1400 Å

F. P. KEENAN, E. S. CONLON, AND D. A. BOWDEN

Department of Pure and Applied Physics, The Queen's University of Belfast, Belfast BT7 1NN, Northern Ireland, UK

W. A. FEIBELMAN[1]

Laboratory for Astronomy and Solar Physics, Code 684.1, NASA–Goddard Space Flight Center, Greenbelt MD 20771

AND

A. K. PRADHAN

Department of Astronomy, The Ohio State University, Columbus OH 43210

[1]Guest observer with the International Ultraviolet Explorer satellite, which is operated and sponsored by the National Aeronautics and Space Adnministration, by the European Space Agency, and by the Science and Engineering Research Council of the United Kingdom.

ABSTRACT

Theoretical O IV electron density sensitive emission line ratios, determined using electron impact excitation rates calculated with the R-matrix code, are presented for R_1 = I(1407.4 Å)/I(1401.2 Å), R_2 = I(1404.8 Å)/I(1401.2 Å), R_3 = I(1399.8 Å)/I(1401.2 Å) and R_4 = I(1397.2 Å)/I(1401.2 Å). The observed values of R_1 – R_4, measured from high resolution spectra obtained with the *International Ultraviolet Explorer* (IUE) satellite, lead to electron densities that are compatible, and which are also in good agreement with those deduced from line ratios in other species. This provides observational support for the accuracy of the atomic data adopted in the present calculations.

Subject headings: atomic data — binaries: symbiotic — planetary nebulae: general — ultraviolet: stars

1. INTRODUCTION

The O IV $2s^2 2p\ ^2P - 2s2p^2\ ^4P$ intercombination lines near 1400 Å have been observed in the spectra of astrophysical sources, including planetary nebulae (Hayes & Nussbaumer 1983), symbiotic stars (Feibelman 1982), and the solar transition region (Sandlin et al. 1986). Flower & Nussbaumer (1975) first pointed out the diagnostic applications of emission line ratios involving these transitions, and presented relative line strengths determined using electron impact excitation rates calculated in the distorted-wave approximation (Eissner & Seaton 1972). Hayes & Nussbaumer (1983) subsequently rederived these ratios using more accurate electron rates deduced with the IMPACT computer code of Crees, Seaton, & Wilson (1978).

Recently Blum & Pradhan (1992) have calculated excitation rates for transitions in O IV using the R-matrix method as adapted for the Opacity Project (Seaton 1987; Berrington et al. 1987), and found results somewhat different from those of Hayes & Nussbaumer (1983). For example, at $T_e = 5000$ K, the Blum & Pradhan rate for the $2s^2 2p\ ^2P_{1/2} - 2s2p^2\ ^4P_{1/2}$ transition is ~15% larger than that of Hayes & Nussbaumer, while for the $2s2p^2\ ^4P_{1/2} - 2s2p^2\ ^4P_{5/2}$ transition the R-matrix data are ~20% larger. In this paper we use the Blum & Pradhan results to derive emission line ratios applicable to gaseous nebulae, and compare these with observations obtained with the *International Ultraviolet Explorer* (IUE) satellite.

2. THEORETICAL RATIOS

The model ion for O IV consisted of the 15 energetically lowest fine-structure levels, namely $2s^22p\ ^2P_{1/2,3/2}$; $2s2p^2\ ^4P_{1/2,3/2,5/2}$, $^2D_{3/2,5/2}$, $^2S_{1/2}$, $^2P_{1/2,3/2}$; $2p^3\ ^4S_{3/2}$, $^2D_{3/2,5/2}$ and $^2P_{1/2,3/2}$. Energies for all these levels were obtained from Fawcett (1975).

Electron impact excitation rates for transitions in O IV were taken from Blum & Pradhan (1992), while for Einstein A-coefficients the calculations of Nussbaumer & Storey (1982) and Dankworth & Trefftz (1977) were adopted. As noted by, for example Seaton (1964), excitation by protons may be important for fine-structure transitions. However Flower & Nussbaumer (1975) found proton rates for transitions within $2s^22p\ ^2P$ and $2s2p^2\ ^4P$ to be typically a factor of 100 smaller than the corresponding electron rates at the temperatures considered here. Hence these rates should have a negligible effect on the theoretical line intensities for O IV.

Using the atomic data discussed above in conjunction with the statistical equilibrium code of Dufton (1977), relative O IV level populations and hence emission line strengths were calculated for a range of electron temperatures and densities. The following assumptions were made in the calculations, (i) that photoexcitation and de-excitation rates are negligible in comparison with the corresponding collisional rates, (ii) that ionization to and recombination from other ionic levels is slow compared with bound-bound rates, and (iii) that all transitions are optically thin. Further details of the procedures involved may be found in Dufton (1977) and Dufton et al. (1978).

In Figures 1 and 2 we plot the theoretical ratios

$$R_1 = I(2s^22p\ ^2P_{3/2} - 2s2p^2\ ^4P_{1/2})/I(2s^22p\ ^2P_{3/2} - 2s2p^2\ ^4P_{5/2})$$

$$= \mathrm{I}(1407.4\ \text{Å})/\mathrm{I}(1401.2\ \text{Å}),$$

$$\mathrm{R}_2 = \mathrm{I}(2s^2 2p\ ^2\mathrm{P}_{3/2} - 2s2p^2\ ^4\mathrm{P}_{3/2})/\mathrm{I}(2s^2 2p\ ^2\mathrm{P}_{3/2} - 2s2p^2\ ^4\mathrm{P}_{5/2})$$
$$= \mathrm{I}(1404.8\ \text{Å})/\mathrm{I}(1401.2\ \text{Å})$$

as a function of electron density for a range of electron temperatures, T_e = 5000 – 40000 K. An inspection of the figures reveals that the temperature dependence of the ratios is small, but that they vary with density for $\mathrm{N}_e \geq 10^2$ cm^{-3}. For example, at T_e = 10000 K, R_1 and R_2 change by factors of 2.8 and 2.1, respectively, between $\mathrm{N}_e = 10^2$ and 10^6 cm^{-3}. However the variation in the ratios between T_e = 10000 and 20000 K is only 11% (R_1) and 9% (R_2) at $\mathrm{N}_e = 10^2$ cm^{-3}, which decreases to 2% (R_1) and 1% (R_2) at $\mathrm{N}_e = 10^6$ cm^{-3}. We note that the ratios

$$\mathrm{R}_3 = \mathrm{I}(2s^2 2p\ ^2\mathrm{P}_{1/2} - 2s2p^2\ ^4\mathrm{P}_{1/2})/\mathrm{I}(2s^2 2p\ ^2\mathrm{P}_{3/2} - 2s2p^2\ ^4\mathrm{P}_{5/2})$$
$$= \mathrm{I}(1399.8\ \text{Å})/\mathrm{I}(1401.2\ \text{Å}),$$

$$\mathrm{R}_4 = \mathrm{I}(2s^2 2p\ ^2\mathrm{P}_{1/2} - 2s2p^2\ ^4\mathrm{P}_{3/2})/\mathrm{I}(2s^2 2p\ ^2\mathrm{P}_{3/2} - 2s2p^2\ ^4\mathrm{P}_{5/2})$$
$$= \mathrm{I}(1397.2\ \text{Å})/\mathrm{I}(1401.2\ \text{Å})$$

have the same density dependence due to common upper levels as R_1 and R_2, respectively, but with

$$\mathrm{R}_3 = 0.987 \times \mathrm{R}_1,$$

$$\mathrm{R}_4 = 0.176 \times \mathrm{R}_2.$$

The present calculations in Figures 1 and 2 may be compared with those of Hayes & Nussbaumer (1983). Our results for R_1 and R_2 are up to ~15%

different from those of Hayes & Nussbaumer, which is principally due to the adoption of improved electron impact excitation rates in the present analysis.

3. RESULTS AND DISCUSSION

Observed values of R_1 – R_4 have been measured from high resolution ultraviolet spectra obtained with the IUE satellite. The objects considered (the planetary nebulae NGC 3918 and NGC 7662, and the symbiotic stars RR Tel and V1016 Cyg) are listed in Table 1, along with the IUE images used in the analysis. Also given are the derived emission line ratios, which were determined using the Goddard Regional Data Reduction Facility. We note that the O IV 1404.8 Å feature is blended with the S IV $3s^2 3p\ ^2P_{1/2} - 3s3p^2\ ^4P_{1/2}$ line. However this S IV transition is predicted to be $\leq$20% of the intensity of the S IV $3s^2 3p\ ^2P_{3/2} - 3s3p^2\ ^4P_{5/2}$ component at 1406.0 Å (Dufton et al. 1982). From the extreme weakness (or absence) of the 1406.0 Å line in our spectra, we estimate that S IV contributes $\leq$3% to the total strength of the O IV/S IV 1404.8 Å blend, and hence may be neglected. The spectra of RR Tel and NGC 7662 are plotted in Figures 3 and 4, respectively, to illustrate the quality of the observational data, and to show the relative strengths of the O IV 1404.8 Å and S IV 1406.0 Å lines.

In Table 2 we summarise the electron densities derived from the observed values of R_1 – R_4 in conjunction with the calculations in Figures 1 and 2, along with the adopted electron temperatures from the references listed. An inspection of the table reveals that for NGC 3918 and NGC 7662 the derived densities are compatible, with values that differ by typically <0.2 dex from the mean estimates ($\overline{log\ N_e}$ = 3.7 and 4.0 for NGC 3918 and NGC 7662, respectively). However in the case of V1016 Cyg, the electron density predicted from R_4 is approximately a factor of 50 lower than those estimated from R_1 and R_3. This is probably due to the fact that the 1397.2 Å line in the V1016

Cyg spectrum is weak and shows an asymmetry in the line profile, implying that it may be blended. We note that the observed R_4 ratio would need to be decreased by $\sim$20% for it to give the same electron density as R_1 and R_3.

Also listed in Table 2 are the electron densities derived from line ratios in species with similar ionization potentials, and hence spatial distributions to O IV, such as I(4711 Å)/I(4740 Å) in Ar IV. The values of log N_e estimated from R_1 – R_4 may be seen to be very similar to those deduced from other line ratios, with discrepancies that average only 0.2 dex, when the R_4 result for V1016 Cyg is excluded. In addition, we note that the observed ratios that are in the high density limit (R_1 – R_4 in RR Tel and R_2 in V1016 Cyg) only differ from the predicted high density values by $\lesssim$10%. These results provide experimental support for the accuracy of the present O IV line ratio calculations, and hence the atomic data employed in their derivation.

We would like to thank A. E. Kingston for his continued interest in the work. ESC is grateful to the Science and Engineering Research Council (UK) for financial support, while DAB acknowledges financial assistance from the Culham Laboratory, the Department of Physics (QUB) and the Department of Education for N. Ireland. AKP acknowledges partial support from NASA grant NAG 5-1644. The IUE archival portion of this work was supported by the Goddard Regional Data Analysis Facility (RDAF). This work was financially supported by NATO travel grant 0469/87.

REFERENCES

Berrington, K.A., Burke, P.G., Butler, K., Seaton, M.J., Storey, P.J., Taylor, K.T., & Yu, Y. 1987, J. Phys. B, 20, 6379.

Blum, R.D., & Pradhan, A.K. 1992, ApJS, 80, 425.

Crees, M.A., Seaton, M.J., & Wilson, P.M.H. 1978, Computer Phys. Comm., 15, 23.

Dankworth, W., & Trefftz, E. 1977, J. Phys. B, 10, 2541.

Dufton, P.L. 1977, Computer Phys. Comm., 13, 25.

Dufton, P.L., Berrington, K.A., Burke, P.G., & Kingston, A.E. 1978, A&A, 62, 111.

Dufton, P.L., Hibbert, A., Kingston, A.E., & Doschek, G.A. 1982, ApJ, 257, 338.

Eissner, W., & Seaton, M.J. 1972, J. Phys. B, 5, 2187.

Fawcett, B.C. 1975, Atom. Data Nucl. Data Tables, 16, 135.

Feibelman, W.A. 1982, ApJ, 258, 548.

Flower, D.R., & Nussbaumer, H. 1975, A&A, 45, 145.

Hayes, M.A., & Nussbaumer, H. 1983, A&A, 124, 279.

———. 1986, A&A, 161, 287.

Kaler, J.B. 1986, ApJ, 308, 322.

Nussbaumer, H., & Storey, P.J. 1982, A&A, 115, 205.

Rowlands, N., Houck, J.R., Herter, T., Gull, G.E., & Skrutskie, M.F. 1989, ApJ, 341, 901.

Sandlin, G.D., Bartoe, J.-D.F., Brueckner, G.E., Tousey, R., & VanHoosier, M.E. 1986, ApJS, 61, 801.

Schmid, H.M., & Schild, H. 1990, MNRAS, 246, 84.

Seaton, M.J. 1964, MNRAS, 127, 191.

———. 1987, J. Phys. B, 20, 6363.

Stanghellini, L., & Kaler, J.B. 1989, ApJ, 343, 811.

FIGURE CAPTIONS

FIG. 1.–The theoretical O IV emission line ratio $R_1 = I(2s^2 2p\ ^2P_{3/2} - 2s2p^2\ ^4P_{1/2})/I(2s^2 2p\ ^2P_{3/2} - 2s2p^2\ ^4P_{5/2}) = I(1407.4\ \text{Å})/I(1401.2\ \text{Å})$, plotted as a function of logarithmic electron density (N_e in cm^{-3}) at electron temperatures of (from top to bottom), T_e = 5000, 10000, 15000, 20000, 30000 and 40000 K.

FIG. 2.–The theoretical O IV emission line ratio $R_2 = I(2s^2 2p\ ^2P_{3/2} - 2s2p^2\ ^4P_{3/2})/I(2s^2 2p\ ^2P_{3/2} - 2s2p^2\ ^4P_{5/2}) = I(1404.8\ \text{Å})/I(1401.2\ \text{Å})$, plotted as a function of logarithmic electron density (N_e in cm^{-3}) at electron temperatures of (from top to bottom), T_e = 5000, 10000, 15000, 20000, 30000 and 40000 K.

FIG. 3.–High resolution IUE spectrum (SWP 20247) of the symbiotic star RR Tel in the wavelength region 1396–1408 Å, where the flux is in units of $ergcm^{-2}s^{-1}$. The O IV lines at 1397.2, 1399.8, 1401.2, 1404.8 and 1407.4 Å are clearly labelled in the figure, as are Si IV 1402.8 Å and S IV 1406.0 Å. An emission feature due to a cosmic ray event is labelled in the figure with a cross.

FIG. 4.–High resolution IUE spectrum (SWP 4106) of the planetary nebula NGC 7662 in the wavelength region 1396–1408 Å, where the flux is in units of $ergcm^{-2}s^{-1}$. The O IV lines at 1397.2, 1399.8, 1401.2, 1404.8 and 1407.4 Å are clearly labelled in the figure, as are Si IV 1402.8 Å and S IV 1406.0 Å. An absorption feature due to a reseau mark is labelled in the figure with the letter R.

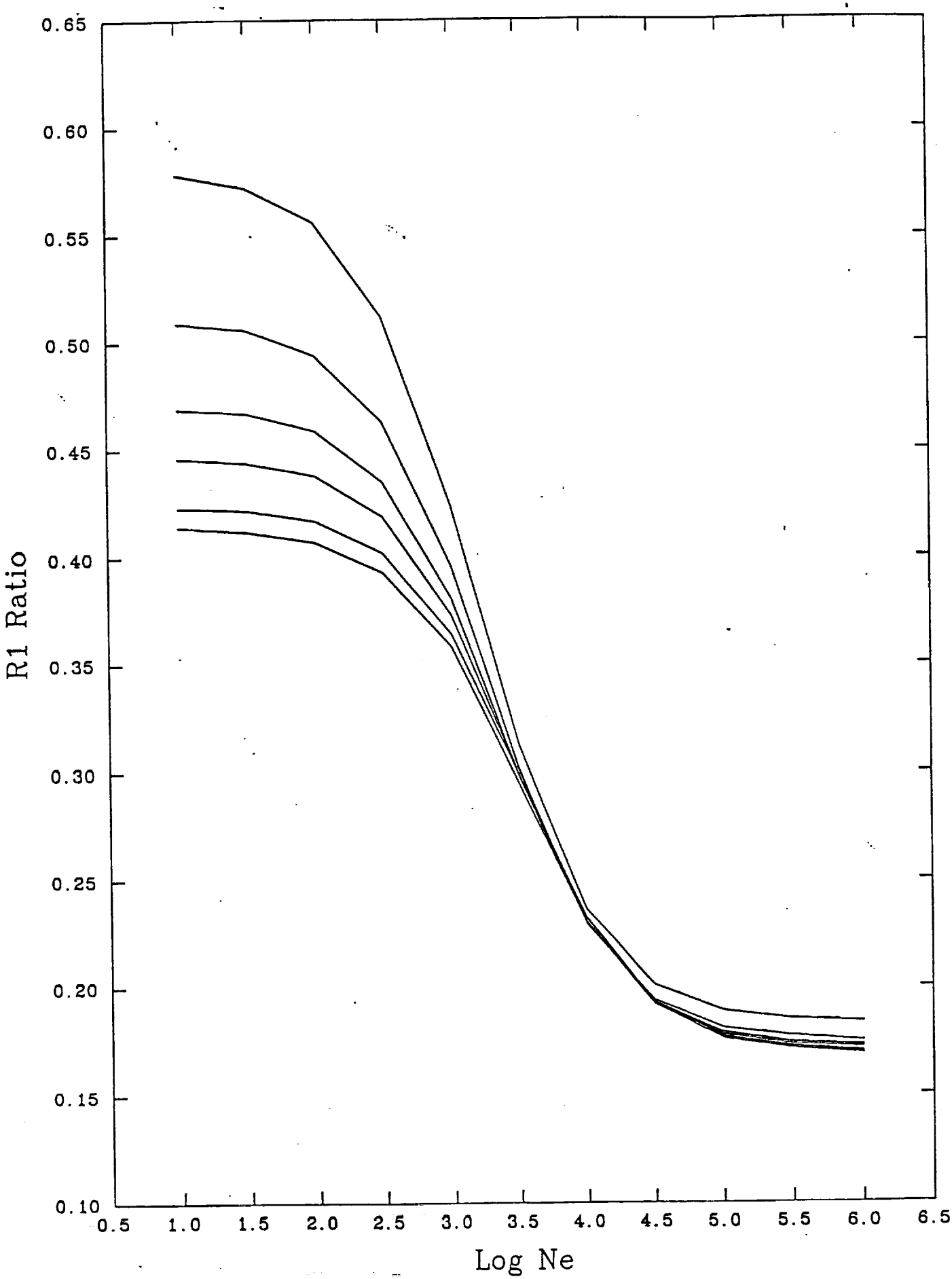
0.65
0.60
0.55
0.50
0.45
0.40
0.35
0.30
0.25
0.20
0.15
0.10
R1 Ratio
0.5
1.0
1.5
2.0
2.5
3.0
3.5
4.0
4.5
5.0
5.5
6.0
6.5
Log Ne

Fig 1

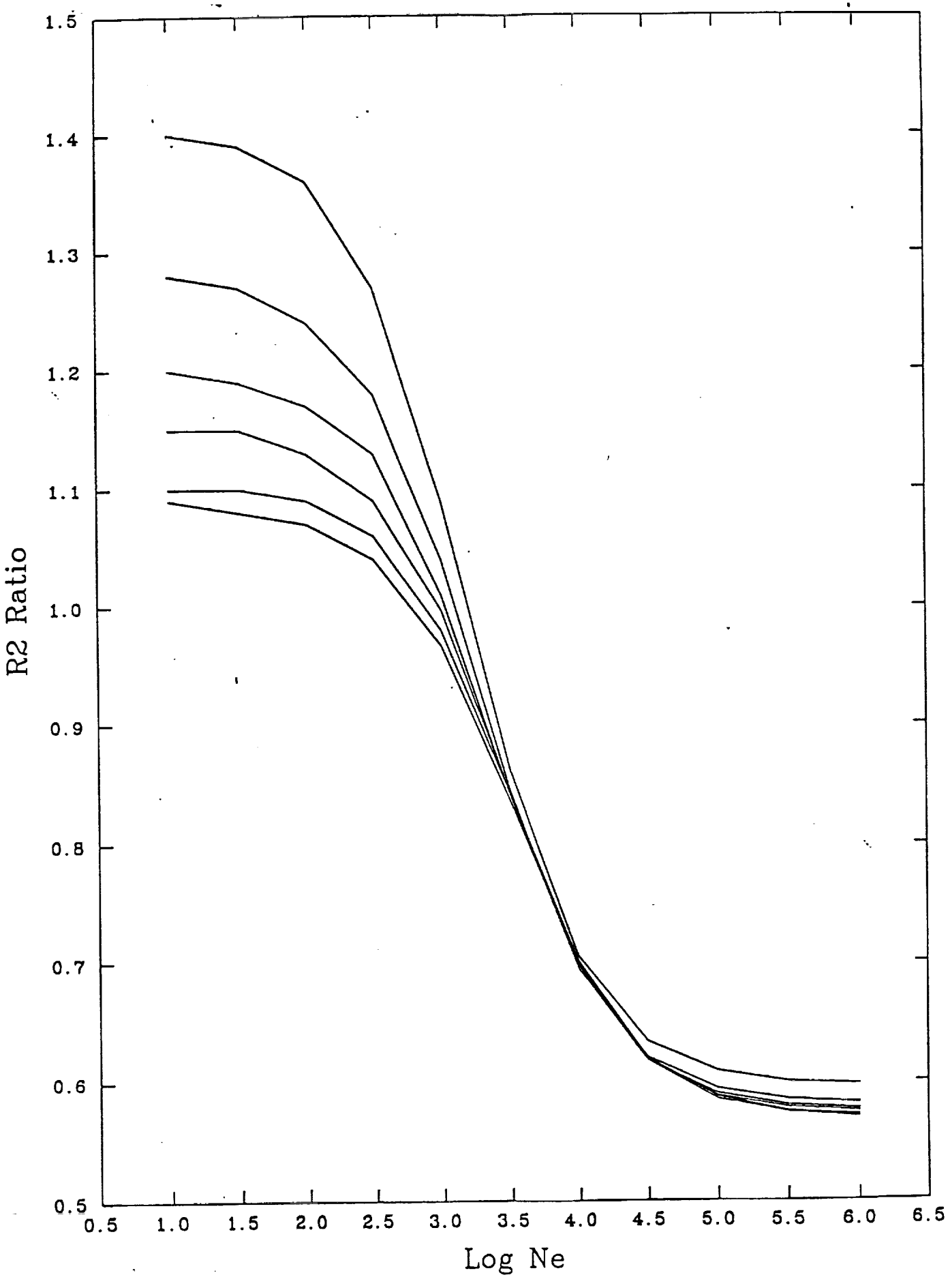
R2 Ratio
Log Ne
1.5
1.4
1.3
1.2
1.1
1.0
0.9
0.8
0.7
0.6
0.5
0.5
1.0
1.5
2.0
2.5
3.0
3.5
4.0
4.5
5.0
5.5
6.0
6.5

FIG 2

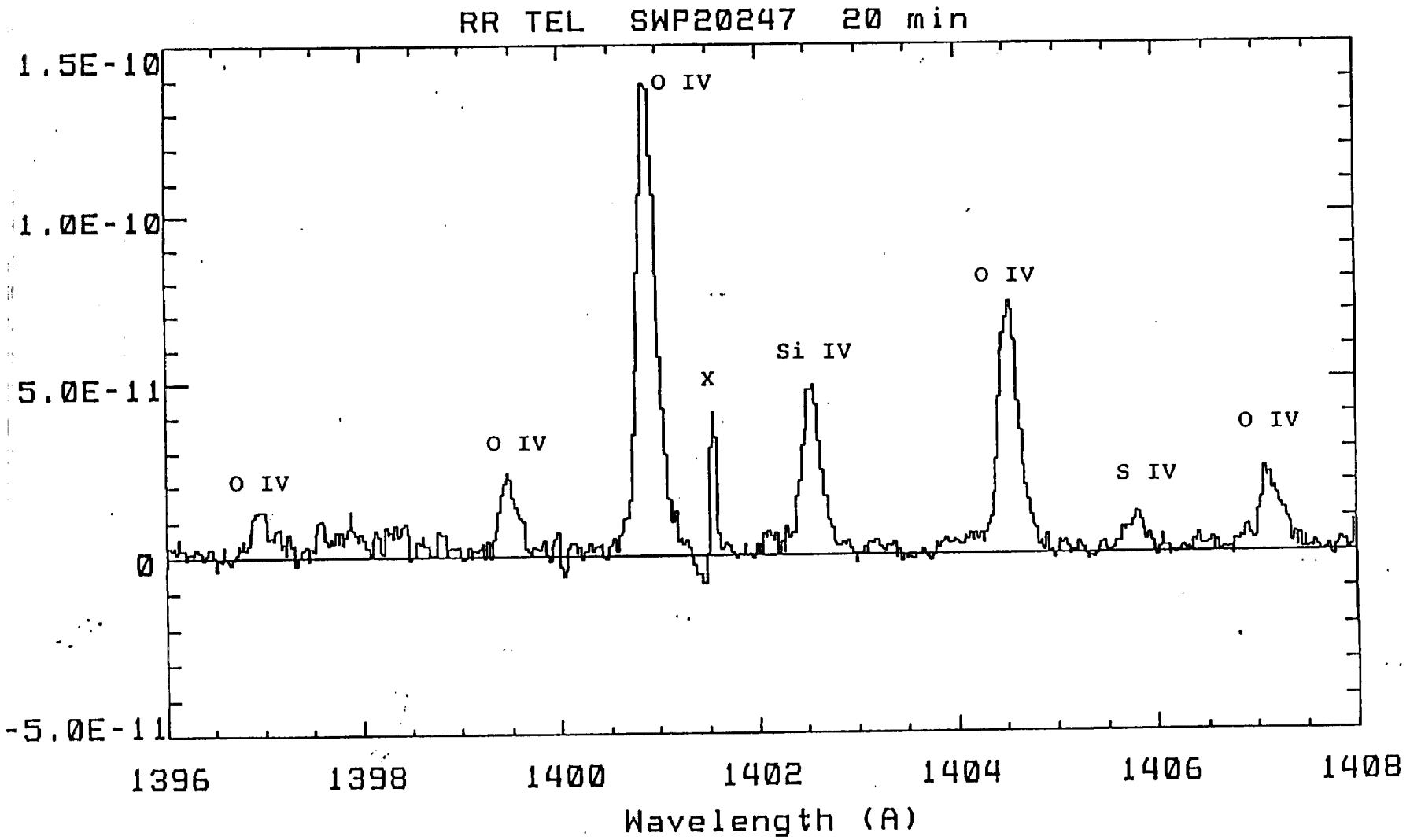
RR TEL SWP20247 20 min
1.5E-10
1.0E-10
5.0E-11
0
-5.0E-11
Calibrated Flux
O IV
O IV
O IV
X
Si IV
O IV
S IV
O IV
1396
1398
1400
1402
1404
1406
1408
Wavelength (A)

FIG 3

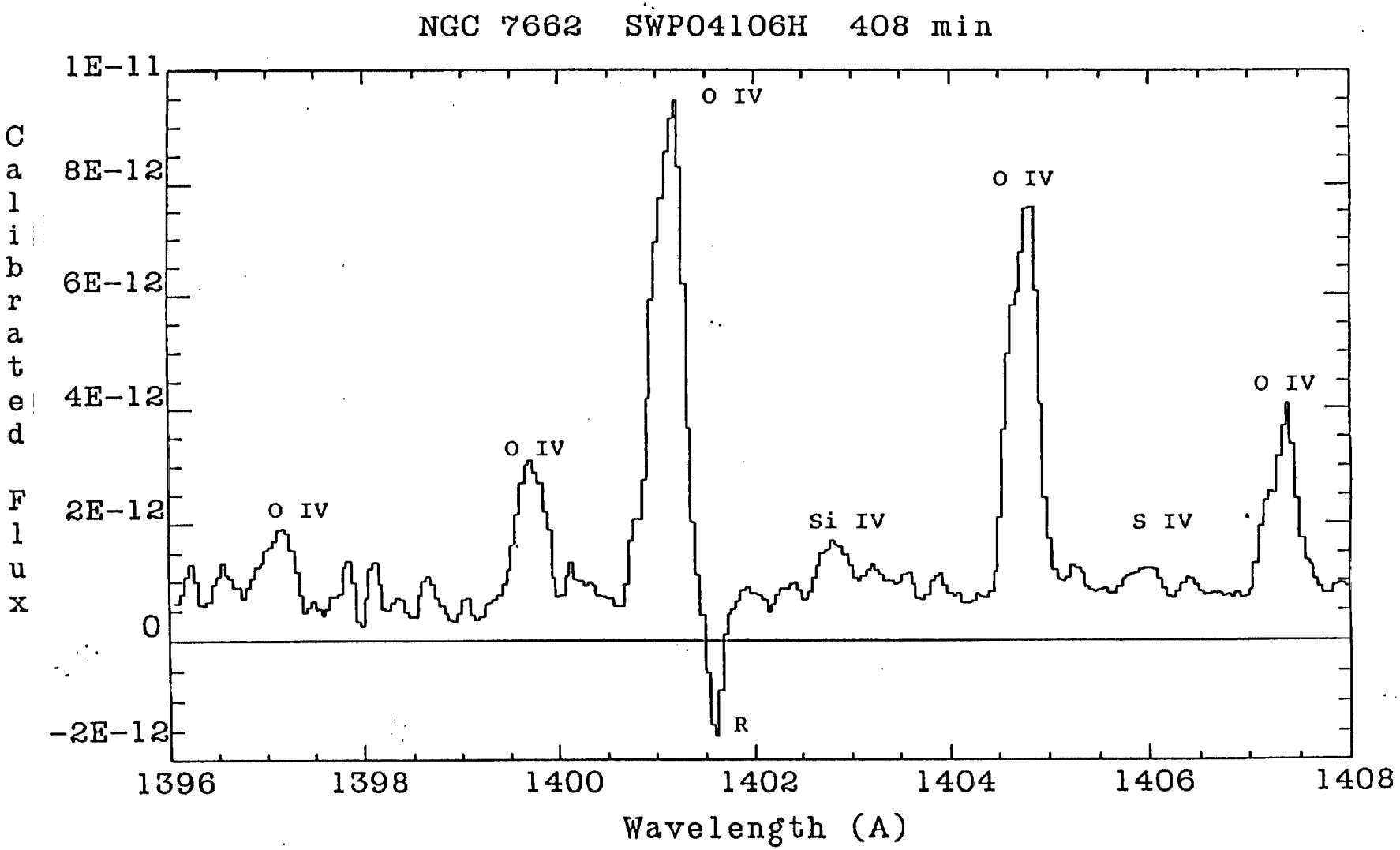
NGC 7662 SWP04106H 408 min
1E-11
8E-12
6E-12
4E-12
2E-12
0
-2E-12
Calibrated Flux
O IV
O IV
O IV
O IV
O IV
Si IV
S IV
R
1396
1398
1400
1402
1404
1406
1408
Wavelength (A)

Fig 4

TABLE 1

OBSERVED O IV LINE INTENSITY RATIOS

Object	SWP Image Number	R_1	R_2	R_3	R_4
NGC 3918	19888	0.23	0.62	0.24	0.16
NGC 7662	4106	0.30	0.69	0.29	0.13
RR Tel	20247	0.15	0.55	0.14	0.10
V1016 Cyg	13432	0.17	0.51	0.19	0.12

TABLE 2

DERIVED O IV LOGARITHMIC ELECTRON DENSITIES

Object	T_e (K)	log N_e (R_1)	log N_e (R_2)	log N_e (R_3)	log N_e (R_4)	log N_e (other)
NGC 3918	14400[a]	3.6	3.9	3.6	3.8	3.5[b]
NGC 7662	12500[c]	4.0	4.3	4.0	3.5	3.8[b]
RR Tel	13000[d]	H[e]	H	H	H	6.4[d]
V1016 Cyg	30000[f]	5.8	H	5.6	4.0	5.9[f]

[a] Rowlands et al. 1989
[b] Stanghellini & Kaler 1989
[c] Kaler 1986
[d] Hayes & Nussbaumer 1986
[e] Indicates that the observed line ratio is smaller than the theoretical high density limit
[f] Schmid & Schild 1990

TABLE 2

DERIVED O IV LOGARITHMIC ELECTRON DENSITIES

Object	T_e (K)	log N_e (R_1)	log N_e (R_2)	log N_e (R_3)	log N_e (R_4)	log N_e (other)
NGC 3918	14400[a]	3.6	3.9	3.6	3.8	3.5[b]
NGC 7662	12500[c]	4.0	4.3	4.0	3.5	3.8[b]
RR Tel	13000[d]	H[e]	H	H	H	6.4[d]
V1016 Cyg	30000[f]	5.8	H	5.6	4.0	5.9[f]

[a] Rowlands et al. 1989
[b] Stanghellini & Kaler 1989
[c] Kaler 1986
[d] Hayes & Nussbaumer 1986
[e] Indicates that the observed line ratio is smaller than the theoretical high density limit
[f] Schmid & Schild 1990